

ICEEECS2024

International Conference on Advances in Electrical-Electronics Engineering and Computer Science

9-10 November 2024
Ankara - Turkiye

PROCEEDINGS

www.iceeecs.com / iceeecs@gmail.com



GAZIANTEP
ISLAM
SCIENCE AND
TECHNOLOGY
UNIVERSITY

SETSCI
Conference Proceedings

SETECH
science-engineering-technology



**International Conference on Advances in Electrical-Electronics Engineering
and Computer Science**

9-10 November 2024, Ankara, Türkiye

Typesetting

Assoc. Prof. Dr. Turgut ÖZSEVEN

Cover Design

Assoc. Prof. Dr. Turgut ÖZSEVEN

Editors

Assoc. Prof. Dr. Turgut ÖZSEVEN

ISBN: 978-625-95366-0-6

Published by SETSCI

Publication Date: November 11, 2024



International Conference on Advances in Electrical-Electronics Engineering and Computer Science

9-10 November 2024, Ankara, Türkiye

CONTENTS

Committee	v
Topics.....	vi

Abstract Papers

Performance Comparison of SQLite across Native and Cross-Platform Frameworks	1
Evaluating the Performance and Efficiency of Caching Algorithms in .NET Applications	2
Comparative Analysis of Change Detection Mechanisms in Modern Web Frameworks	3
Deep Learning-Based In-Store Customer Route Tendency Analysis	4
A Prototype Study on YOLOv10-Based Bird Gesture Recognition.....	5
Deep Learning Based Color and Style Transfer: A Review and Challenges	6
AI Supported Adjustable Oven Rack.....	7
Inverse Prediction of Alloy Composition Based on Physical Properties of Superalloys Modeled by the CALPHAD Methodology Using Explainable Artificial Intelligence	8
Performance Analysis of Artificial Neural Networks in the Diagnosis of Thyroid Diseases.....	9
A Technological Approach to the Rockfall Problem.....	10
Personal Health Data Breaches Increasing with the Proliferation of Digital Health Systems During the COVID-19 Pandemic	11
A New Design Bandpass Filter Working At 28 GHz For 5G Applications	12

Full Papers

The Impact of Electric Vehicles on The Grid.....	1
The Effects of Environmental Factors on Solar Power Plants: The Case of MEYSU Factory	7
DC Energy Technologies: The Key to A Sustainable Tomorrow?.....	10

Development of Machine Learning-Based Sales Cancellation/Return Forecasting Models for the E-Commerce Industry	17
Analysis of Inrush Current Loads in Electric Motors in Low Temperature Tests	22
Failure Mechanisms in Enclosed Electric Motors Due to Insufficient Cooling at High Temperatures	27
Asynchronous Motor Driver PCB Design with MOSFET H Bridge.....	32
Hardware Development and Scale-up of Angular Motion Systems Using BNO055 Sensor and ESP32-WROOM-32 Microcontroller to Measure the Speed of Angular Motion Systems	37
Enhancing Urban Parking Management with SSD-Based Satellite Detection Systems	42
The Importance of Bushing Connections in Transformers	47



International Conference on Advances in Electrical-Electronics Engineering and Computer Science

9-10 November 2024, Ankara, Türkiye

Conference Chair

Köksal Erentürk, Atatürk University, Türkiye

Advisory Committee

Ali Durmuş, Kayseri University, Türkiye

Muharrem Düğenci, Karabük University, Türkiye

Oleksandr Laptiev, Taras Shevchenko National University of Kyivi, Ukraine

Shahnaz N. Shahbazova, Azerbaijan State University of Economics, Azerbaijan

Tanupriya Choudhury, Graphic Era Deemed to be University, Dehradun, India

Zafer Doğan, Tokat Gaziosmanpaşa University, Türkiye

Technical Committee Members

Ahmet Nusret Toprak, Erciyes University, Türkiye

Aydın Çetin, Gazi University, Türkiye

Bahadır Akbal, Aksaray University, Türkiye

Bülent Turan, Tokat Gaziosmanpaşa University, Türkiye

Canan Oral, Amasya University, Türkiye

Cem Emeksiz, Tokat Gaziosmanpaşa University, Türkiye

Emine Gül Cansu Ergün, Başkent University, Türkiye

Ercan Karaköse, Kayseri University, Türkiye

Harun Sümbül, Ondokuz Mayıs University, Türkiye

Haydar Kaya, Karadeniz Technical University, Türkiye

Hilal Arslan, Ankara Yıldırım Beyazıt University, Türkiye

Hussain Falih Mahdi, University of Diyala, Iraq

Ivan Ganchev, University of Limerick, Ireland / University of Plovdiv "Paisii Hilendarski", Bulgaria

İlker Yıldız, Bolu Abant İzzet Baysal University, Türkiye

İsmail İşeri, Ondokuz Mayıs University, Türkiye

Levent Gökrem, Tokat Gaziosmanpaşa University, Türkiye

Levent Seyfi, Konya Technical University, Türkiye

Ljiljana Trajkovic, Simon Fraser University, Canada

M. Gokhan Bakal, Abdullah Gül University, Türkiye

Mahir Kaya, Tokat Gaziosmanpaşa University, Türkiye

Manuel G. Gericota, Polytechnic of Porto, Portugal

Mehmet Akif Erişmiş, Necmettin Erbakan University, Türkiye

Mehmet Bahadır Çetinkaya, Erciyes University, Türkiye

Mete Çelik, Erciyes University, Türkiye

Mohd Asyraf Kassim, Universiti Sains Malaysia, Malaysia

Mustafa Şinasi Ayas, Karadeniz Technical University, Türkiye

Ömür Şahin, Erciyes University, Türkiye

Patrick Goh Kuan Lye, Universiti Sains Malaysia, Malaysia

Rıfat Kurban, Abdullah Gül University, Türkiye

Sachi Nandan Mohantey, Singhidunum University, Serbia

Selami Parmaksızoğlu, Antalya Bilim University, Türkiye

Selen Ayas, Karadeniz Technical University, Türkiye

Serkan Şenkal, Tokat Gaziosmanpaşa University, Türkiye

Taner Çokyaşar, Tarsus University, Türkiye

Secretary

Sadık Önal, Tokat Gaziosmanpaşa University, Türkiye



International Conference on Advances in Electrical-Electronics Engineering and Computer Science

9-10 November 2024, Ankara, Türkiye

TOPICS

Track 1: Biomedical Engineering

Track 2: Computer Science

Track 3: Electrical Engineering

Track 4: Electronic Engineering

Track 5: Energy Systems Engineering

Track 6: Mechatronic Engineering

Track 7: Medical Engineering

Track 8: AI Engineering

Track 9: Software Engineering



**International Conference on Advances in Electrical-Electronics Engineering
and Computer Science**

9-10 November 2024, Ankara, Türkiye

ABSTRACT PAPERS

Published by SETSCI

Publication Date: November 11, 2024

International Conference on Advances in Electrical-Electronics Engineering and Computer Science

9-10 November 2024, Radisson Blu Hotel, Ankara, Türkiye

www.iceeeecs.com

Performance Comparison of SQLite across Native and Cross-Platform Frameworks

Koray Liman ¹⁺, Hüseyin Özkan ^{1*}, Nadir Kocakır ¹ and Cevat Balaban ¹

¹Özdilek Ev Tekstil San. ve Tic. AŞ, Özveri Ar-Ge Merkezi, Bursa, Türkiye

*Corresponding author: huseyin.ozkan@ozdilek.com.tr

⁺Speaker: koray.liman@ozdilek.com.tr

Presentation/Paper Type: Oral / Abstract

Abstract – Mobile applications require high performance to stay competitive with emerging solutions, and database performance plays a critical role in this competition. This study analyzes the performance of the SQLite database across Flutter, Swift, and Kotlin by developing an application with identical functionality in all three languages and testing it on a range of iOS and Android devices, including both high-end and mid-range models. The tests cover table creation, data insertion, deletion, update, and retrieval operations. Results show that Swift achieved the best performance on iOS devices, while Kotlin led on Android devices. Although Flutter provides flexibility through cross-platform support, it lags behind native languages in terms of performance. The Swift-based application completed operations faster on high-end iOS devices, with slightly slower results on mid-range models. Kotlin demonstrated higher operation times than Swift on Android devices but outperformed Flutter. Overall, Flutter exhibited higher processing times across all devices compared to other languages. This study highlights the importance of careful programming language selection based on target platforms and performance needs. In conclusion, native languages are found to be more advantageous in terms of performance than cross-platform languages.

Keywords – SQLite, Flutter, Swift, Kotlin, Performance Analysis

International Conference on Advances in Electrical-Electronics Engineering and Computer Science

9-10 November 2024, Radisson Blu Hotel, Ankara, Türkiye

www.iceeecs.com

Evaluating the Performance and Efficiency of Caching Algorithms in .NET Applications

Hakan Akdoğan^{1*}, Musa Peker¹ and Nadir Kocakır¹

¹Özdilek Ev Tekstil San. ve Tic. AŞ, Özveri Ar-Ge Merkezi, Bursa, Türkiye

*Corresponding author: hakan.akdogan@ozdilek.com.tr

⁺Speaker: hakan.akdogan@ozdilek.com.tr

Presentation/Paper Type: Oral / Abstract

Abstract – This study provides a comprehensive analysis of the performance and efficiency of various caching algorithms within the .NET environment. Specifically, it examines the LRU (Least Recently Used), LFU (Least Frequently Used), ARC (Adaptive Replacement Cache), FIFO (First-In-First-Out), and MRU (Most Recently Used) algorithms. These algorithms were manually implemented to ensure a fair comparison by eliminating any limitations that could arise from external libraries. The evaluation focused on key performance metrics such as speed, memory usage, and data retention times during Get and Put operations. The results showed that the FIFO algorithm offered the fastest data access performance. However, in applications where data retention times are crucial, the ARC algorithm was found to be more consistent and efficient. ARC combines the advantages of LRU and LFU, optimizing memory management and improving overall performance. Additionally, it was observed that algorithms like LFU and LRU consume more memory due to their counters, whereas ARC and FIFO operate with fixed memory usage. Based on these findings, ARC emerges as the most suitable option for complex applications that require efficient memory management, while FIFO is recommended for simpler structures where data retention time is not critical. The overall findings of this study provide valuable insights into how different caching algorithms can be effectively utilized in .NET projects to enhance performance.

Keywords – .NET Caching Algorithms, Performance Optimization, ARC Algorithm, Memory Management, Data Retention Efficiency

International Conference on Advances in Electrical-Electronics Engineering and Computer Science

9-10 November 2024, Radisson Blu Hotel, Ankara, Türkiye

www.iceeecs.com

Comparative Analysis of Change Detection Mechanisms in Modern Web Frameworks

Burak Kadilar ¹⁺, Ferdi Tuna ^{1*} and Nadir Kocakır ¹

¹Özdilek Ev Tekstil San. ve Tic. AŞ, Özveri Ar-Ge Merkezi, Bursa, Türkiye

*Corresponding author: ferdi.tuna@ozdilek.com.tr

+Speaker: burak.kadilar@ozdilek.com.tr

Presentation/Paper Type: Oral / Abstract

Abstract – Change detection is a critical feature in modern web development frameworks, influencing both performance and developer experience. This study provides a comprehensive analysis of the change detection mechanisms in Vue 3, React 18, and Angular 18, focusing on their reactivity systems and their impact on performance. Vue 3 utilizes a reactivity system with reactive objects and Proxies, allowing for efficient updates through automated rendering. React 18, on the other hand, relies on a Virtual DOM, enhancing user experience with its Concurrent Mode, which improves performance by prioritizing user interactions. Angular 18 introduces a Zoneless Change Detection mechanism, offering fine-grained control over change detection without relying on Angular's traditional NgZone. This study highlights the trade-offs between automation and manual control, particularly how Angular's approach allows for more precise performance tuning in complex applications, while Vue 3 and React 18 favor simplicity and ease of use in smaller or less complex projects. The findings suggest that framework choice should align with project requirements, balancing performance optimization and development simplicity. Ultimately, Angular's Zoneless Change Detection is ideal for applications that demand granular control, whereas Vue and React are better suited for projects emphasizing faster development and ease of use.

Keywords – Change Detection, Zoneless Change Detection, Reactivity System, Virtual DOM, Concurrent Mode

International Conference on Advances in Electrical-Electronics Engineering and Computer Science

9-10 November 2024, Radisson Blu Hotel, Ankara, Türkiye

www.iceeecs.com

Deep Learning-Based In-Store Customer Route Tendency Analysis

Erdal Nayir ^{1*}, Arman Kuyucu ¹, Musa Peker ¹ and Nadir Kocakır ¹

¹Özdilek Ev Tekstil San. ve Tic. AŞ, Özveri Ar-Ge Merkezi, Bursa, Türkiye

*Corresponding author: <mailto:erdal.nayir@ozdilek.com.tr>

⁺Speaker: <mailto:erdal.nayir@ozdilek.com.tr>

Presentation/Paper Type: Oral / Abstract

Abstract – Customer behavior analysis plays a critical role in strategic decision-making within the retail sector, especially in optimizing store layout, product placement, and enhancing customer experience. To achieve this, a detailed examination of in-store movements is essential. In this study, an advanced route analysis system was designed to track and analyze the paths followed by customers entering from specific points and to evaluate these movements in percentage terms. Person detection is performed via cameras installed on the store ceiling, utilizing the YOLOX-Tiny algorithm, which ensures high performance even with low-resolution images. The algorithm was trained on a hybrid dataset covering various scenarios, significantly enhancing system accuracy. The system operates by analyzing movements between predefined zones and entry points, offering detailed reports on which areas customers spend the most time, their directional tendencies, and how their in-store paths are formed. This analysis provides store management with valuable insights into customer preferences within the store, enabling data-driven strategic decisions. The system, which runs on low-cost and energy-efficient embedded platforms such as Jetson Nano, delivers high-accuracy results with acceptable FPS rates. The flexibility and scalability of this solution make it applicable not only in retail but also in various industries where customer movement tracking is essential, such as shopping malls, airports, and large event venues.

Keywords – Customer behavior analysis, in-store route analysis, YOLOX-Tiny algorithm, embedded platforms, strategic decision-making

A Prototype Study on YOLOv10-Based Bird Gesture Recognition

Rıdvan Yayla

Bilecik Şeyh Edebali University, Türkiye (ridvan.yayla@bilecik.edu.tr)

Presentation/Paper Type: Oral / Abstract

Abstract – Birds are one of the most abundant types of creatures on Earth. However, it is also known that there are a large number of taxonomically diverse bird species in nature. The bird network has standard behavioural patterns such as flying, perching, feeding and walking. In this study, 2372 bird images are used for five standard bird gestures detection which are flying, perching, swimming, eating, and walking with the Yolov10 algorithm from Caltech-UCSD Birds-200-2011 dataset. Firstly, the dataset is prepared for detection by classifying these gestures. Secondly, the bird gesture images are trained with Yolov10, thirdly the trained model is tested with bird motion short videos and finally, the evaluation results are shown with evaluation metrics. In this prototype study, it was observed that the obtained model had results with accuracy higher than 70%. The study can be used to make sense of bird communication for future studies.

Keywords – *Bird gesture, target detection, classification, deep learning, Yolov10.*

International Conference on Advances in Electrical-Electronics Engineering and Computer Science

9-10 November 2024, Radisson Blu Hotel, Ankara, Türkiye

www.iceeecs.com

Deep Learning Based Color and Style Transfer: A Review and Challenges

Melike Bektaş Kösesoy^{1*} and Seçkin Yılmaz²

^{1*} Department of Computer Engineering, Graduate School, Bursa Technical University, Bursa, Turkey (melike.bektas@btu.edu.tr)

² Department of Computer Engineering, Faculty of Engineering and Natural Sciences, Bursa Technical University, Bursa, Turkey
(seckin.yilmaz@btu.edu.tr)

Abstract – Deep learning methods have been applied in many fields in recent years, and successful results have been obtained. Image processing is one of these areas. One of the image processing applications using deep learning is color and style transfer. Color and style transfer is aimed at transferring the color and texture from the source image to another image (the target image). In color transfer, the colors in the source image are transferred, while in style transfer, texture is transferred as well as color. In the literature, color transfer has been studied for many years, and traditional methods such as PCA have been used in addition to deep learning. On the other hand, studies on style transfer are relatively new and mostly use deep learning methods. In this study, color and style transfer studies in the literature were examined. The methods used in these studies are mentioned, and the current problems in this field are shared.

Keywords – Color Transfer, Neural Style Transfer, Image Colorization, Image Recoloring, CNN.

International Conference on Advances in Electrical-Electronics Engineering and Computer Science

9-10 November 2024, Radisson Blu Hotel, Ankara, Türkiye

www.iceeecs.com

AI Supported Adjustable Oven Rack

Aziz Başdemir^{1*}, Fırat Koçyiğit¹ and Farih Arslan¹

¹*Vestel Home Appliances, Technology Development Department, Manisa, Türkiye*

*Corresponding author: azizbasdemir@vestel.com.tr

+Speaker: aziz.basdemir@vestel.com.tr

Abstract

When early humans discovered fire, they developed various methods to cook food. These methods made food easier to digest, preserved its nutritional value, and eliminated harmful microorganisms. As a result, people began to consume cooked food more quickly and safely, which accelerated the evolution of cooking devices.

With advancing technology, cooking devices have greatly improved the cooking experience, making it more convenient for users. In this context, camera-integrated, AI supported adjustable oven racks have become an essential technology for enhancing modern cooking experiences. These innovative systems ensure that food is cooked under the most optimal conditions, improving cooking quality and making the process easier for users.

The main goal of this work is to continuously update the height and position of food placed in cooking devices during the cooking process, based on color changes detected through image processing. This helps achieve the optimal point in terms of health and eating comfort, while also using heat energy efficiently to ensure the best cooking process.

To achieve these goals, the height of the oven rack inside the cooking device will be automatically adjusted according to the different stages of cooking. This ensures that the food is positioned under ideal cooking conditions throughout the process, increasing energy efficiency. The system's design includes a movable carrier system and components, integrated through 3D modeling. Necessary electromechanical optimizations have been made within the dynamic system, and the prototype has been produced and tested.

Keywords –AI, Cooking Algorithm, Image Processing, Production, CAE, Optimization, Adjustable Oven Rack.

International Conference on Advances in Electrical-Electronics Engineering and Computer Science

9-10 November 2024, Radisson Blu Hotel, Ankara, Türkiye

www.iceeecs.com

Inverse Prediction of Alloy Composition Based on Physical Properties of Superalloys Modeled by the CALPHAD Methodology Using Explainable Artificial Intelligence

Yusuf Alaca^{1*}, Yusuf Uzunoglu²⁺

¹ Hitit University, Department of Computer Engineering, Çorum, Türkiye

² Erciyes University, Department of Materials Science and Engineering, Kayseri, Türkiye

*Corresponding author: yusufalaca@hitit.edu.tr

+Speaker: 4012640009@erciyes.edu.tr

Presentation/Paper Type: Oral / Abstract

Abstract – The CALPHAD methodology models the physical, mechanical, and thermodynamic properties of materials based on a given alloy composition using phase equilibrium calculations and thermodynamic databases. Millions of material data points can be obtained for each alloy composition determined through the CALPHAD approach, varying by temperature. However, finding an alloy with the desired properties requires manually changing the composition and involves time-consuming trial-and-error efforts. In this study, the aim is to find the chemical composition that provides the desired properties at a specific temperature by using the data obtained from the CALPHAD methodology to train artificial intelligence (AI). Accordingly, the physical properties (density, thermal conductivity, linear expansion percentage, Young's modulus, bulk modulus, shear modulus, and Poisson's ratio) of 250 different Ni-Cr-Fe-based superalloys were modeled in the JMatPro software, covering the temperature range of 540-920°C. A dataset of 5000 rows was created from the obtained data, with 80% used to train the AI model and 20% reserved for the validation and testing phases. As a result of the analyses performed with Explainable Artificial Intelligence (XAI) and Artificial Neural Networks (ANNs), the alloy composition providing physical properties such as density, thermal conductivity, linear expansion, Young's modulus, bulk modulus, shear modulus, and Poisson's ratio at a specific temperature was predicted with high accuracy. In conclusion, in addition to obtaining material properties from alloy compositions using the CALPHAD approach, it has become possible to inversely predict the alloy composition with high accuracy for the desired physical properties at a specific temperature using AI techniques.

Keywords – CALPHAD Methodology, Explainable Artificial Intelligence (XAI), Superalloys, Alloy Composition Prediction, Artificial Neural Networks (ANNs), Physical Properties Modeling

Performance Analysis of Artificial Neural Networks in the Diagnosis of Thyroid Diseases

Muhammet Cihat MUMCU^{1*}, Ercan AYKUT²⁺, Sena Nur BENLİ³, Kübra ERDOĞAN⁴, İzzet YAVUZ⁵

^{1,2,5}Electrics Program of Gelisim Vocational School, Istanbul Gelisim University, Istanbul, Türkiye

³Computer Technologies Program of Gelisim Vocational School, Istanbul Gelisim University, Istanbul, Türkiye

⁴Mechatronics Program of Gelisim Vocational School, Istanbul Gelisim University, Istanbul, Türkiye *Corresponding author:

mcmumcu@gelisim.edu.tr

+Speaker: eaykut@gelisim.edu.tr

Presentation/Paper Type: Oral / Abstract

Abstract – The accurate and timely diagnosis of thyroid diseases is crucial for effective treatment and patient management. This study compares artificial neural networks (ANNs), specifically Multi-Layer Perceptron (MLP) and Radial Basis Function (RBF) networks, in the classification of thyroid diseases. A dataset of thyroid disorders from 2,800 patients was used to evaluate and compare the classification accuracy, sensitivity, specificity, and computational efficiency of these models. The dataset includes clinical parameters, such as hormone levels, required to distinguish between thyroid conditions. Model optimization involved analyzing the number of hidden layers and neurons. Cross-validation was applied to train and test the MLP and RBF networks, avoiding overfitting and improving generalization.

Results indicate that both models achieve high classification accuracy, with differences in performance metrics. The MLP model, due to its deeper architecture, shows better generalization, while the RBF model exhibits faster convergence and higher sensitivity for certain thyroid disorders. The findings suggest that both ANN approaches have high accuracy in medical diagnosis and are suitable for automated healthcare systems. This study contributes to the literature on artificial neural networks in medical diagnostics and emphasizes the importance of selecting appropriate models for specific medical applications.

Keywords – Artificial Neural Networks, Automated Healthcare Systems, Deep Learning.

International Conference on Advances in Electrical-Electronics Engineering and Computer Science

9-10 November 2024, Radisson Blu Hotel, Ankara, Türkiye

www.iceeecs.com

A Technological Approach to the Rockfall Problem

Muhammed Çağrı AKSU^{1*}, Hacı Mustafa SANLAV²⁺ and Egemen ÜLKER³

¹ Department of Computer Engineering, Faculty of Engineering, Artvin Çoruh University, Artvin, Türkiye

² Department of Computer Engineering, Faculty of Engineering, Artvin Çoruh University, Artvin, Türkiye

³ Department of Computer Engineering, Faculty of Engineering, Artvin Çoruh University, Artvin, Türkiye

*Corresponding author: cagriaksu@artvin.edu.tr

⁺Speaker: mustafasanlav10@gmail.com

Presentation/Paper Type: Abstract

Abstract – Rockfall incidents pose significant threats to life and property, especially in mountainous regions. This study presents a technological solution to the frequent rockfall issues on the road in Seyitler Village, Artvin. The primary objective is to develop an advanced early warning and monitoring system to prevent potential accidents caused by rockfalls and to enhance safety in the area. Two main systems have been designed for this purpose: an autonomous drone patrol system and an early warning system. The drone patrol system is designed to fly designated routes autonomously, capturing high-resolution images to detect rocks at risk of falling. These images are transmitted to a server via SSH (Secure Shell) and SCP (Secure Copy Protocol) and are analyzed by experts to pinpoint the locations of potentially hazardous rocks. This process allows for remote monitoring and a proactive approach to road safety, identifying risks before accidents occur. The semi-automated system is based on an Internet of Things (IoT) infrastructure, enabling local governments and disaster management units to monitor risks effectively and respond quickly to any incidents. The second component, the early warning system, consists of accelerometer sensors installed on rockfall protection barriers in high-risk areas, paired with ESP32 microcontrollers. These sensors detect vibrations, and if the vibrations exceed a certain threshold, the data is sent to warning lights positioned at the beginning and end of the road. The activation of these lights alerts drivers and pedestrians to potential danger, allowing them to evacuate the area. This early warning system is especially useful in situations where rock movements are triggered by factors like heavy rainfall, erosion, or sudden temperature changes. Wireless data communication supports the system, and solar panels power it, ensuring easy portability to various locations. The integration of IoT devices and autonomous flight technologies in these systems enables early detection of rockfall hazards and the activation of warning mechanisms during critical moments, offering a comprehensive and innovative solution. This cost-effective alternative to the high-priced monitoring and warning systems commonly found in the literature utilizes low-cost, wireless communication-supported microcontrollers and sensor technologies, making the system reliable, accessible, and efficient. It serves as a model for high-risk road routes, particularly in Turkey's mountainous regions. By using IoT devices, the system provides continuous monitoring of rockfall hazards, facilitating real-time data collection, analysis, and rapid assessment of risks. It is expected that this IoT-based solution could serve as a model in other areas facing similar risks, contributing to disaster management in an innovative and practical manner.

Keywords – Internet of Things, Rockfall Problem, Drone, Rockfall Monitoring, Disaster Management

International Conference on Advances in Electrical-Electronics Engineering and Computer Science

9-10 November 2024, Radisson Blu Hotel, Ankara, Türkiye

www.iceeecs.com

Personal Health Data Breaches Increasing with the Proliferation of Digital Health Systems During the COVID-19 Pandemic

Cihan Ünal^{1*}, Hakan Yıldırım²⁺

¹Computer Programming, Hacettepe University, Ankara, Turkey

²Computer Engineering, Ankara Bilim University, Ankara, Turkey

*Corresponding author: cihan.unal@hacettepe.edu.tr

⁺Speaker: cihan.unal@hacettepe.edu.tr

Presentation/Paper Type: Abstract

Abstract – This study examines vulnerabilities in many countries. Based on case studies from Turkey, allegations of personal health data theft and misuse were investigated, and the impact of these breaches on individuals' privacy was analyzed. Furthermore, within the framework of regulations such as the Personal Data Protection Law (KVKK) and the General Data Protection Regulation (GDPR), the legal measures aimed at preventing such breaches and the legal rights of citizens were discussed. The technical and legal measures that can be taken to minimize the impact of data breaches were also explored while emphasizing the responsibilities that individuals and institutions should assume during this process. The study concludes by emphasizing the importance of protecting personal health data during crises like COVID-19 and the necessity of increasing awareness-raising activities on this issue, supported by recommendations.

Keywords – Personal health data, COVID-19 data breaches, Data Security, GDPR, Privacy during the pandemic

International Conference on Advances in Electrical-Electronics Engineering and Computer Science

9-10 November 2024, Radisson Blu Hotel, Ankara, Türkiye

www.iceeecs.com

A New Design Bandpass Filter Working At 28 GHz For 5G Applications

Burak AÇIKALIN*, Nursel AKÇAM²⁺ and Burak DÖKMETAŞ³

¹Electrical and Electronic Engineering/Engineering Faculty, Turkish Aeronautical Association University, City, Country

¹Electrical and Electronic Engineering/Engineering Faculty, Gazi University, Ankara, Turkey

¹Electrical and Electronic Engineering/Engineering Faculty, Kafkas University, Kars, Turkey

*Corresponding author: bacikalin@thk.edu.tr

⁺Speaker: bacikalin@thk.edu.tr

Presentation/Paper Type: Oral / Abstract

Abstract - With advancing technology, people's demand for faster and more reliable communication is increasing. In order to meet these, there are important studies on the structures used in 5G applications. In this study, a new band-pass filter design and results that allow signal transmission at 28 GHz frequency were observed. The structure of the filter consists of parallel coupled structures and step impedance structure. In order to get results at the desired frequency, a defected ground structure was applied. With this structure, both frequency shift and our reflected signal ratio value were improved. It was designed to show efficient results at high frequencies such as 28 GHz. Rogers 5880 substrate material, which shows quality performance at high frequencies, was preferred in the filter design. The dimensions of the structure were designed as $18 \times 14 \text{ mm}^2$ and 1.27 mm in height in order to be compact. Since the filter has a symmetrical structure, the structure shows the same results on both sides. The filter, whose calculations and discrete element design were made in the ADS program, was drawn in 3D in the CST program and the results were obtained. According to the program analysis results, a return loss ratio of -50 dB (S11) and an insertion loss of -3 dB (S21) were obtained at a bandwidth of 1.26 GHz and a center frequency of 28 GHz. The filter operates efficiently at these values. It is thought that the results obtained will be an important step for new designs in 5G technology.

Keywords – 5G, Center Frequency, Return Loss Ratio, Parallel Coupled



**International Conference on Advances in Electrical-Electronics Engineering
and Computer Science**

9-10 November 2024, Ankara, Türkiye

FULL PAPERS

Published by SETSCI

Publication Date: November 11, 2024

The Impact of Electric Vehicles on The Grid

Abidin KEÇECİ^{1*}, Bülent ÇAVUŞOĞLU²

¹Department of Electrical and Electronics Engineering/Institute of Science, Atatürk University, Erzurum, TURKEY

²Department of Electrical and Electronics Engineering, Atatürk University, Erzurum, TURKEY

**(abidinkececi@gmail.com)*

Abstract – The unlimited nature of consumption and needs contrasts with the scarcity of usable resources, necessitating the optimal use of available resources. Alongside the careful protection of the environment and human health, it is crucial to meet needs with maximum efficiency. With the aid of measuring instruments and sensors added to traditional grids, grids are becoming smart, allowing for rapid resolution of system failures, security issues, losses, and requirements through detection, monitoring, and control. The quick and minimal-error communication between grid elements is of great importance. This paper aims to raise awareness about the economic benefits for the grid and users through a V2G (Vehicle-to-Grid) technology simulation, focusing on the advantages and disadvantages of using V2G technology, ensuring that the energy needs between the producer and consumer are met promptly and adequately without any system disruption within a smart grid infrastructure aided by 5G communication technology.

Keywords – EV, Electric vehicle, V2G, G2V, 5G

I. INTRODUCTION

Due to environmental pollution, global warming, dwindling fossil fuel reserves, and rising prices, the search for alternative energy sources has intensified, particularly in vehicles where electricity is increasingly used in place of petroleum and derivative fuels. Electric vehicles (EVs) offer advantages such as zero exhaust emissions, quiet operation, and lower energy consumption compared to internal combustion engines. However, they face disadvantages like range anxiety, high costs, battery technology issues, and insufficient charging stations.

According to the International Energy Agency (IEA), the stock and sales of EVs worldwide have been gaining dominance in the automotive sector. The EV stock exceeded 40 million in 2023, with sales surpassing 16 million in 2024, leading to a rise in both fast and slow charging stations. [1], [2], [3], [4]

The IEA's Global EV Outlook 2024 report predicts that by 2030, the number of charging points will exceed 15 million, with electricity consumption from EVs making up 8.1% of final electricity consumption, up from 0.5% in 2023. The EV fleet is expected to displace 6 million barrels per day (mb/d) of diesel and gasoline by 2030. [5]

The concept of EVs exchanging power with the grid first emerged in 1997 through the work of Kempton and Letendre [6], who coined the terms G2V (Grid-to-Vehicle) for charging and V2G (Vehicle-to-Grid) for discharging, investigating the economic potential of energy flow. The increasing number of EVs, technological advancements in smart grids, and daily fluctuations in energy demands drive this change. Price fluctuations in energy due to these daily variations allow EV owners to charge at lower costs and profit during peak demand times. Thus, EVs can act both as energy consumers and distributed storage devices, supporting the grid.

The increasing number of electric vehicles and their simultaneous charging as distributed loads on the grid during the day necessitate alternative studies to prevent significant

grid imbalances. These studies include literature reviews compiling academic research on G2V (Grid-to-Vehicle) and V2G (Vehicle-to-Grid) Technologies [7], [8], [9], [10], [11], [12], [13], steps to be taken for the development of V2G technology, including policy regulations [14], research aimed at resolving the range issue of electric vehicles, efforts to shorten charging times, studies on the criteria for selecting the locations of charging stations, advances in battery technology, research on the electric motors used in electric vehicles, studies on the microprocessors found in electric vehicles and charging stations, V2G studies focusing on the supportive impact of electric vehicles on the grid, instead of being a load, and the economic gains for the electric vehicle user, advantages in the energy system and disadvantages in the case of unplanned charging [15], [16], [17], [18], [19], [20], [21], [22], [23], [24], [25], [26], [27], [28], [29], [30], [31], [32], [33], [34], implementations of V2G technology [35], [36] etc. These areas of research have collectively inspired many dimensions of electric vehicle technology.

Although the electronic equipment in electric vehicles causes some issues in the grid, there are also solutions to these problems. The power electronics equipment in electric vehicles, the charging times, the differences in power values, and the uncertainties in the charging locations affect the stability of the power system. If electric vehicles are charged by drawing power from the grid in an unplanned manner, it causes instability in the grid voltage. To eliminate this negative effect, the location and power of electric charging stations should be planned considering the total load profile in the network structure of the energy grid. The excess/deficiency in the power drawn from the grid and the amount of energy produced in the system causes deviations in the grid frequency. If more power is needed than the existing energy supply in the grid, there will be a drop in grid frequency; if more energy is supplied than the demanded power, there will be an increase in grid frequency. Small-scale fluctuations occur in the grid due to changes in the energy consumption/production values

of electric vehicles and the amount of energy produced in the grid. If these fluctuations are not controlled, they may cause aging in the units of the energy system, leading to sudden outages in the grid. Planned control charging and strategies for load management should be developed against such adverse effects.

Electric vehicles and charging stations contain a lot of electronics. The electronic equipment gives electric vehicles and charging stations a nonlinear characteristic, causing harmonics in the current drawn from the grid. Current harmonics lead to overheating of components/equipment in electric vehicles and charging stations and reduce their lifespan. When electric vehicles draw power from the grid, the main voltage drops, and disconnecting them causes a voltage rise. This situation damages circuit equipment. When electric vehicles are loaded on a single phase of the grid, unbalanced loading occurs. This causes different amplitude values in the three phases of the grid, leading to overheating of protective equipment on the phases. Wide-area controls should be implemented in the grid against such adverse effects, and harmonic filtering systems should be used. Many electric vehicles connected to the grid as a load will require additional power from the grid, necessitating extra energy production. This situation will lead to overloading of system connection elements and a reduction in transformer lifespan. Load management strategies should be developed against such adverse effects, coordinated charging applications should be established, and distributed charging systems should be created in the grid.

Electric vehicles also provide positive contributions to the grid. The amount of energy drawn from the grid varies throughout the day. With energy management, the energy demand that may occur during high peak times can be spread over time, thus managing the grid loads, supporting renewable energy sources, increasing energy efficiency, improving the system power factor, and achieving energy savings. The stored energy in electric vehicles can be supplied to the grid during high demand times and they can be charged when the demand is low. When there is an energy flow as a fleet of vehicles, it will have a relieving effect on the grid. This also contributes to the efficient use of energy. Balancing supply and demand will support keeping the grid frequency stable. The integration of electric vehicles into the grid, with filtering and reactive power compensation circuit elements for improving harmonics and power factor, contributes to improving the power quality of the grid.

Electric vehicles integrated into the grid both in V2G (discharge mode) and G2V (charge mode) situations assist the grid as both producers and consumers. Energy planning can be done by processing the data obtained from electric vehicles and the grid through the network. Assigning the electric vehicle as a production unit like an energy storage unit when consumption is high and as a grid load when energy demand is low can support grid stability. The planning should consider the times when the electric vehicle will be used for driving, the amount of energy it will consume, its waiting times in parking areas, and its charging status while parked.

II. MATERIALS AND METHOD

A. 5G SYSTEM PERFORMANCE

The development process in 5G communication has culminated with the works of Claude E. Shannon (Shannon

Theory), Robert G. Gallager (Low-Density Parity-Check Code), and most recently Erdal Arkan (Polar Coding). The transition to 5G was achieved through the test studies conducted in the laboratory environment by Erdal Arkan related to polar coding.

Polar coding is an algorithm that ensures secure and fast data transmission in a noisy environment. It significantly enhances 5G communication performance by minimizing the losses experienced in communication due to noise. [37]

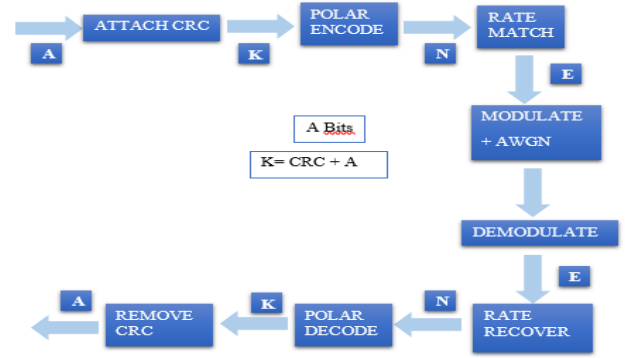


Fig. 1 5G Communication Topology

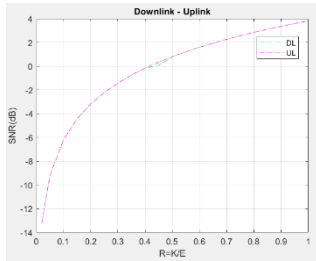
In 5G communication, the data in bits transmitted by the sender is first encrypted through polar coding to ensure it is sent with minimal errors and then passed on to modulation. With modulation, the data is superimposed on a much higher frequency carrier signal to be sent over long distances. Subsequently, noise that may exist in the environment is introduced into the process, and demodulation is performed in the channel to remove the modulation. Finally, the encrypted data is decrypted and the final data is transmitted to the receiver. (Figure 1)

A simulation study was conducted in MATLAB to analyze the performance of data flow with polar coding. The data (A) entering polar coding, when following the flow shown in Figure 2, was analyzed in terms of the variation in SNR (dB) noise value depending on the $R=K/E$ ratio, both in the downlink and uplink directions. The $R=K/E$ ratio was examined separately for downlink and uplink directions, increasing from approximately 0 to 1 in increments of 0.05, and the data flows were analyzed individually.

In the downlink and uplink directions, the value A was kept as a fixed bit value with intermittent increments. In the downlink direction, a 24-bit CRC was added, and in the uplink direction, an 11-bit CRC was added to form the K value. The E value was adjusted based on the increase in the R value. The N polar code value was kept constant at 128. The SNR (dB) noise value exhibited a logarithmic change, ranging from approximately -13 to +3.8. (Graph 1)

A	DL (DOWNLINK) CRC=24 (A+CRC=K)						UL (UPLINK) CRC=11 (A+CRC=K)						
	N	K	E	K/E	SNR (dB)	BLER	BER	K	E	K/E	SNR (dB)	BLER	BER
24	128	48	2400	0	-13,179	0	0	35	1750	0	-13,179	0	0
26	128	50	1000	0,1	-9,2	0	0	37	740	0,1	-9,2	0	0
28	128	52	520	0,1	-6,1897	0	0	39	390	0,1	-6,1897	0	0
30	128	54	360	0,2	-4,4288	0	0	41	272	0,2	-4,4076	0,1	0,033
32	128	56	280	0,2	-3,1794	0	0	43	216	0,2	-3,1996	0	0
34	128	58	232	0,3	-2,2103	0	0	45	180	0,3	-2,2103	0,2	0,094
36	128	60	200	0,3	-1,4185	0,1	0,058	47	158	0,3	-1,4553	0,1	0,039
38	128	62	178	0,3	-0,77	0	0	49	140	0,4	-0,749	0	0
40	128	64	160	0,4	-0,1691	0,1	0,038	51	126	0,4	-0,1177	0,1	0,058
42	128	66	146	0,5	0,09069	0,2	0,05	53	118	0,4	0,33424	0,1	0,038
44	128	68	136	0,5	0,8	0,3	0,091	55	110	0,5	0,8	0,1	0,05
46	128	70	128	0,5	1,1892	0,3	0,117	57	104	0,5	1,1987	0,1	0,046
48	128	72	120	0,6	1,5918	0,3	0,121	59	98	0,6	1,6066	0,4	0,196
50	128	74	114	0,6	1,9336	0,5	0,142	61	94	0,6	1,9323	0,3	0,072
52	128	76	110	0,7	2,2045	0,4	0,14	63	90	0,7	2,2613	0,4	0,131
54	128	78	104	0,8	2,5609	0,1	0,044	65	86	0,8	2,5944	0,6	0,219
56	128	80	100	0,8	2,8412	0,8	0,273	67	84	0,8	2,8283	0,5	0,188
58	128	82	96	0,9	3,1257	0,9	0,397	69	82	0,8	3,0607	0,7	0,181
60	128	84	94	0,9	3,3218	0,8	0,28	71	80	0,9	3,292	0,9	0,288
63	128	87	92	0,9	3,5676	0,9	0,357	74	78	0,9	3,5817	0,9	0,232
65	128	89	90	1	3,7618	1	0,282	76	76	1	3,8103	0,9	0,242

Table 1. 5G Communication Performance



Graph 1. SNR (dB) – K/E Change

B. V2G Analysis

An electric vehicle integrated into the grid with V2G (discharge mode) and G2V (charge mode) can act as both a producer and a consumer. During the day, it can draw energy from or supply energy to the grid depending on the energy prices in the electricity market and the supply/demand of energy. In situations where energy demand is low and energy prices are low during the day, it acts as a consumer in G2V (charge mode). When energy demand is high and energy prices are high, it supplies the energy stored in its battery to the grid in V2G (discharge mode). To visualize the contribution of electric vehicles to the grid in V2G (discharge mode) and the load they create in G2V (charge mode), a simulation was created using MATLAB Simulink by modeling a section of the grid. The system analysis was carried out based on the number of vehicles at the charging station. The analyzed section of the grid consists of five parts. In a 60Hz system, a 15MW diesel power plant acts as the central power station, and the energy needed by the grid is supplied by a 4.5MW wind power plant (WPP) and an 8MW solar power plant (SPP) as renewable energy sources that support the central power station. On the energy consumption side, there is a residential load of 10MW with a power factor of 0.15, an industrial load of 0.16 MVA, and a total electric vehicle load of 8MW with 200 vehicles (200*0.4MW). The analysis was performed using MATLAB Simulink (Figure 2).

To reflect reality, the electric vehicles were divided into 10 charging stations with a variable number of vehicles at each station (Figure 3).

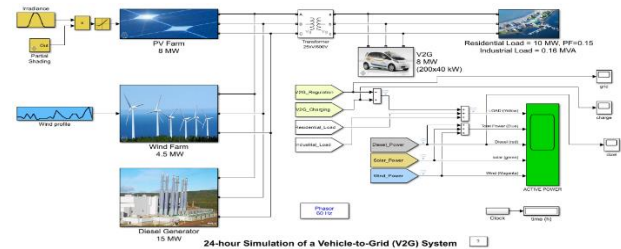


Fig. 2 Sampled System

In the analysis, the WPP and SPP data were based on daily meteorological data (wind speed, humidity, sunlight angle, sunlight duration, etc.), and the amount of energy they could produce hourly over 24 hours was considered constant. In this system example, the diesel power plant acts as the central power station, meeting demand with energy production data that varies according to the user's consumption data at hourly intervals throughout the day. The analysis compared the diesel power plant's production data based on the electric vehicle consumption data, assuming the WPP, SPP, residential load, and industrial load were fixed variables. In the analysis, for 200 vehicles across 10 charging stations: in case 1, with 60 vehicles charging (30%) and 140 vehicles feeding the grid (70%); in case 2, with 120 vehicles charging (60%) and 80 vehicles feeding the grid (40%); and in case 3, with 180 vehicles charging (90%) and 20 vehicles feeding the grid (10%), it was observed that electric vehicles functioned as both consumers and energy storage units at varying times of the day. They were able to trade energy by taking advantage of fluctuating energy prices and could contribute to central power plants and renewable energy production sources during times of high demand. The most important assumption in the

analysis was that a communication network and infrastructure based on 5G technology existed, the electric vehicles had G2V and V2G capabilities, and the sampled grid section was part of a smart grid connection.

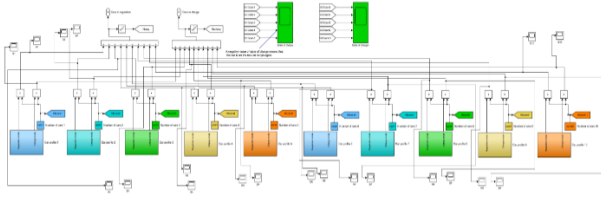
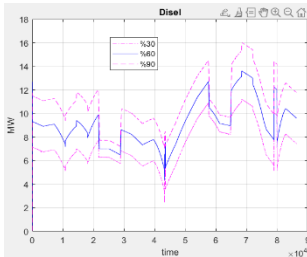


Fig. 3 Electric Vehicles Connected to Charging Stations

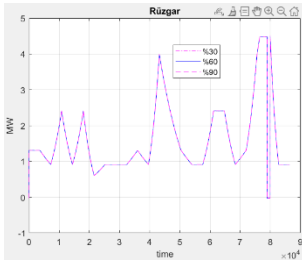
CHARGING STATION	1. CASE (%30 C / 70% D)		2. CASE (%60 C / 40% D)		3. CASE (%90 C / 10% D)	
	G2V	V2G	G2V	V2G	G2V	V2G
1.	21	0	42	0	63	0
2.	15	0	30	0	45	0
3.	6	0	12	0	18	0
4.	12	0	24	0	36	0
5.	6	0	12	0	18	0
6.	0	49	0	28	0	7
7.	0	35	0	20	0	5
8.	0	14	0	8	0	2
9.	0	28	0	16	0	4
10.	0	14	0	8	0	2
TOTAL	60	140	120	80	180	20

Table 2. Vehicles in V2G – G2V Charging Stations for Three Scenarios

The change in total power drawn from the grid by the diesel power plant, wind power plant, solar power plant, and electric vehicles was monitored for the three different scenarios.



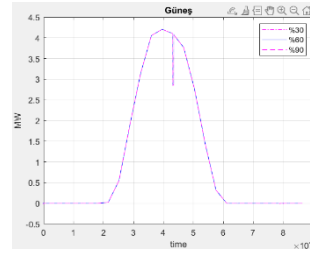
Graph 2. Diesel Power Plant Energy Production



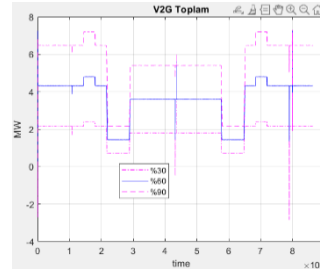
Graph 3. WPP Energy Production

In scenarios with 30% G2V – 70% V2G (1st case), 60% G2V – 40% V2G (2nd case), and 90% G2V – 10% V2G (3rd case), it was observed that the diesel power plant worked harder to meet the demand in the grid when the number of vehicles

drawing energy for charging increased. Conversely, when the number of vehicles feeding the grid in V2G mode increased, the diesel power plant operated to meet the lower demand in the grid (Graph 2).



Graph 4. SPP Energy Production



Graph 5. EV Cumulative Impact

Since the meteorological data was assumed to be constant in all three scenarios, there was no change in the energy production of the wind power plant and solar power plant over 24 hours (Graph 3) (Graph 4).

In all three scenarios, when the cumulative effect of the G2V and V2G modes of the electric vehicles on the total energy drawn from the grid was monitored, an increase in the total energy drawn from the grid was observed as the number of charging vehicles increased (Graph 5).

III. RESULTS

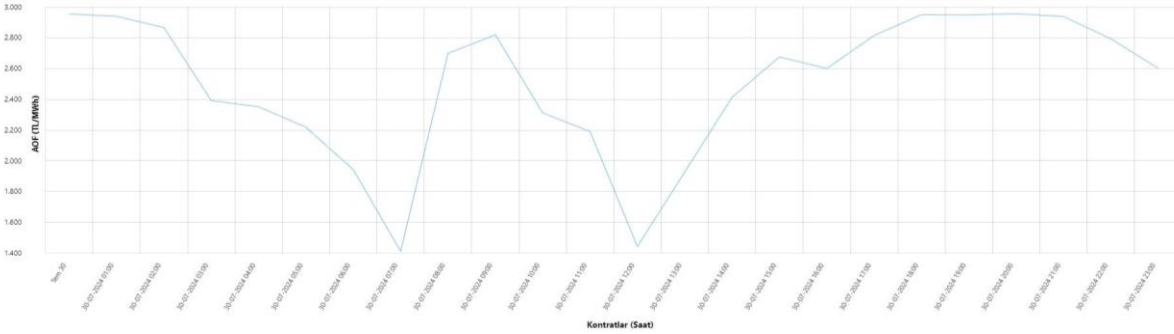
In the analysis study, considering the impact of electric vehicles on the grid in G2V and V2G modes, depending on the vehicle density at charging stations, an interpretation based on the pricing mechanism in the energy market during the day will help better understand the decision-making process of an electric vehicle as a producer/consumer. Here, the decision is influenced not only by energy market pricing but also by the equipment and features of the electric vehicle, and most importantly, by the battery's aging characteristics in G2V and V2G modes, as well as the vehicle's usage during the day. Therefore, it is necessary to examine the cumulative effect of the owner's preferences and the renewal of the vehicle's equipment by including detailed variables such as these in the process.

IV. DISCUSSION

Energy Market Operations Inc. (EPIAŞ) data has been used to make interpretations based on the daily market pricing in the energy market, disregarding the detailed variables affecting the choice.

Through the "Transparency Platform" created by EPIAŞ, it is possible to access the pricing curves formed in the energy market on daily, weekly, monthly, and yearly bases. Here, the pricing curve formed during the day is in TL/MWh based on

the weighted average price. Graph 6 shows the pricing curve that occurred on 30.07.2024.



Graph 6. EPIAŞ GIP (Intraday Market) Weighted Average Price on 30.07.2024

According to EPIAŞ data on 30.07.2024, an electric vehicle can achieve a high profit in V2G (discharge mode) at an energy price peak of 2,955 TL/MWh (at the hours of 00:00-01:00-18:00-19:00-20:00-21:00), while it can benefit from low prices in G2V (charge mode) at an energy price range of 1,411 TL/MWh - 1,441 TL/MWh (at the hours of 07:00-12:00). Assuming the highest and lowest pricing and that the electric vehicle returns to a charged state once, a profit of 1,544 TL/MWh (2,955-1,411) can be achieved. If this situation is repeated twice during the day (charge-discharge), the profit can be doubled.

V. CONCLUSION

With globalization and technological developments, electricity consumption and the number of electricity consumers have increased. Environmental needs are as indispensable in life as energy needs. Environmental concerns and the depletion of energy resources have led countries to develop strategies focused on renewable energy sources and maximizing the efficiency of the energy produced. In this direction, academic studies that support each other and pave the way for future research have been guiding.

Technological advancements in charging technologies, battery capacity and sizes, maximum range at full charge, charging time, and easy access to charging stations will contribute to the increasing market share of electric vehicles. Additionally, electric vehicles will help reduce environmental pollution by replacing internal combustion engines.

Within the scope of this study, the potential negative impacts of V2G technology on the grid, as well as proposed solutions, and the contributions of V2G technology to the grid and vehicle owners, have been emphasized. Through simulations, the contribution that vehicles equipped with V2G technology can make to the economy and meeting energy demand while remaining idle at charging stations has been demonstrated in a case study.

V2G technology, smart grids, and 5G communication are systems open to development that support each other. Each stage of development in these systems will support employment processes and provide different types of employment opportunities. The most significant development will be the efficient use of energy, where individuals who are consumers within the energy system during the day will support the grid as energy producers, leading to the consumption of fewer fossil-based energy sources by central

power stations. Another important development is that consumers will be able to cover their transportation costs more cheaply by taking advantage of low energy prices at different times of the day.

ACKNOWLEDGMENT

I would like to thank my valuable family, who have always supported me, for their unwavering support.

REFERENCES

- [1] The IEA website. [Online]. (2024) Global electric car stock 2013-2023 Available: <https://www.iea.org/data-and-statistics/charts/global-electric-car-stock-2013-2023>
- [2] The IEA website. [Online]. (2024) Electric car sales 2012-2024 Available: <https://www.iea.org/data-and-statistics/charts/electric-car-sales-2012-2024>
- [3] The IEA website. [Online]. (2024) Publicly installed accessible light-duty vehicle charging points by slow chargers and region, 2015-2023 Available: <https://www.iea.org/data-and-statistics/charts/publicly-installed-accessible-light-duty-vehicle-charging-points-by-slow-chargers-and-region-2015-2023>
- [4] The IEA website. [Online]. (2024) Publicly installed accessible light-duty vehicle charging points by fast chargers and region, 2015-2023 Available: <https://www.iea.org/data-and-statistics/charts/publicly-installed-accessible-light-duty-vehicle-charging-points-by-fast-chargers-and-region-2015-2023>
- [5] The IEA website. [Online]. (2024) Global EV Outlook 2024 Available: <https://www.iea.org/reports/global-ev-outlook-2024>
- [6] W. Kempton and S.E. Letendre "Electric vehicles as a new power source for electric utilities" Transportation Research Part D: Transport and Environment, Pages 157-175, 1997
- [7] F. Karapınar "Integration of Electric Vehicles in Smart Grids and V2G Applications From Vehicle to Grid" M. Eng. Thesis. Erciyes University, Kayseri, Turkey 2023
- [8] M.A Hassan., E Abdullah., N. H. K. Ali N., N. M. Hidayat, M. Umair and A.Johari "Vehicle-to-grid system optimization for electric vehicle – a review" 6th International Conference on Clean Energy and Technology 2023 (CEAT 2023), Penang, Malaysia, 2023
- [9] M. Wan, H. Yu, Y. Huo, K. Yu, Q. Jiang and G. Geng "Feasibility and Challenges for Vehicle-to-Grid in Electricity Market: A Review" Energies 17, no. 3: 679, 2023
- [10] Y. Cao "Study on the interaction of vehicle-to-grid and its impact on power quality of electric grid" The 2023 International Conference on Mechatronics and Smart Systems, Oxford, UK, 2023
- [11] B. Bibak and H.Tekiner-Mogulkoç "A comprehensive analysis of Vehicle to Grid (V2G) systems and scholarly literature on the application of such systems" Renewable Energy Focus, 2021
- [12] A. Alsharif, C.W. Tan, R. Ayop, A. Dobi and K.Y. Lau "A comprehensive review of energy management strategy in Vehicle-to-Grid technology integrated with renewable energy sources" Sustainable Energy Technologies and Assessments, 2021
- [13] M. Sarp and N. Altın "Review on Vehicle-to-Grid Systems: The Most Recent Trends and Smart Grid Interaction Technologies" Gazi University Journal of Science, vol.33, no.2, pp.394-411, 2020
- [14] B.K.Sovacool, J.Kester, L. Noel and G.Z. Rubens "Actors, business models, and innovation activity systems for vehicle-to-grid (V2G) technology: A comprehensive review" Renewable and Sustainable Energy Reviews, 2020

- [15] A.S. Türkoğlu “Optimal Management of Large-Scale V2G in Different Sizes of Distribution System Environments” M. Eng. Thesis. Yıldız Technical University, İstanbul; Turkey, 2023
- [16] A.K. Aktar “The Most Economical Use of Vehicle-To-Grid Charging Technology in Electricity Distribution Networks” PhD Thesis. Muğla Sıtkı Koçman University, Turkey, 2023
- [17] M. Yavuz “Multi-Agent Reinforcement Learning Base Energy Management With P2P/V2G” M. Eng. Thesis. İstanbul Okan University, İstanbul, Turkey, 2023
- [18] K. Şahinkaya “Monte Carlo Based Control Algorithm for Economic Feasibility of V2G Applications” M. Eng. Thesis. Middle East Technical University, Ankara, Turkey, 2019
- [19] J. Waldron, L. Rodrigues, S. Deb, M. Gillott and S. Naylor “Exploring Opportunities for Vehicle-to-Grid Implementation through Demonstration Projects”, *Energies*, 2024
- [20] J.Li and A.Li “Optimizing Electric Vehicle Integration with Vehicle-to-Grid Technology: The Influence of Price Difference and Battery Costs on Adoption, Profits, and Green Energy Utilization” *Sustainability* 16, no. 3: 1118. 2024
- [21] M. Umair, N. M. Hidayat, N.H.N. Ali, E. Abdullah, A.R. Johari and T. Hakomori “The effect of vehicle-to-grid integration on power grid stability: A review” 6th International Conference on Clean Energy and Technology 2023 (CEAT 2023), Penang, Malaysia, 2023
- [22] Y.R. Rodrigues, A.C.Z. Souza and P.F. Ribeiro “An inclusive methodology for Plug-in electrical vehicle operation with G2V and V2G in smart microgrid environments” *International Journal of Electrical Power & Energy Systems* Volume 102, P 312-323, 2018
- [23] Y. Zheng, Y. Shanga, Z. Shao and L. Jiana “A novel real-time scheduling strategy with near-linear complexity for integrating large-scale electric vehicles into smart grid” *Applied Energy* Volume 217, p 1-13, 2018
- [24] J. Lin, B. Xiao., H. Zhang, X. Yang and P. Zhao “A novel underfill-SOC based charging pricing for electric vehicles in smart grid” *Sustainable Energy, Grids and Networks*, 2021
- [25] R. Yapıcı, D. Güneş and N., Yörükleren “Possible Effects of Electric Charging Stations on the Distribution Network” *Chamber of Electrical Engineers*, 2017
- [26] C. Heilmann and G. Friedl “Factors influencing the economic success of grid-to-vehicle and vehicle-to-grid applications—A review and meta-analysis” *Renewable and Sustainable Energy Reviews*, 2021
- [27] M. Nurmuhammed and T. Karadağ “A Review on Locating the Electric Vehicle Charging Stations and Their Effect on the Energy Network” *Gazi University Journal of Science*, 2021
- [28] S.R. Etesami, W. Saad, N.B. Mandayam and H.V. Poor “Smart routing of electric vehicles for load balancing in smart grids” *Automatica* 2020
- [29] Z. Liao, M. Taiebat and M. Xu “Shared autonomous electric vehicle fleets with vehicle-to-grid capability: Economic viability and environmental co-benefits” *Applied Energy*, 2021
- [30] M. Inci, Ö. Çelik, A. Lashab, K.Ç Bayındır, J.C. Vasquez and J.M. Guerrero J.M. “Power System Integration of Electric Vehicles: A Review on Impacts and Contributions to the Smart Grid” *Applied Sciences* 14, 2024
- [31] A. Srivastava, M. Manas and R.K. Dubey R.K. “Electric vehicle integration’s impacts on power quality in distribution network and associated mitigation measures: a review” *Journal of Engineering and Applied Science* 70, 2024
- [32] F.B. Özkanlı and Z. Demir “Integration of Electric Vehicles Into the Smart Grid” *Eskisehir Technical University Science and Technology Journal*, 2021
- [33] I. Pavić, H. Pandžić and T. Capuder “Electric vehicle based smart e-mobility system – Definition and comparison to the existing concept” *Applied Energy*, 2020
- [34] H.F. Feshki Farahani “Improving voltage unbalance of low voltage distribution networks using plug-in electric vehicles” *Journal of Cleaner Production* V. 148 p. 336-346, 2017
- [35] K. Zagrajek, M. Kłos, D.D. Rasolomampionona, M. Lewandowski and K. Pawlak “The Novel Approach of Using Electric Vehicles as a Resource to Mitigate the Negative Effects of Power Rationing on Non-Residential Buildings” *Energies* 17, 2024
- [36] S. Adak, H. Cangi, R. Kaya and A.S. Yilmaz “Effects of Electric Vehicles and Charging Stations on Microgrid Power Quality”, *Gazi University Journal of Science*, 2022
- [37] E. Arıkan “Channel polarization: A method for constructing capacity-achieving codes for symmetric binary-input memoryless channels” *IEEE Transactions on Information Theory* vol. 55, no. 7, pp. 3051-3073, 2009
- [38] The EPIAŞ website. [Online]. (2024)GIP Weighted Average Price Available:<https://seffaflik.epias.com.tr/electricity/electricity-markets/intraday-market-idm/idm-weighted-average-price>

The Effects of Environmental Factors on Solar Power Plants: The Case of MEYSU Factory

Fırat ÖZBAY^{1*}, Ali DURMUŞ¹

¹Elektrik Elektronik Mühendisliği, Kayseri Üniversitesi, Kayseri, Türkiye
*(firat.ozbay@meysu.com.tr)

Abstract– Today, the use of fossil fuels to meet energy needs has become unsustainable due to their limited resources and environmental impacts. This situation has heightened the importance of clean, eco-friendly, and sustainable alternatives, particularly renewable energy sources such as solar, wind, and biomass. Solar energy is the most widespread and effective among these alternatives. The efficiency of solar panels determines the success in converting sunlight falling on the panel surface into electricity. Generally, the efficiency of solar panels ranges between 15% and 20%, while in 2021, the best-performing panels were slightly below 23%. This efficiency depends on the type, design, and quality of the cells used, as well as the quality of the glass and other components. The collection and storage efficiency of a solar cell relies on the design of transparent conductors and the thickness of the active layer. Additionally, panel cleanliness is an important factor. For example, the rooftop solar energy system of the MEYSU factory, with an installed capacity of 2000 kW, meets approximately 25% of the company's energy needs. In this study, electricity production in conditions where the panels were dirty was compared with production values after cleaning, taking into account the environmental factors around the factory. The obtained data showed an increase of approximately 17.38% in electricity production by cleaning the panels. Thus, regularly cleaning the panels at certain intervals is very important for efficiency in solar power plants.

Keywords – Solar power plant, environmental factors, efficiency, panel cleaning, renewable energy.

Güneş Enerji Santrallerinde Çevresel Faktörlerin Etkileri MEYSU Fabrikası Örneği

Özet – Günümüzde, enerji ihtiyacının karşılanmasında fosil yakıtların kullanımı sınırlı kaynakları ve çevresel etkileri nedeniyle sürdürülemez hale gelmiştir. Bu durum, temiz, çevreci ve sürdürülebilir alternatiflerin, özellikle güneş, rüzgâr ve biyokütle gibi yenilenebilir enerji kaynaklarının önemini artırmıştır. Güneş enerjisi, bu alternatifler arasında en yaygın ve etkili olanıdır. Güneş panellerinin verimliliği, panel yüzeyine düşen güneş ışığının elektriğe dönüşümündeki başarıyı belirler. Genel olarak, güneş panellerinin verimliliği %15 ila %20 arasında değişirken, 2021'de en iyi performans gösteren paneller %23'ün biraz altında kalmıştır. Bu verimlilik, kullanılan hücre tipine, tasarımına ve kalitesine, cam ve diğer bileşenlerin niteliğine bağlıdır. Bir güneş hücresinin toplama ve depolama verimliliği, şeffaf iletkenlerin tasarımı ve aktif katman kalınlığına bağlıdır. Ayrıca, panel temizliği de önemli bir faktördür. Örneğin, MEYSU fabrikasının çatı güneş enerji sistemi, 2000 KW kurulu güç ile firmanın enerji ihtiyacının yaklaşık %25'ini karşılamaktadır. Bu çalışmada fabrika etrafındaki çevresel faktörler göz önüne alınarak panellerin kirli olduğu durumdaki elektrik üretimi ile temizlendikten sonraki üretim değerleri karşılaştırmalı olarak analiz edilmiştir. Elde edilen veriler panellerin temizlenmesi ile yaklaşık %17.38'lik bir elektrik enerjisi üretiminde artış elde edilmiştir. Böylelikle güneş enerji santrallerinde özellikle panellerin belli periyotlarla temizlenmesi verimlilik açısından oldukça önemlidir.

Anahtar Kelimeler – Güneş enerji santrali, çevresel faktörler, verimlilik, panel temizliği, yenilenebilir enerji.

I. GİRİŞ

Günümüzde, küresel enerji talebinin artmasıyla birlikte, fosil yakıtlara dayalı geleneksel enerji kaynaklarının sınırlı doğası ve çevresel etkileri giderek daha fazla tartışma konusu olmaktadır. Bu durum, temiz, çevreci ve sürdürülebilir enerji kaynaklarına yönelik bir talep artışına yol açmıştır. Bu alternatif kaynakların başında yenilenebilir enerji gelmektedir. Yenilenebilir enerji, doğal kaynaklardan elde edilen ve sonsuz döngüsel süreçlerle yenilenebilen enerji türlerini ifade eder. Bu tür enerji kaynakları, çevresel etkileri

minimal seviyede tutarak enerji ihtiyacını karşılar ve fosil yakıtların aksine sınırsız bir potansiyele sahiptir [1].

Alternatif enerji kaynakları arasında güneş enerjisi, özellikle ön plana çıkmaktadır. Güneş enerjisi, dünya üzerinde mevcut olan en büyük ve en temiz enerji kaynağıdır. Güneşten gelen ışığın ve ısı enerjisinin kullanılmasıyla elde edilen güneş enerjisi, doğal olarak yenilenebilir ve sınırsızdır. Güneş ışığının fotovoltaik (PV) hücreler aracılığıyla elektriğe dönüştürülmesiyle güneş panelleri enerji üretimine katkı sağlar. Bu süreç, çevre dostu olması ve güneşin her yerde ve

üretim tecrübesi; ailenin ilk kuşak temsilcisi olan merhum Osman Güldüoğlu'nun reçel, helva, akide şekeri ve lokum üretimine başladığı 1948 yılına dayanmaktadır.

2024 yılı Ocak–Ağustos ayları arası toplam elektrik tüketimimiz 7.020.759,90 KWh olup, ortalama aylık elektrik tüketimi 877.596,23 KWh'tir. Tesis çatı üzeri 2000 KW GES kurulu güce sahiptir. Bu GES kurulu güç ile son bir yılda 2.415.235 KWh elektrik üretimi sağlanmıştır.

Güneş paneli temizliği, her mevsim başlangıcında ve düzenli aralıklarla yapılmalıdır. Temizlik için özel solar fırçalar kullanılmalı ve en iyi sonuç için ultra deiyonize saf su veya alkol bazlı temizleyiciler tercih edilmelidir. Saf su, çözünmüş maddelerden arındırıldığı için panellerin temizliği için idealdir. Panel temizliği yapılmaması durumunda üretimde azalma ve panellerde bozulmalar olası durumdur. Tablo 1'de Meysu fabrikasına ait GES'in verim tablosu verilmiştir.

Tablo 1. Meysu Çatı Üzeri Ges İle 2023 Yılı Üretim Verim Tablosu

Ges Enerji Üretim		Aktif Tüketilen Enerji
Ay / Yıl (2023)	Üretim KWh	Miktar KWh
Mart	131894	640478,7
Nisan	192035	427634,4
Mayıs	248415	539883,6
Haziran	249340	517741,5
Temmuz	299847	662558,7
Ağustos	254232	809928,9
Eylül	227936	685501,2
Ekim	173608	567318
Kasım	106162	714688,2
Aralık	92273	652733,1
TOPLAM	1975742	6218466,3
Ges Enerji Üretim Ve Aktif Tüketilen Enerji Toplamı ; 8194208		
Ges enerji üretimimizle toplam enerji tüketimimizin %24,11 ile yaklaşık %25'ni karşılamaktadır.		

Solarrelax | Ges Takip Sistemi ile alınan üretim verileri temizlik öncesi ile temizlik sonrası üretim verileri arasında yaklaşık %17.38 verim sağlanmıştır.

Table 2. Meysu Ges Temizlik Öncesi Üretim Verileri

ÜRETİM TARİHLERİ		TOPLAM ÜRETİM
BAŞLANGIÇ	BİTİŞ	
1.03.2023	30.06.2023	821.741 KWh

Table 3. Meysu Ges Temizlik Sonrası Üretim Verileri

ÜRETİM TARİHLERİ		TOPLAM ÜRETİM
BAŞLANGIÇ	BİTİŞ	
30.06.2023	31.10.2023	964.640 KWh

IV. SONUÇ

Çevresel faktörler ve hava koşulları, çatı üzeri GES'lerin performansını doğrudan etkileyen önemli unsurlardır. Bu etkileri minimize etmek için doğru sistem tasarımı, düzenli bakım ve temizlik, uygun panel ve ekipman seçimi, ve çevresel koşulların sürekli izlenmesi gerekmektedir. Gölgeleme analizleri ve hava koşullarına dayanıklı ekipman kullanımı, GES'in verimliliğini artırmada önemli rol oynamaktadır.

KAYNAKLAR

- [1] C. E. Özsoy, and D. İ. N. Ç. Ahmet, "Sürdürülebilir kalkınma ve ekolojik ayak iz," *Finans Politik ve Ekonomik Yorumlar*, vol. 619, pp. 35-55, 2016.
- [2] A. Muhammadi, M. Wasib, S. Muhammadi, S. R. Ahmed, A. H. Lahori, S. Vambol, and O. Trush, "Solar Energy Potential in Pakistan: A Review." *Proceedings of the Pakistan Academy of Sciences: B. Life and Environmental Sciences*, vol. 61, pp.1-10, 2024.
- [3] M. E. Bilgili, and A. Akyüz, "Çukurova Koşullarında Tarımsal İşletme Çatılarında Fotovoltaik Sistemlerin Tekno-Ekonomik Yönden Tasarımı," *Toprak Su Dergisi*, pp. 61-69, 2019.
- [4] B. Y. Liu, and R. C. Jordan, "The interrelationship and characteristic distribution of direct, diffuse and total solar radiation," *Solar Energy*, vol. 4(3), pp. 1-19, 1960.
- [5] D. H. Li, G. H. Cheung, and J. C. Lam, "Analysis of the operational performance and efficiency characteristic for photovoltaic system in Hong Kong," *Energy conversion and management*, vol. 46(7-8), pp. 1107-1118, 2005.
- [6] Gautam, A., Hameed, S., Khalid, A., & Khan, S. A. (2012). The impact of dust on solar PV performance: Investigation on PV surface cleaning. *Solar Energy*, 85(4), pp. 1-8. <https://doi.org/10.1016/j.solener.2012.01.005>
- [7] Skoplaki, E., & Palyvos, J. A. On the temperature dependence of photovoltaic module electrical performance: A review of efficiency/power correlations. *Solar energy*, 83(5), pp. 614-624, 2009.
- [8] Duffie, J. A., & Beckman, W. A. *Solar engineering of thermal processes*. John Wiley & Sons. 2013.
- [9] Gupta, R., Yadav, S., & Khatri, S. K. Impact of environmental factors on performance of solar photovoltaic module: A review. *Journal of Solar Energy Research*, 5(1), pp. 45-55, 2019. <https://doi.org/10.1016/j.jsr.2019.01.005>
- [10] Chow, T. T. A review on photo voltaic/thermal hybrid solar technology. *Applied Energy*, 87(2), pp. 365-379, 2010.
- [11] Sayigh, A. A. M. *Solar energy engineering*. Academic Press. 1978.
- [12] Dubey, S., Sarvaiya, J. N., & Seshadri, B. Temperature dependent photovoltaic (PV) efficiency and its effect on PV production in the world—a review. *Energy Procedia*, 33, pp. 311-321, 2013.
- [13] Luque, A., & Hegedus, S. (Eds.). *Handbook of Photovoltaic Science and Engineering*. John Wiley & Sons. 2013.
- [14] Skoplaki, E., & Palyvos, J. A. On the temperature dependence of photovoltaic module electrical performance: A review of efficiency/power correlations. *Solar Energy*, 83(5), pp. 614-624, 2009.
- [15] Parida, B., Iniyani, S., & Goic, R. A review of solar photovoltaic technologies. *Renewable and Sustainable Energy Reviews*, 15(3), pp. 1625-1636, 2011.
- [16] Dunlop, J. P. *Photovoltaic systems*. American Technical Publishers. 2012.
- [17] Carr, A. J., & Pryor, T. L. A comparison of the performance of different PV module types in temperate climates. *Solar Energy*, 76(1-3), pp. 285-294, 2004.

DC Energy Technologies: The Key to A Sustainable Tomorrow?

Hatice Aydın^{1*}, Muciz Özcan²

¹Electrical and Electronics Engineering Department, Necmettin Erbakan University, Konya, Türkiye

²Electrical and Electronics Engineering Department, Necmettin Erbakan University, Konya, Türkiye

*23821113001@ogr.erbakan.edu.tr) Email of the corresponding author

Abstract – Development of semiconductor technology, the introduction of computers, smart devices and many household appliances into our lives, especially in the last 20 years, the increase in interest in renewable energy sources, the density of the population in the grid and the increase in the number of electric vehicles have shaken the throne of AC, which has been in use for more than a century. DC is making a strong comeback with these developing technologies. DC-powered digital consumer devices today account for one-fifth of total power consumption. It is projected that in the next 20 years, 50 percent of our total loads will consist of DC consumption, an increase with even more accelerating momentum than expected. In addition, the importance of energy saving, is increasing day by day. Increasing number of devices that produce and use DC, there is a great opportunity to save energy. By distributing DC power to DC devices instead of converting it to AC along the way, it is possible to avoid the significant energy losses that occur each time electricity is converted. In this paper, DC from the past to the future, technologies using DC and its advantages over AC are analyzed, considering the above-mentioned developments.

Keywords – AC versus DC, Advantages of DC, DC Energy, DC Technologies, Energy Sustainability

I. INTRODUCTION

AC (Alternating Current) has been promoted as a superior option for power distribution and transmission ever since electricity was invented. Nonetheless, one of the pioneers of electricity, Thomas Edison, advocated for the usage of DC (Direct Current). There was no way to control and magnify the DC voltage at the load at the time. As a result, there was a significant degree of loss and voltage fluctuation at various load sites during the transfer of DC power from the generator to the load. To address this issue, Westinghouse suggested using AC distribution. Thanks to the alternating current system Tesla worked on with Westinghouse to amplify and transmit voltage over long distances, the hydraulic power of Niagara Falls was discovered and the electricity generated there was transmitted to the American continent and then to the whole world [1], [2].

Although the AC and DC power transmission paradigms clashed in the early days of the electric power system, one side seems to win because of its ability to convert voltage levels. The power system might be DC today if DC technology had been able to achieve this capability. Conversely, electromagnetic transformers provided AC the ability to change the voltage level, which gave AC the advantage in the conflict between currents. It became a medium for the generation, transmission, distribution and utilization of electrical energy in the form of residential loads [3].

AC continues to be the main power source in our electrical infrastructure, despite the fact that a lot has changed since the invention of electricity. Nonetheless, the advancement of power converters and DC energy sources has brought about a renewed interest in DC [4].

DC was forced to wait until High Voltage Direct Current (HVDC) transmission technology was developed before DC was once again included in the power grid. Reactive power losses and high electrical currents caused by line

charging/discharging were prevented, and HVDC transmission was successful. Then, DC appeared on the generating side of the electrical system in the shape of renewable energy sources, which are power generation sources driven by both environmental and economic considerations.

Power electronic DC/DC converters can increase the voltage produced by photovoltaic cells, which provide DC power directly in solar power systems. Through the development of DC/DC converters, DC has obtained transformers in the field of power electronics. DC/DC converters are intended to modify the voltage level and enable the DC voltage to be raised and lowered, whilst DC/AC inverters and AC/DC rectifiers perform the tasks of altering the kind of electricity.

As for wind power, many wind farms provide AC power, which they then must convert to DC because of frequency fluctuations. After that, this DC is delivered back into the AC power system at a steady frequency for conversion. On the side of power generation, DC is therefore present.

DC power is in high demand on the home front due to the enormous rise in contemporary electronic loads. In addition to the typical domestic electronic loads, the contemporary notion of Light Emitting Diode (LED) lighting generates an additional DC electrical energy consumer.

In addition to this, variable speed drives used in air conditioning (heating and cooling) result in the conversion of input AC power to DC, which is subsequently converted back to AC and supplied to the compressor motor. The total demand for DC power for contemporary residential buildings may surpass the demand for AC power if these loads are regarded as loads that also require DC power. The home distribution system is the only segment of the global electric power system in which DC power is not widely used in practical applications.

A study examined the energy savings of residential buildings with in-building power distribution systems that combine AC and DC power sources. According to the findings, energy

savings from DC amount to 5% of total energy consumption in the absence of battery storage in the home and 14% in the presence of storage.

A comparison between AC and DC power distribution systems is provided by another study, which points out that the advancements in DC energy sources and power electronic converters have sparked a renewed interest in DC power distribution. For varying power electronic converter efficiencies and system voltage levels, different results are shown. For very high levels of power electronic converter efficiency and at a higher voltage level than AC, the reviewers demonstrate that DC becomes superior to AC [3].

II. MATERIALS AND METHOD

A. Differences between AC and DC

AC is a form of energy in which the electric current changes direction periodically, usually in the form of a sinusoidal wave. AC voltage also has positive and negative half-waves. Care must be taken in AC circuits as the current flows in both directions.

DC is an electrical form of energy with a constant voltage level, where the direction of the electric current is always the same. DC voltage has negative and positive poles. DC always flows in the same direction. Pure DC consists of a straight line.

The main differences between DC and AC:

- Direction: In DC voltage the direction of current is constant, whereas in AC voltage it is constantly changing.
- Waveform: DC voltage has a flat waveform, AC voltage has a sinusoidal waveform.
- Conductivity: DC has better conductivity because it is unidirectional, while AC may suffer conduction loss due to its frequency.
- Power Loss: DC causes less energy loss during power transfer because it minimizes the loss due to resistances in transmission lines.

B. Systems Using DC

A centralized power grid approach supported exponential growth in the AC electricity industry as it expanded and soon reached larger communities. Even if DC use is still common today, major AC system components including transformers, transmission lines and towers, switchgear and circuit breakers, light bulbs, motors, etc. were utilized extensively. This section focuses on structures that run on DC energy.

1) Energy Storage, Distributed Generation, and Microgrids

Power grids are becoming more decentralized, with growing pressure to integrate renewable and distributed energy sources. Many of these require power electronics interfaces to connect. Fuel cells and microgrids will likely play key roles in future systems. Several renewable sources, like solar panels, naturally produce DC power. Wind turbines can be optimized by combining some capacity with power electronics, often using a DC bus. Converting DC to AC and back to DC leads to efficiency losses that could be avoided. As the grid evolves, finding ways to efficiently integrate diverse energy sources and minimize unnecessary power conversions will be increasingly important. Fig. 1 shows the converter structure in renewable energy sources. Our current AC

distribution system has almost no energy storage, but as DC energy becomes available, there will naturally be an increase in storage systems [5].

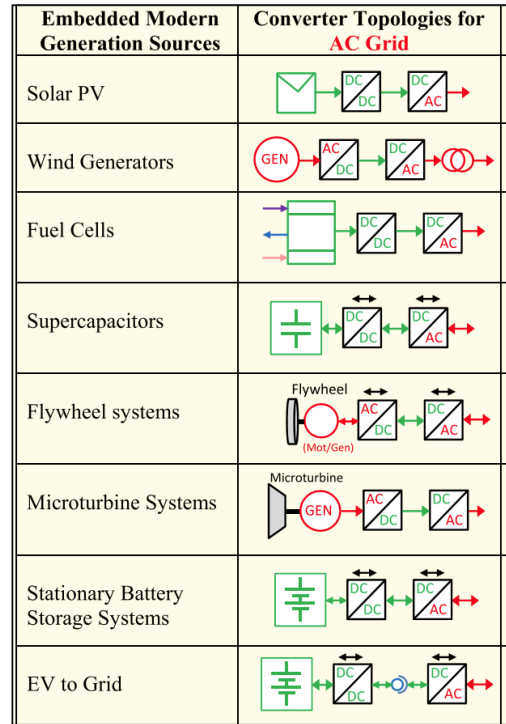


Fig. 1 Converter structure used in the connection of distributed generation plant to the AC grid

2) Electric Vehicles and Batteries

Laptops and other portable electronics are frequently used with battery chargers. This argument will also be impacted by the development of electric vehicle technology in the future. Fleets of electric vehicles not only have the potential to become substantial electricity consumers, but when these vehicles are grid-connected, their batteries can also enhance system resilience and energy storage by recharging the grid.

3) Computers, Lighting and Household Electronics

Computer servers and other electronic devices have grown to constitute substantial system loads. The way that lighting is produced is also evolving as more people pick energy-efficient substitutes for incandescent lights. A DC power supply is needed for these devices.

4) Air Conditioning (Cooling and Heating) Based on Variable Speed Drives

The AC power at the input is converted to DC and then converted back to AC and fed to the compressor motor.

5) Electrolysis Devices

DC power is required for chemical processes such as water electrolysis.

6) Ships

Currently, ships are using more and more power electronic converters. Motor control is incredibly accurate and energy-efficient when power electronic converters are used. But using rectifiers that are Diode Front Ends (DFEs) can cause harmonic distortion issues in the AC bus when converters are employed. There is no harmonic distortion when Active Front

Ends (AFEs) are utilized. But the price of Active Front Ends is steep. Harmonic distortion on the AC bus will be less of an issue if all power electronic converters share a single DC bus. We will just require half of the power electronics equipment. The future of shipboard electrical systems appears to be the utilization of a common DC bus to connect a small AC bus and high-power consumers. [6].

7) Telecommunications

A DC distribution system offers the convenience of plug-and-play functionality without the need for synchronization. This efficient system is commonly found in telecommunication networks and data centers, where it serves as a reliable power source at low voltage levels (48 Vdc). Similar to traditional DC distribution systems, these systems exhibit similar characteristics [7].

The standard measure of reliability in such a system is five nines (99.999%), whereas for comparison, the usual requirement for AC bulk power systems is three nines (99.9%). The permitted downtime for each is much different, at 5 minutes and 9 hours annually, respectively. The ability to link the core battery stack directly to the common bus explains how DC systems may attain such great reliability. This type of approach is common in both the consumer electronics and telecommunications sectors. [8].

8) Semiconductors

Power electronic converters (PECs) are devices that improve the performance of DC distribution networks. Their development was made possible by the emergence of the semiconductor industry in the 1960s. Semiconductor technology is constantly evolving, making PECs more compact, dependable, efficient, and economical. As a result, DC distribution systems are beginning to outperform AC distribution systems in terms of efficiency, dependability, cost, and size[7].

9) Data Centers

Data centers are the foundation of the online world. They host anywhere from a few dozen to thousands of servers, each with its own processors, hard disks and memory.

Large enterprises rely on facilities in various industries such as technology, consulting, finance and research for their operations. Despite their importance, these facilities are known for being energy intensive. One prominent example is the Lakeside Technology Center located in Chicago, which stands as one of the largest data centers globally. Its energy consumption surpasses that of the O'Hare International Airport, ranking it as the second-largest energy consumer in the region with over 100 megawatts consumed. On a national scale, these data centers account for a significant amount of electricity usage, totaling 14.6 terawatt-hours per year according to a report by Lawrence Berkeley National Laboratory (LBNL).

Systems with low voltage DC operating at 48 Vdc are made for use in places like data centers. It takes at least three conversion stages from the AC input to the load to produce this voltage level. Even while DC distribution systems' components are subjected to higher electrical voltages than those of typical AC systems, they are more dependable in data centers. The fact that these systems employ fewer conversion stages accounts for their increased reliability. Fig. 2 shows the

measured fault currents for UPSs in NTT plants when AC and DC are applied. In DC the fault is zero [7] .



Fig. 2 Data on the reliability of power systems for 23,000 DC and 10,000 UPS systems (NTT Facilities)

10) AC and DC Distribution Grids

Regarding energy security and environmental effect, renewable energy technologies provide numerous advantages. The technical issue lies in integrating intermittent power sources with the system while maintaining power quality. The literature has put up a number of suggestions for enhancing power quality in AC grids.

When designed as DC distribution grids, they enable the connection of additional distributed generation (DG) and offer consumers a better quality of power than AC distribution grids. Consequently, the proposal of DC grids leads to a noteworthy decrease in issues related to power quality, losses and fault periods, and protection failures. The positive aspects of DC and AC distribution systems are contrasted in Table 1 [9]. LV and MV protection devices are available for both AC and DC lines, with respect to protection costs.

Although DC technology has advanced, AC technology is still more attractively priced.

DC voltages can pose increased safety risks as the lack of a natural current zero crossing point makes it more difficult to interrupt DC circuits, increasing the potential for electric shock and arc flash hazards. Appropriate safety measures, such as the use of specialized circuit breakers and grounding systems, are crucial to mitigate these risks in DC-based applications [9], [10], [11].

The absence of zero crossing current and grounding are the two main problems that arise especially for DC grid systems [5], [12].

Table 1. Advantages of DC and AC distribution system

	DC distributed power system	AC distributed power system
1	Integration of renewable energy sources	Voltage conversion
2	Reliability and uninterrupted supply	Circuit breaker protection
3	Voltage stability	Voltage stability
4	Fluorescent lighting and electronics	
5	Variable speed drives	
6	Power quality	
7	60 Hz. health concerns	
8	Lack of harmonic effect	

11) AC and DC Transmission Grids

Currently, most of the power transmission lines utilize three-phase AC technology. However, in recent years, HVDC technology has become more popular for power transmission

Table 2. Comparison between AC and DC transmission systems

	AC	DC
Transmission costs		
Investment costs		
Right of way (ROW)	High	Low
Tower	High	Simpler and cheaper
Insulators	High	Low
Conductors	High	Low
Terminal equipment	Low	High
Operating costs		
Losses	High	Low
Skin effect	Available	None
Dielectric losses	High	Low
Corona effects	High	Low
Compensation	Through reactive power	Low
Technical issues		
Control of transmitted power	Need for reactive power control	Full
Transient and dynamic stability	Bad	Good.
Fault currents	Limited	High
Power conveying capacity	Distance dependent	No distance dependency
Voltage control	Load dependent	No reactive power (Q) control
Line compensation	Available	None
Interconnection	Need for synchronization and large power oscillations	Asynchronous connection
Grounding impedance	High	Low
Reliability	Similar	Similar
Availability	Similar	Similar
Application Fields	Short distances (<50 km)	Wires that are both underwater and underground massive power transmission over large distances AC system connections made asynchronously power flow stability in an integrated power system

due to its advantages such as high-power density, controlled emergency support, no contribution to short circuit level and greater stability. Furthermore, the transmission capacity can be increased by conversion of AC lines to DC lines [9]. Table 2 shows a comparison of AC and DC networks in transmission lines.

In situations when power must be transmitted over long distances, such as through subterranean and underwater lines, DC transmission systems are more suitable over AC transmission systems. [9].

12) HVDC Transmission Lines

HVDC systems provide greater flexibility compared to AC systems, presenting notable benefits for the integration of offshore wind farms into terrestrial grid frameworks. A Voltage Source Converter (VSC) HVDC transmission system facilitates rapid and adaptable management of both active and reactive power, effectively alleviating the transmission of voltage and frequency fluctuations attributed to variations in wind energy generation. Recent technological advancements have expanded the capabilities of VSC HVDC systems, allowing for operation at elevated voltage levels and power capacities, thus rendering multi-terminal HVDC (MTDC) systems a feasible technical option [13].

Table 3 lists the HVDC grids in operation. There are some notable ones, such as Rio Madeira in Brazil, the longest HVDC installation ever built (2375 km). The Jinping-Sunan 7800 kV ultra-high voltage direct current (UHVDC) installation in China is the world's most powerful transmission line with a rated capacity of 7.2-7.6 GW. Their number is constantly increasing due to the multiple advantages that HVDC offers for

power transmission over long distances (4,800 km for overhead lines and 450 km for cable systems) [9].

Fig. 3 shows the image of the 500 kV HVDC transmission line and pole. In the industry where DC grids, which are called super grids, are slowly being established, grid operators are making their plans accordingly.



Fig. 3 500 KV HVDC transmission line

When the use of HVDC is analyzed in terms of our country, there is the Black Sea HVDC transmission line between Georgia and Turkey, which has a back-to-back topology and has a transmission capacity of 350 MW. There are also 2 possible HVDC projects on the agenda. The transfer of electrical energy generated at the Akkuyu Nuclear Power Plant and an HVDC transmission line project planned to solve the electrical energy problem of Cyprus [14].

Table 3. HVDC grids in utilization

Country	Number of Lines	Country	Number of Lines
Africa	2	Austria	1
Brazil	2	Denmark-Germany	1
Canada	7	Denmark-Sweden	1
Canada-USA	2	Estonia-Finland	1
Paraguay	1	Finland-Sweden	1
USA	14	France-UK	1
China	6	Greece-Italy	1
India	8	Ireland-Scotland	1
Japan	3	Italy	2
Philippines	1	Norway	1
South Korea	1	Norway-Denmark	1
Thailand-Malaysia	1	Norway-Netherlands	1
Russia	2	Sweden	1
UK	1	Sweden-Germany	1
Australia	1	New Zealand	1
Australia-Tanzania	1	Turkey-Georgia	1

According to a study conducted by the Turkish National Committee of the World Energy Council, in addition to the above planned HVDC grids, it is recommended that new HVDC grids be built in Akkuyu-Istanbul, Black Sea and other regions shown in Fig. 4 in terms of energy supply and security.



Fig. 4 HVDC grid scenario in Turkey

C. Advantages Of Using DC

1) Integration of Renewable Energy Sources

Integrating DC renewable energy sources into a premise DC bus is considerably simpler. They can integrate seamlessly with renewable energy sources. Doing so will save between 2.5% and 10% of the project developed each.

2) Reliability and Uninterrupted Supply

The use of DC-DC converters in renewable energy systems allows for efficient voltage regulation and power management, further increasing the efficiency and reliability of these systems.

In addition, the increasing demand for dependable information technology necessitates the implementation of uninterruptible power supplies. Each of these systems must incorporate DC battery storage capable of sustaining application operations during unforeseen AC outages.

Constant power devices, such as those found in telecommunications and industrial applications, benefit from the consistent voltage provided by DC systems because their power requirements are not affected by fluctuations in voltage. This stability ensures reliable operation and minimizes the risk of equipment damage or failure.

3) Voltage Stability

The voltage stability of DC distribution system components, especially if DC and AC distribution will coexist as they should, may exacerbate, if not alleviate, our calculations and challenges. Nevertheless, the active input stages of power supplies not only enhance the power factor but also have the capacity to inject reactive power into AC sources, thereby aiding in voltage control and ensuring voltage stability.

4) Fluorescent Lighting and Electronics

Electronic ballasts for fluorescent lights work best when powered by DC. The shift from less efficient incandescent lighting to sophisticated lighting technologies, such as compact fluorescent bulbs and eventually solid-state lighting, offers a realistic chance to deploy DC distribution systems. This approach would eliminate at least one conversion stage currently necessary in every luminaire. A parallel consideration applies to household electronic devices, all of which necessitate DC power and must convert the AC provided to them.

5) Variable Speed Drives

Both production and load scenarios benefit from variable speed drives, which facilitate the alignment of input and output power. This congruence can lead to enhanced efficiency, increased convenience, or a combination of both. Furthermore, the implementation of variable speed control is more readily attainable when utilizing a DC power source.

6) Power Quality

While power electronics are frequently perceived as contributors to inadequate power quality, power electronic converters integrated within an AC system have the capacity to comply with the majority of power quality standards and, in many cases, enhance AC power quality. Power factor correction must be incorporated into the earliest stages of DC power supplies. Furthermore, excellent design approaches and effective filtering protocols ensure that harmonic power quality remains within acceptable bounds.

It is due to the use of power electronics conversion not only to prevent poor power quality but also to improve power quality.

7) 60-Hz Health Concerns

Potential health concerns arising from human exposure to 60-Hz distribution may lead us to greater use of DC distribution systems [15].

8) Reactive Losses

A DC system has only active power. There are no heavy electrical currents and/or losses due to reactive power losses [3].

9) High Energy Transmission Capacity

DC voltages can be efficiently transmitted over long distances with minimal power loss, making them well suited

for applications where power needs to be distributed over large geographical areas. The absence of the need for frequency conversion also simplifies the design and implementation of power transmission systems, reducing complexity and increasing overall efficiency. More power is transmitted with a conductor of the same cross-section.

10) Better Voltage Regulation and Control Capability

DC transmission can be better controlled.

11) Asynchronous Connection Opportunity

It enables asynchronous connection, which is not possible in AC systems [3].

III. RESULTS

If local DC generation is accessible, such as through solar photovoltaics, it can provide energy directly to DC loads without necessitating conversion to AC. This approach yields cost savings by eliminating additional conversion losses and related equipment. The conversion from DC to AC is not always efficient, leading to energy losses ranging from 5 to 20 percent as heat.

When comparing energy savings in residential buildings utilizing a combination of AC and DC within in-building power distribution systems, findings indicate that energy savings through DC reach 5% of total energy consumption in homes without battery storage and increase to 14% in homes equipped with storage [3].

DC transmission systems are more economically advantageous than AC systems for long-distance applications, effectively addressing several drawbacks associated with AC transmission, including the necessity for synchronization, the requirement for line compensation, and the challenges posed by high ground impedance [9].

In a 2004 study on DC distribution efficiency in data centers, Lawrence Berkeley National Laboratory (LBNL) reported that DC distribution consumes 28% less power than a typical AC distribution in data centers [7].

The Electric Power Research Institute (EPRI) found in their research that in the data center space, this means that the UPS used go through AC to DC to AC conversions, the AC electricity supplied by the backup system is subsequently transformed back into DC within the servers. This conversion process produces heat, necessitating the implementation of energy-intensive cooling systems in server rooms. Notably, the energy required to operate the air conditioning is approximately twice that needed to power the servers themselves.

At NTT Facilities in Tokyo, four DC-powered data centers eliminated AC-DC converters in their battery backup systems (fed directly from DC), reducing power consumption by 15 percent compared to traditional AC configurations. Intel estimated the annual power savings for a mid-sized data center in the US at \$1.2 million.

IV. DISCUSSION

DC distribution systems possess several key advantages over AC distribution. These include enhanced efficiency and reliability, simpler integration of renewable energy sources and energy storage systems, and reduced costs. Additionally, DC systems do not encounter issues related to reactive power and frequency stabilization, leading to decreased copper losses.

Many loads necessitate DC power, including consumer electronics, LED lighting systems, and devices utilizing variable speed motor drives. DC distribution systems are currently used mostly in telecommunications systems, data centers, DC buildings, and microgrids. Because of its multiple benefits, new plants are being established around the world using DC distribution. A voltage level of 380 Vdc has gained acceptance among organizations implementing DC distributed plants, due to its high efficiency, reliability, and reduced copper costs. The enhanced efficiency of DC distribution primarily results from fewer power conversion stages. Furthermore, the radial bus structure is particularly advantageous for residential buildings, as it offers lower costs and meets minimal reliability requirements [7].

V. CONCLUSION

DC energy is important for energy efficiency, reliability and special applications. However, the advantages and disadvantages of AC and DC should be evaluated depending on the requirements of the project.

The use of DC energy becomes more economical with lower energy loss, lower maintenance costs and better voltage control. Energy savings due to less power loss will enable more economical delivery of electrification services to remote areas. Connecting more renewable energy sources will reduce carbon greenhouse gases, increase the use of green energy and create employment opportunities.

An escalating number of DC consuming devices, including computers, televisions, and monitors, are being integrated into contemporary buildings. The power provided to these devices requires conversion from AC back to DC. Transitioning to a DC infrastructure would mitigate additional losses and simplify the overall power system.

Furthermore, emerging Silicon Carbide technology has the potential to improve the efficiency of power electronic converters used in DC systems. With the development of DC/DC converters, AC is more efficient compared to electromagnetic transformers.

Considering these developments in the DC field, we can say that the second war of currents has already begun, or we have entered another process where both currents can be used with hybrid structures [16].

REFERENCES

- [1] P. Fairley, "Edison's revenge: The rise of DC power," MIT Technology Review. Available: <https://www.technologyreview.com/2012/04/24/256131/edison-revenge-the-rise-of-de-power/>
- [2] P. Fairley, "DC versus AC: The second war of currents has already begun [in my view]," *IEEE Power and Energy Magazine*, vol. 10, no. 6, 2012, Doi: 10.1109/MPE.2012.2212617.
- [3] F. Dastgeer and H. E. Gelani, "A Comparative analysis of system efficiency for AC and DC residential power distribution paradigms," *Energy Build*, vol. 138, pp. 648–654, Mar. 2017, Doi: 10.1016/j.enbuild.2016.12.077.
- [4] M. Starke, L. M. Tolbert, and B. Özpineci, "AC vs DC distribution: A loss comparison," *IEEE*, 2010.
- [5] S. Sarangi, B. K. Sahu, and P. K. Rout, "Distributed generation hybrid AC/DC microgrid protection: A critical review on issues, strategies, and future directions," *Int J Energy Res*, vol. 44, no. 5, pp. 3347–3364, Apr. 2020, Doi: 10.1002/er.5128.
- [6] N. Remijn and B. Krijgsman, "Advantages of common DC busses on ships," *IEEE*, 2010.
- [7] V. A. Prabhala, B. P. Baddipadiga, P. Fajri, and M. Ferdowsi, "An overview of direct current distribution system architectures

- & benefits,” *Energies (Basel)*, vol. 11, no. 9, Sep. 2018, Doi: 10.3390/en11092463.
- [8] T. Dragičević, J. C. Vasquez, J. M. Guerrero, and D. Škrlec, “Advanced LVDC electrical power architectures and microgrids: A step toward a new generation of power distribution networks,” *IEEE Electrification Magazine*, vol. 2, no. 1, pp. 54–65, Mar. 2014. Doi: 10.1109/MELE.2013.2297033.
- [9] E. Planas, J. Andreu, J. I. Gárate, I. Martínez De Alegría, and E. Ibarra, “AC and DC technology in microgrids: A review,” *Renewable and Sustainable Energy Reviews*, vol. 43, pp. 726–749, 2015, Doi: 10.1016/j.rser.2014.11.067.
- [10] M. H. Ashfaq, J. A. Selvaraj, and N. A. Rahim, “Control strategies for bidirectional DC-DC converters: An overview,” *IOP Conf Ser Mater Sci Eng*, vol. 1127, no. 1, p. 012031, Mar. 2021, Doi: 10.1088/1757-899x/1127/1/012031.
- [11] F. Mumtaz, N. Zaihar Yahaya, S. Tanzim Meraj, B. Singh, R. Kannan, and O. Ibrahim, “Review on non-isolated DC-DC converters and their control techniques for renewable energy applications,” *Ain Shams Engineering Journal*, vol. 12, no. 4, pp. 3747–3763, Dec. 2021, Doi: 10.1016/j.asej.2021.03.022.
- [12] C., D. Xu and K., W., E. Cheng, “A survey of distributed power system-AC versus DC distributed power system,” *IEEE*, 2010.
- [13] F. Gonzalez-Longatt and C. A. Charalambous, “Power flow solution on multi-terminal HVDC systems: Super grid case,” in *International Conference on Renewable Energies and Power Quality*, 2012. [Online]. Available: <https://www.researchgate.net/publication/235769646>
- [14] G. Önal, “Türkiye’ nin HVDC yol haritası,” *Dünya Enerji Konseyi Türk Milli Komitesi*, 2017.
- [15] Hammerstrom and Donald, “AC versus DC distribution systems—Did we get it right?” *IEEE*, 2007.
- [16] N. Ertugrul and D. Abbott, “DC is the future [Point of View],” in *Proceedings of the IEEE*, Institute of Electrical and Electronics Engineers Inc., May 2020, pp. 615–624. Doi: 10.1109/JPROC.2020.2982707.

Development of Machine Learning-Based Sales Cancellation/Return Forecasting Models for the E-Commerce Industry

Zehra Sude Sari¹, Batuhan Taşkapı² Gökay Dağdaş³, Mehmet Fatih Akay⁴

¹Dept. of Data Science, Inveon, İstanbul, Turkey

²Dept. of Customer Operations, Inveon, İstanbul, Turkey

³Dept. of Customer Operations, Inveon, İstanbul, Turkey

⁴Dept. of Computer Engineering, Çukurova University, Adana, Turkey
(sude.sari@inveon.com)

Abstract – E-commerce is evolving rapidly, creating a more competitive market environment. With this development, gaining a competitive advantage has become even more crucial. Companies implement various strategic moves to maintain their position in this competitive market. Strategies and forecasts have a high ranking among these strategies. Predicting sales cancellations and returns is crucial for companies to anticipate future challenges and stay ahead. The aim of this study is to develop sales cancellation/return prediction models for the e-commerce sector. To achieve this, sales cancellation/return prediction models have been generated using Multi-Layer Perceptron (MLP), Random Forest (RF), Extreme Gradient Boosting (XGBoost), Support Vector Machine (SVM), and Logistic Regression (LR). A weekly dataset has been created using 4909 rows of sales cancellation/return data. The performance of the models has been evaluated using precision, recall, F1 score, and accuracy. Among all the methods, it has been observed that RF and XGBoost delivered the best performance.

Keywords – Machine Learning, Customer Behavior Analysis, Sales Cancellation/Return Prediction, E-commerce, E-commerce Analytics

I. INTRODUCTION

E-commerce sector has undergone a significant transformation with the widespread adoption of the Internet and the rapid development of digital technologies, resulting in substantial growth within the industry. Online shopping has become increasingly popular among consumers, replacing traditional retail shopping methods. In 2023, the volume of e-commerce in Turkey increased by 115.15% compared to the previous year, reaching 1.85 trillion Turkish Lira (approximately \$77.89 billion). During the same period, the number of transactions increased by 22.25%, totaling 5.87 billion. The share of e-commerce within the total trade volume also rose significantly, from 10.1% in 2019 to 20.3% in 2023. Furthermore, the sector's growth potential remains strong, with the Ministry of Trade projecting that the e-commerce volume will reach 3.4 trillion Turkish Lira and the number of transactions will rise to 6.67 billion by 2024 [1].

In order to remain competitive in this dynamic sector, e-commerce companies need both short-term and long-term financial planning. Financial planning is a process that enables businesses to effectively manage their future financial resources based on an analysis of income and expenditure. However, sales cancellations and return processes pose significant challenges for companies. When sales are canceled or returned, financial plans based on expected revenues from sold products can result in budget deficits when sales are canceled or products are returned.

Sales cancellations and returns cause financial problems, increase costs, negatively impact customer satisfaction, and complicate inventory management. While sales cancellations generally do not incur shipping costs because the product has not yet been dispatched, returns incur shipping costs after the

product has been delivered to the customer, which reduces profit margins. A study by Fast Company revealed that processing a return can cost as much as 59% of the original sales price [2]. Furthermore, tracking, storing, and restocking returned products necessitates additional resources and personnel. Ineffective management of cancellations and returns can lead to serious financial and operational consequences for businesses.

Particularly for products with expiration dates, such as perishable goods and seasonal fashion items, returns create significant challenges for reselling. These products require additional processes, making the return process even more complex. For instance, defective or damaged goods may need to be repaired or repackaged, adding labor and costs. In this context, anticipating cancellations and returns can provide significant advantages for companies. If a product has a high likelihood of being returned, the business can strategically delay its shipment or manage the return process more efficiently. These strategies help minimize unnecessary shipping costs and enable businesses to achieve financial savings.

This study is organized as follows: Section 2 covers relevant literature. The dataset, overview of methods and sales return/cancellation prediction models have been described in Section 3. Section 4 and 5 presents the results and discussion. Section 6 concludes the paper.

II. LITERATURE REVIEW

Studies on predicting product returns and order cancellations in e-commerce are extensive, underscoring the growing need for accurate forecasting methods in this sector. Various methodologies have been applied to address these challenges, including probabilistic models, multimodal

frameworks, machine learning techniques, and ensemble learning approaches. [3] analyzed sellers' optimal pricing and inventory policies in the context of order cancellations under cash-on-delivery (COD) systems. The study examined customer behaviors related to order cancellations when using the same payment method. Machine learning models, which offered new insights beyond earlier research that relied on periodic review systems and lacked experimental data analysis, were employed. The model's accuracy was assessed, with the Logistic Regression (LR) model having the highest prediction accuracy of 84% and a precision rate of 69%. In another study, [4] proposed an interpretable feature method to enrich the available Passenger Name Record (PNR) information. The prediction performance of two classes of models was empirically evaluated to determine whether they could cross-fertilize each other to improve cancellation prediction. The researchers combined Bayesian Networks (BN) and Lasso Regression (LR). They added to the body of research by suggesting an understandable feature interaction and a forecasting method that used both types of efficient models together. Further, [5] observed that the average return rate of fashion products purchased online ranged from 13% to 96%, based on a large dataset. Machine-based prediction was employed to automatically extract interpretable features from images, and the analysis demonstrated how to select and design fashion products that were less likely to be returned. Similarly, [6] aimed to develop personalized strategies to boost sales, employing current, frequency, and monetary (CFM) models based on digital transformation techniques to better understand and segment potential customers. The underlying reasons behind vendor behaviors were determined using K-means and hierarchical clustering. A real-world dataset was analyzed by [7] to predict accommodation order cancellations, employing XGBoost with optimized hyperparameters to achieve successful outcomes. Meanwhile, [8] proposed a multi-channel pricing and order optimization model with two return policies—full return and non-return. To overcome nonlinearity in the model, a linearization technique was used. The study used Support Vector Machine (SVM) to turn historical data into uncertainty clusters. This turned the model into an approximate mixed integer linear programming model that can be solved with commercial software. A comparison with the box uncertainty set indicated that the data-driven uncertainty set was less conservative and yielded higher profits for the retailer. In the context of online ride-hailing, [9] presented a deep learning model designed to predict the probability of order cancellations. The Didi Chengdu Express public dataset was used to test the Deep Residual Network-Based Ride-Hailing Order Cancellation Probability Prediction Model (DeepOCP). The results showed that the model was good at predicting how likely it was that a user would cancel an online ride-hailing order. A study by [10] suggested using a large dataset to show how important it is for probabilistic forecasters to be well-calibrated in order to make accurate predictions with high precision and good recall. The study recommended using calibrated models selectively, emphasizing the need to avoid predictions for some instances when confidence was low. The increasing trend of real-time order cancellations in live streaming e-commerce (LSE) was analyzed by [11], focusing on the factors that influenced these cancellations. Data were collected from 768 TikTok live streaming rooms in China, including 4,984 product promotion videos, 1.29 million comments, and information from 513,551

viewers. Using emotional contagion theory, the study examined the impact of emotional expressions by live-stream hosts on viewers and how these influenced real-time order cancellations. Finally, [12] proposed a multimodal analysis framework for predicting product returns in e-commerce environments. The model considered multimodal features and their correlations from different data sources, with experiments conducted using a dataset from Taobao live streaming. The findings highlighted the utility of multimodal signals in predicting product returns, allowing live streaming platforms and consumers to anticipate which products would likely have high return rates. Additionally, the study suggested that sellers and anchors could use these predictions to improve product descriptions and interaction strategies.

III. MATERIALS AND METHOD

A. DATASET

A dataset has been created with the sales cancellation/return data received from one of Inveon's customers. The dataset contains 4909 cancellation/return data across 10000 rows. Table 1 shows the attributes in the dataset with their descriptions.

Table 1. Attributes in the dataset

Attributes	Description
CustomerId	Unique Customer Identifier
OrderDiscount	Discount on the Order
OrderTotal	Total Order Value After Discount
CountryId	Customer's Country Identifier
ProductId	Unique Product Identifier
Price	Product Price Including Tax
Discount	Discount Amount Including Tax
AllowEmail	Permission for Email Communication
AllowSms	Permission for SMS Communication
OrderCount	Total Number of Orders by the Customer
ReturnCount	Number of Returns or Cancellations
Month	Month of the Order
Day	Day of the Order
Hour	Hour of the Order
Return	Status of the Order

B. OVERVIEW OF METHODS

1. Multi-Layer Perceptron

MLP function is a complex function that produces numerical outputs from numerical inputs. The input layer acquires raw data from the domain, the hidden layer extracts features, and the output layer generates a prediction. This represents the architecture of a MLP. A deep neural network comprises numerous hidden layers. Conversely, increasing the number of hidden layers may lead to vanishing gradient

problems, requiring the implementation of specialized techniques. The hyperparameters of the MLP, encompassing the quantity of hidden layers and hidden neurons, must be chosen meticulously [13].

2. Random Forest

RF is a widely utilized ensemble learning method applicable to regression, classification, clustering, and interaction detection. In contrast to a solitary decision tree (DT), which is often unstable and biased, RF constructs a multitude of trees, mitigating these concerns through the utilization of multiple DTs. Each tree is generated from a bootstrap sample, and at each node, a random selection of variables is utilized. Out-of-Bag (OOB) error rates are employed to evaluate the precision of each tree. The ultimate classification is determined by a majority vote across all trees. Key error metrics comprise the mean reduction in the Gini coefficient and accuracy. To enhance the RF model, users must modify two critical parameters: the overall quantity of trees and the number of variables evaluated at each node [14].

3. Extreme Gradient Boosting

XGBoost is an efficient gradient tree boosting algorithm that builds decision trees sequentially. It is known for its speed and effectiveness, especially in handling structured datasets for label classification. XGBoost combines predictions from multiple decision trees using the "bagging" technique and enhances model performance by reducing sequential errors. Gradient descent further refines these errors. XGBoost also improves the traditional gradient boosting by eliminating missing data issues and using parallel processing to reduce overfitting [15].

4. Support Vector Machine

SVM is a technique for pattern recognition grounded in statistical learning theory. SVM were initially designed for classification; however, their primary applications now encompass regression and the classification of small, high-dimensional, non-linear datasets. SVM are founded on the VC-dimension of statistical learning theory and the principle of minimizing structural risk. Learning occurs without error identification utilizing a constrained sample size, and the model's precision is evaluated. The minimal deviation of the hyperplane from the sample points is employed to ascertain the optimal universal capability. SVM encompass both linear and non-linear regressions. The kernel function, which assesses the similarity between data points, and the cost loss function, or regularization parameter, are critical parameters. (i.e., among reflectance values.) [16].

5. Linear Regression

In technical and scientific applications, LR is one of the most prevalent models for determining the relationship between two variables. Two categories of statistical methods—Type I, known as Ordinary Least Squares (OLS), and Type II, referred to as Standard Major Axis (SMA)—have been developed for LR, contingent upon the characteristics of the data set. In optical oceanography, the rationale for selecting a specific method to calculate a linear regression fit is often overlooked and seldom substantiated by statistical evidence [17].

C. SALES CANCELLATION/RETURN PREDICTION MODELS

Results have been obtained with 10-fold cross-validation using MLP, RF, XGBoost, SVM and LR algorithms on the dataset. To maximize the performance of each algorithm, hyperparameter optimization has been performed with grid search. The hyperparameter ranges used for grid search are provided in Table 2.

Table 2. Hyperparameter Ranges Used for Grid Search

Method	Hyperparameter Range
MLP	Layer number: (1 - 3) Neuron count: (32 - 128) Epochs: (5 - 10)
RF	N Estimators: (50 - 200) Max Depth: (10) Min Samples Split: (2 - 10)
XGBoost	N Estimators: (50 - 100) Max Depth: (None - 10) Learning Rate: (0.1 - 0.2) Max Leaves: (25 - 100)
SVM	C: (1 - 1000) Degree: (4) Gamma: (0.1 - 0.5)
LR	C: (0.001 - 10) Max Iter: (1000) Penalty: (L1, L2)

IV. RESULTS

The confusion matrices of these models are shown in Figure 2 to Figure 6.

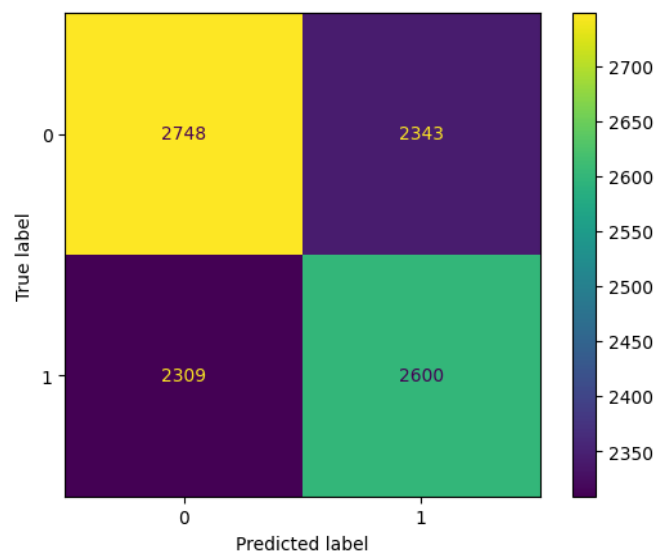


Figure 2. Confusion matrix obtained with MLP

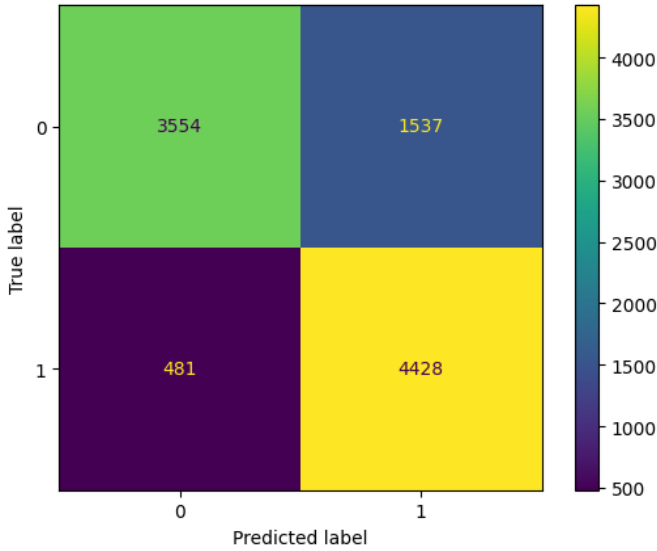


Figure 3. Confusion matrix obtained with RF

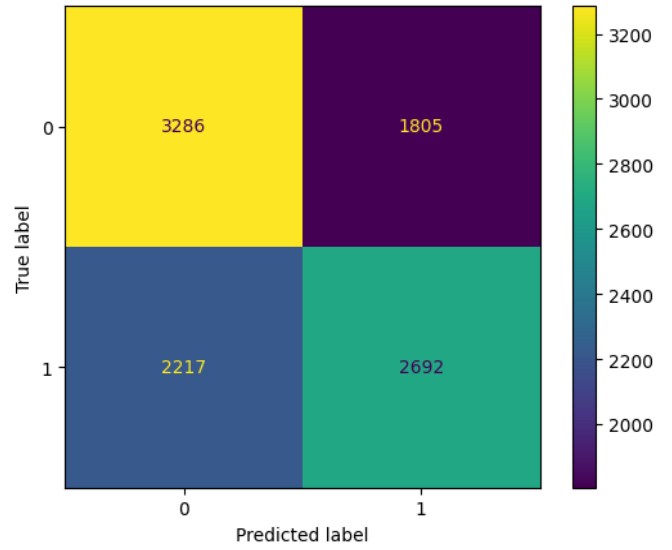


Figure 6. Confusion matrix obtained with LR

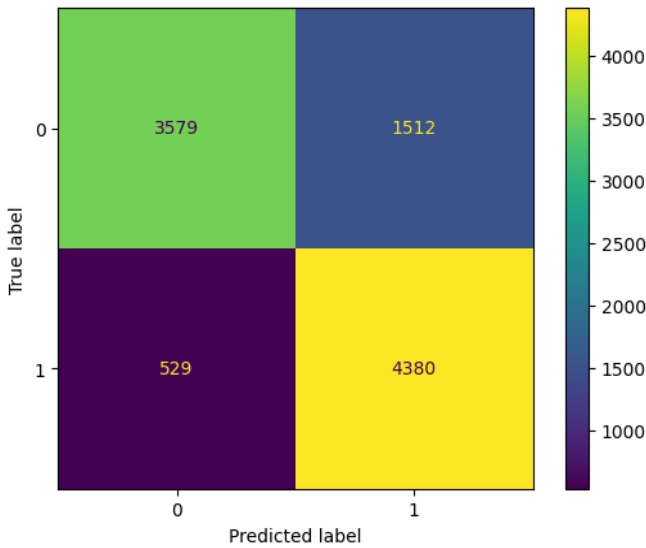


Figure 4. Confusion matrix obtained with XGBoost

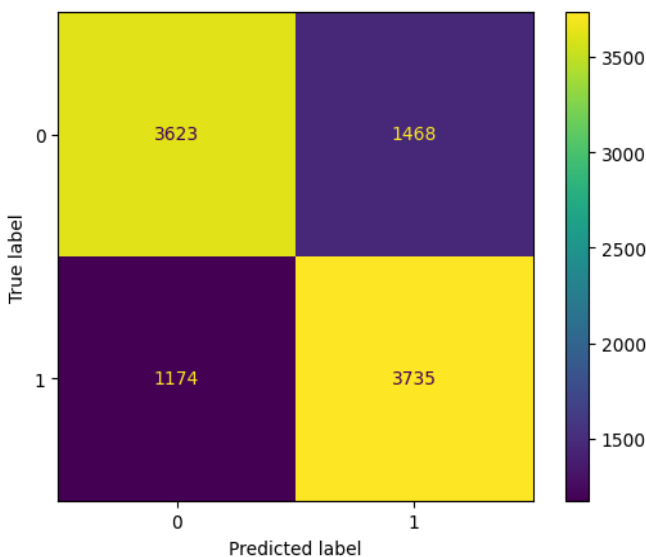


Figure 5. Confusion matrix obtained with SVM

The comparison of precision, recall, F1-score, and accuracy values of the results obtained with the sales cancellation and return models developed using MLP, RF, XGBoost, SVM, and LR is given in Table 3.

Table 3. The Obtained Results

Algorithms	Precision	Recall	F1-Score	Accuracy
MLP	0.53	0.53	0.53	0.53
RF	0.74	0.90	0.81	0.80
XGBoost	0.74	0.89	0.81	0.80
SVM	0.72	0.76	0.74	0.74
LR	0.60	0.55	0.57	0.60

V. DISCUSSION

Based on the results,

- RF and XGBoost models demonstrated superior performance compared to other algorithms, achieving the highest F1-score and accuracy, along with high recall rates. These characteristics suggest that these models are the most suitable for predicting cancellations and returns in e-commerce.
- The MLP model produced the lowest results across all evaluation metrics, indicating that it struggles to capture the relevant features of the dataset effectively.
- The SVM model exhibited balanced performance in terms of F1-score and accuracy. However, it was not as effective as RF and XGBoost, indicating that while it is an acceptable option, it is not the optimal choice for this problem.
- The LR model achieved a reasonable level of accuracy and F1-score, but it underperformed in terms of recall compared to other models. This suggests that LR may be less suitable in scenarios where minimizing false negatives is critical.

VI. CONCLUSION

This study utilized several machine learning algorithms to develop forecasting models for predicting sales cancellations

and returns. Among the models evaluated, XGBoost and RF demonstrated the best overall performance, particularly excelling in accuracy and recall. This suggests that these models are more robust in effectively identifying potential cancellations and returns. The SVM model also provided balanced results across most evaluation metrics, while the LR and MLP models exhibited comparatively lower effectiveness. Notably, the LR model had the lowest performance metrics, indicating a higher occurrence of false positives and false negatives.

To further enhance the accuracy of these forecasting models, future work will focus on leveraging the strengths of various feature selection algorithms to better assess the impact of features on model performance. Instead of changing the feature set, this approach aims to provide a more accurate evaluation of the contribution of existing features, ultimately helping e-commerce companies make more precise and proactive decisions, thereby reducing operational inefficiencies and increasing overall profitability.

REFERENCES

- [1] Ministry of Trade of the Republic of Turkey. (May 2024). E-commerce outlook report in Turkey.
- [2] Chaturvedi, H. (2022, May 30). Product returns are wasteful for companies and the planet. Here's how to change that. Fast Company
- [3] Adebajo, S., & Banchani, E. (2023). DEVELOPMENT OF MACHINE LEARNING TECHNIQUES FOR DETERMINING OPTIMAL PRICING AND INVENTORY POLICY WITH ORDER CANCELLATION UNDER THE CASH-ON-DELIVERY PAYMENT SCHEME. *Advance Journal of Current Research*, 8(12), 18-41.
- [4] Chen, S., Ngai, E. W., Ku, Y., Xu, Z., Gou, X., & Zhang, C. (2023). Prediction of hotel booking cancellations: Integration of machine learning and probability model based on interpretable feature interaction. *Decision Support Systems*, 170, 113959.
- [5] Dzyabura, D., El Kihal, S., Hauser, J. R., & Ibragimov, M. (2023). Leveraging the power of images in managing product return rates. *Marketing Science*, 42(6), 1125-1142
- [6] Jauhar, S. K., Chakma, B. R., Kamble, S. S., & Belhadi, A. (2024). Digital transformation technologies to analyze product returns in the e-commerce industry. *Journal of Enterprise Information Management*, 37(2), 456-487.
- [7] Liu, Z., Jiang, P., Wang, J., Du, Z., Niu, X., & Zhang, L. (2023). Hospitality order cancellation prediction from a profit-driven perspective. *International Journal of Contemporary Hospitality Management*, 35(6), 2084-2112.
- [8] Qiu, R., Ma, L., & Sun, M. (2023). A robust omnichannel pricing and ordering optimization approach with return policies based on data-driven support vector clustering. *European Journal of Operational Research*, 305(3), 1337-1354.
- [9] Sun, H., Lv, Z., Li, J., Xu, Z., & Sheng, Z. (2023). Will the Order Be Canceled? Order Cancellation Probability Prediction Based on Deep Residual Model. *Transportation Research Record*, 2677(6), 142-160.
- [10] Sweidan, D., Johansson, U., Alenljung, B., & Gidenstam, A. (2023, July). Improved Decision Support for Product Returns using Probabilistic Prediction. In *2023 Congress in Computer Science, Computer Engineering, & Applied Computing (CSCE)* (pp. 1567-1573). IEEE.
- [11] Wang, Z., Luo, C., Luo, X. R., & Xu, X. (2024). Understanding the effect of group emotions on consumer instant order cancellation behavior in livestreaming E-commerce: Empirical evidence from TikTok. *Decision Support Systems*, 179, 114147.
- [12] Xu, W., Zhang, X., Chen, R., & Yang, Z. (2023). How do you say it matters? A multimodal analytics framework for product return prediction in live streaming e-commerce. *Decision Support Systems*, 172, 113984.
- [13] Al Bataineh, A., & Manacek, S. (2022). MLP-PSO hybrid algorithm for heart disease prediction. *Journal of Personalized Medicine*, 12(8), 1208.
- [14] Park, S., & Kim, J., Landslide susceptibility mapping based on random forest and boosted regression tree models, and a comparison of their performance. *Applied Sciences*, 9(5), 942, 2019.
- [15] Park, S., & Kim, J., Landslide susceptibility mapping based on random forest and boosted regression tree models, and a comparison of their performance. *Applied Sciences*, 9(5), 942, 2019.
- [16] Yuan, H., Yang, G., Li, C., Wang, Y., Liu, J., Yu, H., ... & Yang, X. (2017). Retrieving soybean leaf area index from unmanned aerial vehicle hyperspectral remote sensing: Analysis of RF, ANN, and SVM regression models. *Remote Sensing*, 9(4), 309.
- [17] Bellacicco, M., Vellucci, V., Scardi, M., Barbieux, M., Marullo, S., & D'Ortenzio, F. (2019). Quantifying the impact of linear regression model in deriving bio-optical relationships: the implications on ocean carbon estimations. *Sensors*, 19(13), 3032.

Analysis of Inrush Current Loads in Electric Motors in Low Temperature Tests

Gizem Fırat¹

¹*Koluman Otomotiv Endüstri A.Ş., University of Turkish Aeronautical Association, Ankara, Turkey*
**(gizem.firat@koluman.com)*

Abstract – This study examines the effects of inrush current loads on electric motors operating under low-temperature conditions. While electric motors have a wide range of applications in industrial and military environments, they face significant performance challenges in low-temperature settings. In particular, inrush current loads reduce the efficiency of the motor, leading to overheating, wear, and, ultimately, component failure in long-term use. In this study, the fluctuations in inrush current occurring under low-temperature conditions were evaluated. Experimental data reveal that when the motor operates in low temperature environments, current loads increase significantly, which, in turn, raises the motor's energy consumption. The focus is on the necessity of improvement strategies, particularly for electric motors used in harsh military applications. The research also explores strategies to manage inrush current loads at low temperatures. In conclusion, this study highlights the negative effects of inrush current loads experienced by electric motors under low-temperature conditions and suggests design and operational improvements for motors operating in such environments.

Keywords – *Inrush current, Surge current, Cold environment operation, Operational enhancements, Design improvement*

I. INTRODUCTION

Electric motors are widely used in various areas of industry and have an important place in military systems with the development of the defense industry. In this context, reliability is one of the most important criteria for military systems, and induction motors meet this need by offering long-term and trouble-free operating performance thanks to their robust and simple structure [1]. Their brushless construction makes them more resistant to wear, thus minimizing the need for regular maintenance [2]. Additionally, the absence of wearable components such as brushes or commutators reduces maintenance costs and frequency, which in turn allows for a reduction in maintenance time and costs in military operations [3]. Especially in applications that require low noise, such as submarines and unmanned aerial vehicles, the silent operation of induction motors offers a significant advantage, as it reduces the risk of detection [4]. Additionally, induction motors play an effective role in reducing the costs of military operations due to their high efficiency and low energy consumption. Their high starting torque supports the efficient operation of military vehicles carrying heavy loads [5]. AC motors help reduce energy consumption in military vehicles by providing high energy efficiency, which is critical, especially in battery-powered systems [6]. Squirrel cage rotor induction motors are among the most widely used types of electric motors. These motors are long-lasting because they do not contain wear-prone parts such as brushes and commutators [7]. However, the use of these motors also comes with some disadvantages. First of all, the speed control of squirrel cage induction motors is the most complex among alternating current motors. The motor speed varies depending on the supply frequency, which necessitates the use of additional

systems, such as variable frequency drives (VFDs), to control the speed of the motor. Therefore, this increases both cost and system complexity [8]. In addition, squirrel cage induction motors may initially fall short in applications that require high torque. The starting torque may be insufficient under certain load conditions, which can be problematic when heavy loads need to be started suddenly [9]. In long-term operation, these motors may experience heating problems, and overheating can adversely affect their performance and increase the risk of failure. Therefore, it is crucial to design appropriate cooling systems [10]. Low temperature ambient conditions can cause some disadvantages that adversely affect the performance of these motors. For example, low temperatures increase the viscosity of the motor's oils, which raises the coefficient of friction and creates more resistance between the moving parts. As a result, the operation of the motor becomes difficult, and energy efficiency decreases [11]. Under low temperature conditions, the starting torque of squirrel cage induction motors can also be reduced. In cold weather, the motor can produce low torque while drawing more current than normal, making it difficult to operate heavy loads [12]. At low temperatures, motors usually operate by consuming more energy; this can create heating problems in the internal structure of the motor, and overheating reduces its efficiency and increases the risk of failure [13]. Low temperatures can also reduce the overall efficiency of the motors. Cold weather adversely affects their operation, leading to increased energy consumption and significant cost increases in long-term operation [14]. Finally, low temperatures can affect the physical properties of the motor's materials. In particular, insulation materials can lose their mechanical strength in cold weather, which can lead to electrical failures [15]. In this

study, the performance of a 3-phase squirrel cage induction motor under low temperature conditions was investigated. The motor was subjected to a test temperature of -33°C in accordance with MIL-STD-810G, Method 502.5, Procedure II. MIL-STD-810G is a document developed within the scope of military standards, designed to ensure the durability of military equipment, systems, and materials against various environmental conditions. This standard provides a set of testing and evaluation methodologies for assessing the performance of military equipment in different climatic and environmental conditions. In this context, Method 502.5 was developed specifically to analyze material and system performance under low temperature conditions [16]. The standard establishes the criteria necessary to ensure the reliable operation of military systems in harsh conditions. These criteria cover parameters such as freezing, material deformation, functionality of internal components, and overall durability. Low temperature tests stand out as a critical requirement for adapting to the climatic conditions specific to the regions where military operations are conducted, ensuring that the equipment performs its duties effectively. The reliability and performance of electric motors are especially critical in military applications. In this context, understanding how the motor operates under low temperature conditions is essential for the design and implementation processes. The test process began with conditioning the motor at a temperature of -33°C for 6 hours. This conditioning time is critical for observing the effects of low temperature, such as the increased viscosity of engine oils, and for assessing the impact of these effects on engine performance. The inrush current can cause the current drawn by the motor at startup to be several times the rated current. This high current can lead to overheating of the windings and other components of the motor. Overheating shortens the life of the motor and can cause various malfunctions. This effect becomes even more pronounced, especially under low temperature conditions [17]. Additionally, the inrush current can place an overload on the electrical components inside the motor, which can lead to electrical faults such as short circuits in the windings or insulation breakdown. Low temperature conditions can increase the likelihood of such failures occurring [18]. Low temperature conditions can affect the mobility and efficiency of the internal components of electric motors, making it difficult for the motor to operate effectively. The motor under test is a 3-phase AC motor with a speed of 1445 rpm, a power of 1.5 kW, and a torque of $10\text{ N}\cdot\text{m}$. These characteristics make it suitable for a variety of applications, while also highlighting the performance issues that can be encountered at low temperatures. In particular, the high starting torque of the motor offers a significant advantage when heavy loads need to be moved. However, within the scope of this study, analyzing the peak currents experienced by the motor during startup is a critical component for understanding its performance under low temperature effects. During the test, the motor was driven by a counterload with a capacity of $8\text{ N}\cdot\text{m}$. This load provides a scenario that closely resembles the actual operating conditions of the motor, allowing for observation of how it performs under low temperature effects. Thus, critical parameters of the motor, such as low-temperature starting currents and torque generation, were examined. As a result, this study aims to systematically evaluate the effects of low temperature environments on the performance of 3-phase squirrel cage induction motors and to analyze inrush peak

currents. The findings will provide important data for the design and use of electric motors in military and industrial applications and will contribute to future motor development processes.

II. MATERIALS AND METHOD

In this section, the materials used and the methods applied for the analysis of the inrush current loads of the 3-phase squirrel cage induction motor under low temperature conditions will be presented. In the study, a special test procedure was developed to determine the critical parameters affecting the performance of the motor. Below are the details of the materials used in the test process and the methods applied.

A. Test Motor

The test motor used in this study is a 3-phase squirrel cage induction motor powered by 400 V alternating current (VAC). The motor has a 4-pole structure and is designed with a star connection. The star connection type reduces the starting current of the motor, resulting in more stable operation and thus increasing the performance of the motor. The rated speed of the motor is set at 1445 rpm; this speed is an important parameter that directly affects the performance of the motor. The rated power of the test motor is set at 1.5 kW, which indicates the motor's ability to effectively handle a given load. The torque capacity of the motor is determined to be 10 Newton-meters ($\text{N}\cdot\text{m}$). This torque value reveals the load-carrying ability of the motor, and the fact that it produces high torque at startup provides a significant advantage in moving heavy loads. In terms of energy efficiency, the motor is classified in the IE3 efficiency class and has an F class heating rating. Additionally, the motor features a closed servo body structure that protects its internal components from external factors, thereby enhancing its durability and supporting long-term operation. The motor is equipped with two NTC (Negative Temperature Coefficient) temperature sensors. These sensors continuously monitor the internal temperature of the motor, providing critical data to ensure the performance and safety of the motor.



Figure 1 Closed body design test motor

The motor is controlled by a long-delay type circuit breaker. This type of circuit breaker is activated to protect the motor when a certain current limit is reached. However, unlike traditional circuit breakers, the long-delay type circuit breaker provides a range limit that varies over time rather than a single current limit. This feature allows for tolerance against temporary current surges that occur when the motor draws

high current during startup, offering more effective protection against sudden and transient load fluctuations that can affect the motor's operation. As a result, it enhances the reliability of the motor while also helping to prevent unnecessary interruptions.

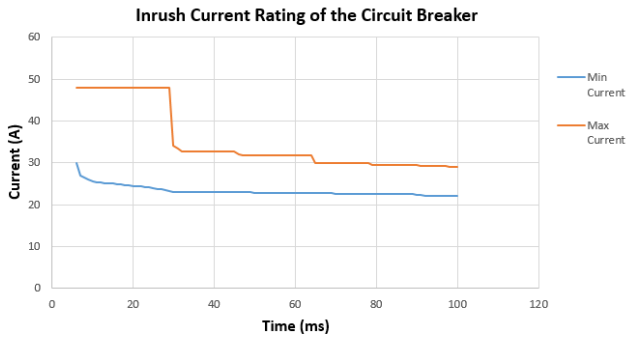


Figure 2 Inrush current rating of the circuit breaker

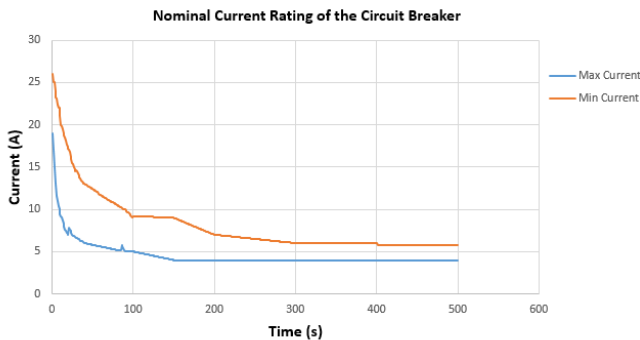


Figure 3 Nominal current rating of the circuit breaker

B. Counter Load Test Setup

A dynamic counter load of 8 N·m has been applied to the motor. A test setup capable of applying this load to the motor has been established. This arrangement is designed to evaluate the performance of the motor under real working conditions and simulates the load the motor will encounter during operation. The dynamic counter load allows for the assessment of how the motor responds to various torque demands and is a critical element for analyzing the motor's behavior, especially under low temperature conditions. The test setup includes all the necessary components to monitor and evaluate the motor's performance. These components consist of load cells, control systems, and data collection equipment. Load cells continuously monitor the dynamic load applied to the motor, while control systems assist in optimizing the motor's operation. Additionally, data collection equipment records the data obtained during the motor's operation, facilitating the gathering of information required for performance analysis.

C. Test Chamber

The test environment was conducted in a test chamber designed to meet military standards. This chamber has been accredited according to MIL-STD-810G, Method 502.5, Procedure II, providing an ideal setting for comprehensively evaluating the motor's performance under low-temperature conditions. The accreditation ensures the compliance and validity of the testing process with international standards,

thereby enhancing the reliability of the data obtained. Additionally, the control systems within the chamber continuously monitor temperature and other environmental parameters, ensuring that the motor is exposed to realistic operating conditions throughout the test duration. This setup allows for a thorough assessment of the motor's functionality and durability in extreme cold, facilitating an accurate analysis of its performance under specified conditions.

D. Test Equipment

During the test, various equipment was used to monitor the motor's performance and record the data obtained. At the start of the test, an oscilloscope was employed to measure the motor's inrush current with greater precision. Since the inrush current is expected to be a short-lived phenomenon occurring within milliseconds, the oscilloscope was chosen for its ability to detect rapid and momentary current fluctuations with high accuracy. Once the motor's current stabilized, the initial measurements taken with the oscilloscope were followed by longer-term and steady current monitoring using a Fluke clamp meter. This process was conducted to verify the current readings under stable operating conditions. The clamp meter monitored the motor's steady-state current levels to detect any deviations in performance during the test.



Figure 4 Current measurement during the test

Thermocouples have been placed on the motor body, and inside the motor, there are two NTC (Negative Temperature Coefficient) sensors. These sensors are used to measure the external body temperature and the internal winding temperature of the motor, collecting crucial data during the test. This setup ensures continuous monitoring of the motor's thermal behavior, allowing for a detailed analysis of the temperature variations affecting both the outer surface and the critical internal components. The motor's circuit breaker box has been placed outside the environmental test chamber. This arrangement was made to prevent the circuit breaker box from being affected by temperature fluctuations, keeping it at a constant room temperature. By doing so, the impact of temperature conditions on the circuit breaker box was eliminated, allowing for a focused evaluation of the motor's performance under low-temperature conditions.

E. Test Procedure

The test motor was evaluated for functionality under low-temperature conditions according to MIL-STD-810G Method 502.5 Procedure I for storage at a constant temperature of -33°C and according to MIL-STD-810G Method 502.5 Procedure II for operation at a constant temperature of -32°C.

The motor was connected to the test bench and followed the test procedure steps at room temperature, during which the data collected was recorded. As no issues were observed, the test chamber was sent to -33°C . According to the thermocouple data connected to the motor body, the temperature was stabilized at -33°C with a tolerance of 2 degrees, and a 6-hour waiting period was completed. During this waiting period, the test setup and the test motor remained unpowered. Following the 6-hour waiting period, the low-temperature operation test of the motor began; the test procedure commenced with 2 minutes of no-load operation, followed by applying a counter load of 8 N·m, which corresponds to 80% of the nominal torque capacity, for 6 minutes. The total test duration of 8 minutes was considered as one cycle. A total of 6 cycles were conducted during the test, which means the motor was operated continuously for 48 minutes. Throughout the test, the motor's operating temperature, current, voltage, and torque values were recorded, and the motor's performance was observed. The obtained data was analyzed to assess the functionality and durability of the motor under low-temperature conditions.

III. RESULTS

The operation test was initiated following a 6-hour waiting period. During the first 2 minutes, the motor was operated in an unloaded condition. Throughout the test, the motor's inrush current was measured at 22 A, with a starting time of 132 ms. In preliminary tests conducted under ambient conditions, the motor's inrush current was recorded at 15 A, and the starting time was measured at 110 ms. These results indicate an increase in the motor's inrush current and an extension of the starting time under test conditions. At the 91st second of the test, the motor's fuse blew, resulting in the interruption of the supply voltage. Concurrently, at the 91st second, the current drawn by the motor was observed to be 5.1 A via a clamp meter. This situation is considered a consequence of the excessive current conditions encountered during the motor's startup process. During the test, it was observed that the current drawn by the motor gradually decreased from 8 A to 5.1 A by the 91st second. This indicates that the current value began to stabilize as the internal structure of the motor warmed up. The test setup was returned to its initial state and restarted. The first cycle was completed with 2 minutes of unloaded operation followed by 6 minutes of loaded operation. During the first cycle, the current drawn by the motor was observed to be 5.1 A. Without any interruption, the second cycle commenced. During this process, the motor casing temperature rose from -35°C to 0°C . The internal sensor data indicated a reading of 9.2°C for the first sensor and 11.3°C for the second sensor.

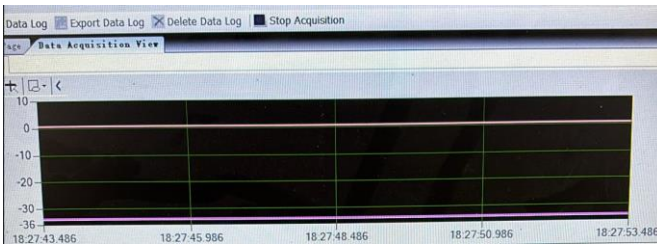


Figure 5 Motor body thermocouple temperature value

After completing the second cycle, the direction of the motor was reversed counterclockwise while transitioning to the third cycle. During the direction change of the motor, the circuit

breaker tripped again. This event occurred as the motor was subjected to sudden load variations during the direction change, leading to an excessive current that triggered the protective mechanism of the circuit breaker. During the direction change of the motor, the current exceeded the fuse trip current of 24 A in conjunction with the counter load. The circuit breaker was reactivated. A 3-second waiting period was added to the test software during the motor's direction change, and the testing process continued accordingly. Starting from the third cycle, the motor successfully completed a total of 6 cycle tests, which corresponds to a duration of 32 minutes. Throughout the testing period, a significant increase in both the casing and internal temperatures of the motor was observed. At the end of the 6th cycle, the motor casing temperature reached 28°C , while the internal temperature rose to 98°C . These temperature increases are considered a result of the loads and environmental factors to which the motor was subjected under operating conditions. A total of 6 cycles were successfully completed in the tests conducted at room temperature. No waiting time was applied during the direction change, and the circuit breaker's overcurrent protection limits were not exceeded. The motor's internal temperature was measured at 68°C , while the body temperature was recorded at 36°C . The starting current was observed to be 16 A for 110 ms, and the maximum nominal current drawn by the motor was recorded at 3.8 A. In the low-temperature conditions, the starting current of the motor was noted to be 22 A for 132 ms. At the 91st second of the test, the circuit breaker cut off the supply due to excessive current draw without a load on the motor. Additionally, when transitioning to the third cycle, the power supply was also cut off due to excessive current during the motor's direction change. A 3-second waiting period was added during this direction change. The test under low-temperature conditions also completed a total of 6 cycles, with the internal temperature of the motor reaching 98°C and the body temperature measured at 28°C . During the test, the nominal current value of the motor started at 8 A and decreased to 4.6 A.

Table 1 Table 1. Test comparison data

Parameter	Room Temperature	Low Temperature Condition
Number of Cycles	6 cycles	6 cycles
Waiting Time	None	3 seconds
Circuit Breaker Status	Overcurrent limit not exceeded	Cut off due to overcurrent
Motor Internal Temperature	68°C	98°C
Motor Body Temperature	36°C	28°C
Starting Current	15 A (110 ms)	22 A (132 ms)
Nominal Current	Maximum 3.8 A	8 A - 4.6 A
Status at 91 Seconds	-	Cut off due to overcurrent
Direction Change Status	-	Cut off due to overcurrent

IV. DISCUSSION

The comparative analysis of tests conducted under room temperature and low temperature conditions reveals significant differences in motor performance and operational

REFERENCES

stability. In the tests carried out at room temperature, the motor successfully completed six cycles without any waiting time during direction changes and did not exceed the circuit breaker's overcurrent protection limits. The internal temperature of the motor was recorded at 68 °C, while the outer casing temperature was noted at 36 °C, indicating effective thermal management under these conditions. The starting current was observed to be 16 A for 110 ms, with a maximum nominal current recorded at 3.8 A, demonstrating the motor's capability to effectively handle the initial load. In contrast, the tests conducted under low temperature conditions presented distinct challenges. The starting current was recorded at 22 A for 132 ms, indicating a significant increase in electrical demand at startup. This led to an overcurrent situation at the 91st second when the motor was unloaded, resulting in the circuit breaker tripping. A similar overcurrent condition was observed during the motor's direction change before proceeding to the third cycle, necessitating a 3-second waiting time. Under low temperature conditions, the internal temperature of the motor rose to 98 °C, while the casing temperature was measured at 28 °C, indicating that the motor was subjected to significant stress. During the testing period, the nominal current decreased from 8 A to 4.6 A, which is correlated with the increase in internal motor temperature and rising electrical resistance over time. Rapid changes in internal and external temperatures during motor operation, particularly in low temperature conditions, can lead to condensation formation and short-term leakage current situations. The heating associated with low temperature conditions may cause the moisture in the air to condense, resulting in accumulation within motor components and a decrease in electrical conductivity. Condensation can lead to water pooling in critical parts, especially in the electric motor windings, triggering electrical problems such as short circuits and failures. Short-term leakage currents are directly related to this condensation, causing unwanted electrical currents to develop.

V. CONCLUSION

In conclusion, the comparative analysis of tests conducted under room temperature and low-temperature conditions has highlighted significant factors affecting motor performance and reliability. At room temperature, the motor successfully completed six cycles without any waiting time during direction changes, demonstrating effective thermal management. However, the challenges encountered under low-temperature conditions raise concerns about the operational reliability of the motor and negatively impact its performance. Notably, the increased starting current and the resulting instances of overcurrent in low-temperature conditions create stress on critical motor components, raising the potential risk of failure. Furthermore, considering the relationship between rapid temperature changes and condensation within the motor, the occurrence of short-duration leakage currents cannot be overlooked. These findings indicate the necessity for optimizing motor design and operational conditions to account for such scenarios. Thus, this research provides essential data that can guide future efforts aimed at improving motor performance and reliability. Consequently, it is critical to comprehensively evaluate environmental factors and temperature management strategies to ensure that motors can operate safely and efficiently under low-temperature conditions.

- [1] "Applications of induction motors," *Electrical and Computer Engineering*, pp. 128-167, 2004. doi:10.1201/9781420030815.ch5.
- [2] J. Smith and R. Davis, "Induction Motors in Harsh Environments: Military Applications," *Defense Technology Review*, 2016.
- [3] K. Thompson and D. Baker, "Maintenance-Free Induction Motors in Military Applications," *Defense Engineering Journal*, 2017.
- [4] L. Zhang and X. Yu, "Noise Reduction in Electric Motors: A Study on Military Submarines," *Journal of Military Engineering*, 2019.
- [5] A. Patel and M. Kor, "High Starting Torque Induction Motors for Armored Vehicles," *Military Vehicle Technology Journal*, 2020.
- [6] L. Johnson and A. Patel, "Energy Efficiency in Military Electric Drive Systems," *IEEE Transactions on Military Technology*, vol. 5, no. 4, pp. 305-314, 2019.
- [7] N. E. O. F. W., "Squirrel Cage Induction Motors: A Review of Performance in Harsh Environments," *Journal of Electric Power Systems*, 2018.
- [8] K. R. Ranjan and S. K. Jain, "Challenges in the Speed Control of Squirrel Cage Induction Motors," *International Journal of Electrical Engineering and Technology*, vol. 9, no. 1, pp. 15-24, 2018.
- [9] M. H. Rashid, "Performance Analysis of Squirrel Cage Induction Motors under Different Load Conditions," *IEEE Transactions on Industry Applications*, vol. 55, no. 3, pp. 2385-2392, 2019.
- [10] J. H. Wang and L. T. Lee, "Thermal Performance Analysis of Squirrel Cage Induction Motors," *Journal of Electrical Engineering and Technology*, vol. 17, no. 1, pp. 102-111, 2022.
- [11] M. H. Rashid and H. P. Das, "Effects of Low Temperature on Induction Motor Lubrication," *IEEE Transactions on Industry Applications*, vol. 54, no. 2, pp. 1680-1685, 2018.
- [12] R. S. Kumar and A. K. Gupta, "Impact of Low Temperatures on Starting Torque of Induction Motors," *International Journal of Electrical Engineering & Technology*, vol. 10, no. 1, pp. 45-53, 2019.
- [13] J. H. Wang and M. K. Li, "Thermal Analysis of Squirrel Cage Induction Motors Under Low Temperature Conditions," *Journal of Thermal Engineering*, vol. 6, no. 1, pp. 200-209, 2020.
- [14] A. P. Singh and B. R. Sharma, "Energy Efficiency Challenges for Induction Motors in Cold Environments," *International Journal of Energy Research*, vol. 45, no. 9, pp. 1230-1240, 2021.
- [15] K. R. Ranjan and S. K. Jain, "Material Degradation of Insulation in Induction Motors at Low Temperatures," *Journal of Electrical Materials*, vol. 41, no. 4, pp. 1034-1042, 2022.
- [16] U.S. Department of Defense, "MIL-STD-810G, Method 502.5, Procedure II," 2014.
- [17] D. G. L. Shires and D. J. Adams, "Thermal Performance of Induction Motors in Low Temperature Applications," *IEEE Transactions on Industrial Electronics*, vol. 63, no. 5, pp. 2946-2954, 2016.
- [18] M. S. V. R. Mohan, "Electrical Failures in Induction Motors: Causes and Prevention," *IEEE Industrial Applications Society Annual Meeting*, pp. 1-8, 2018.

Failure Mechanisms in Enclosed Electric Motors Due to Insufficient Cooling at High Temperatures

Gizem Fırat^{1*}

¹*Koluman Otomotiv Endüstri A.Ş., University of Turkish Aeronautical Association, Ankara, Turkey*
^{*}*(gizem.firat@koluman.com)*

Abstract – This study examines the failure mechanisms of a three-phase AC induction electric motor with a closed body design, intended to provide IP protection, due to insufficient cooling under high-temperature conditions. Overheating at elevated temperatures adversely affects the motor's performance, leading to the deterioration of insulation materials and ultimately motor failures. The cooling performance of the motor, designed to rely on convection through its closed body design, has been evaluated in detail. During the experiments, temperature data were continuously recorded on both the inner and outer surfaces of the motor. The motor was operated at regular intervals under an 80% load, and its cyclic performance was monitored. The study also analyzed the effects of inadequate cooling on the motor's cycle life using analytical methods. The research findings aim to provide strategic recommendations for design and operational processes to improve the reliability of electric motors, particularly those used in military and industrial applications.

Keywords – *Electric motors, Enclosed motor body, High temperature conditions, Accelerated life analysis, Overheating*

I. INTRODUCTION

Electric motors are widely used in various fields, including industrial automation, transportation, and numerous engineering applications. These motors have become an essential part of modern technology due to their high efficiency and compact design advantages. However, the performance of these motors can vary significantly depending on operating conditions, particularly temperature levels. Electric motors operating at high temperatures may encounter several issues, such as wear and degradation of motor components. Insufficient cooling can lead to overheating in critical motor parts, which may trigger motor failures. High temperatures can negatively affect motor windings, insulation materials, and bearings, reducing overall efficiency and shortening the service life of the motor. Additionally, overheating due to insufficient cooling can result in electrical malfunctions, short circuits, and mechanical damage [1]. Enclosed electric motors play a crucial role in military systems, providing high durability and reliability under demanding conditions. These motors are designed to operate in harsh environmental conditions, making ingress protection (IP) ratings, particularly IP 67 and above, essential. IP protection ratings indicate the degree of protection that motors offer against external factors, particularly water and dust. Military applications often involve systems exposed to significant amounts of dust, water, humidity, and other challenging climatic conditions. Therefore, enclosed motor designs are vital to enhancing motor performance and longevity. These designs protect internal components through robust sealing features [2]. The impact of high temperatures on motor performance is a critical issue, particularly in military applications. Electric motors typically perform optimally

within specific temperature ranges, depending on the operating conditions. However, high temperatures can cause thermal stress and wear in internal motor components, leading to decreased efficiency, power losses, and long-term failures. Enclosed motors face thermal management challenges under high-temperature conditions, which can result in performance loss and reduced motor lifespan. The effects of high temperatures include the degradation of insulation materials, changes in the viscosity of lubricants, and deformation of mechanical components. Therefore, understanding the impact of high temperatures on motor performance is crucial for optimizing motor design and maintenance processes [3]. Thermal management involves controlling the temperature of internal motor components and ensuring that these components remain within their optimal operating temperature range. Cooling techniques can range from passive methods, such as natural cooling, to active cooling systems. Natural cooling dissipates heat by exposing the motor's exterior surface to air, but this method is generally inadequate for high-power motors. As a result, active cooling techniques, such as fan cooling or liquid cooling systems, provide more effective solutions [4]. High temperatures can adversely affect the performance of critical components, such as windings, bearings, and other vital motor parts. The thermal properties of materials used in motor design play a significant role in thermal management. Consequently, motor manufacturers continuously research new technologies and materials to develop and optimize thermal management strategies [5]. In AC induction motors, heat generation mechanisms stem from various physical and electrical processes during motor operation. These mechanisms lead to the heating of motor components, impacting the motor's performance, efficiency, and durability. The energy loss that occurs as current passes

through the resistance of the windings is one of the most significant factors contributing to motor heating. This loss, also known as Joule loss, is expressed as the square of the current multiplied by the resistance. Higher current values result in increased heat generation in the windings [1]. Magnetic losses occur in the stator and rotor cores of the motor. These losses consist of two primary components: hysteresis loss and eddy current loss. Hysteresis loss arises from the continuous change in the direction of the magnetic field, causing internal losses within the magnetic material. Eddy current loss results from circular currents induced within the core by the rotating magnetic field [6]. Mechanical losses are caused by friction between the moving parts of the motor and air resistance. Bearings, gears, and other mechanical components contribute to friction, which impacts motor performance and generates heat. Additionally, air resistance during rotor movement contributes to heat generation [7]. The insulation materials used in motor windings must operate effectively within a specific temperature range. High temperatures can cause the degradation of insulation materials, resulting in overheating of motor components. Insufficient insulation exacerbates heat generation mechanisms, leading to motor failures [8]. Motor operation under load is another critical factor that affects heat generation. When a motor operates under high load, it draws more current, which generates more heat in the windings and magnetic components. This heating can lead to motor overheating and potential failures [9]. This study aims to examine the failure mechanisms that enclosed electric motors face due to insufficient cooling at high temperatures. By addressing these issues, the study seeks to highlight the effects of these problems on motor performance and reliability, providing valuable insights into improving motor design, cooling strategies, and overall operational efficiency in various engineering and military applications.

II. MATERIALS AND METHOD

This study aims to examine the failure mechanisms encountered by enclosed electric motors under high-temperature conditions. Specifically, it focuses on the thermal stress, wear, and electrical failures that arise in the motor's internal components due to insufficient cooling. The tests are designed to assess motor performance at elevated temperature levels, analyze the effectiveness of cooling methods, and determine the durability of motor components. The materials used in the study and the methods followed are detailed below.

A. Test Motor

The motor utilized in this study is a 3-phase squirrel cage induction motor, powered by a 400V alternating current (VAC) supply. It features a 4-pole design and operates with a star connection configuration, which helps reduce the starting current, resulting in smoother operation and improved performance. The motor's rated speed is 1445 rpm, a critical parameter that directly influences its operational efficiency. Its rated power output is 1.5 kW, indicating the motor's capability to effectively manage a specified load. The motor's torque capacity is specified at 10 Newton-meters (N·m), reflecting its ability to handle significant loads, and its high torque during start up offers a notable advantage for moving heavy objects. In terms of energy efficiency, the motor belongs to the IE3 efficiency class and has a heating rating of Class F. Additionally, its closed servo body design shields the internal

components from external elements, enhancing its durability and enabling reliable, long-term operation. The motor is also equipped with two NTC (Negative Temperature Coefficient) temperature sensors, which continuously monitor its internal temperature, providing vital data for ensuring optimal performance and safety.



Figure 1 Test motor

B. NTC Sensors

NTC (Negative Temperature Coefficient) sensors are passive components that exhibit a decrease in resistance as temperature increases, and they are widely used in electric motors and various industrial applications. These sensors are made from semiconductor materials and play a crucial role in monitoring the internal temperatures of motors due to their sensitivity to temperature changes. NTC sensors are known for their low cost, fast response times, and high accuracy. The working principle is based on the reduction of sensor resistance as temperature rises, and this change is monitored through a voltage divider circuit. By continuously tracking motor temperatures, excessive overheating conditions can be prevented when temperatures exceed a certain threshold. The use of NTC sensors ensures the safe and efficient operation of electric motors while preventing damage caused by overheating [10]. Temperature measurements are carried out using NTC (Negative Temperature Coefficient) sensors. Due to their inherent structure, NTC sensors exhibit a parabolic curve at high temperatures, meaning that even the smallest changes in temperature can lead to significant variations. Specifically, calibration offsets need to be applied after reaching a temperature of 90 °C. In this study, two NTC sensors are integrated within the enclosure of a squirrel cage AC induction motor. These sensors were calibrated prior to the commencement of the testing process.

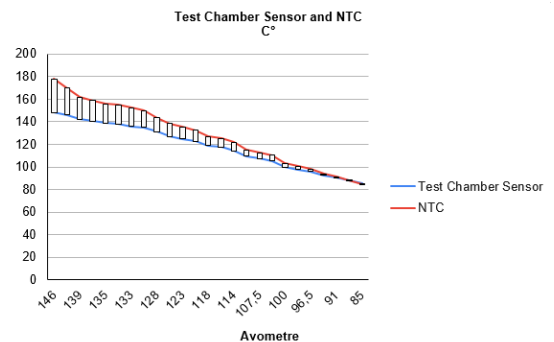


Figure 2 Test chamber sensor and NTC sensor data

C. Counter Load Test Setup

A dynamic counter load of 8 N·m has been applied to the motor during high-temperature testing conditions. A specialized test setup has been developed to impose this load on the motor, which is intended to evaluate its performance under realistic operating scenarios, simulating the actual loads the motor is expected to face. This dynamic counter load is essential for analyzing how the motor reacts to varying torque requirements, particularly in high-temperature environments. The testing apparatus is equipped with all the necessary components to monitor and assess the motor's performance effectively. This includes load cells that continuously track the dynamic load exerted on the motor, control systems that aid in optimizing motor operation, and data acquisition devices that capture the information gathered throughout the motor's functioning, enabling a thorough performance evaluation.

D. Test Chamber

The testing was carried out in a chamber specifically designed to comply with military standards. This chamber has been certified according to MIL-STD-810G, Method 501.5, Procedure II, creating an optimal environment for thoroughly assessing the motor's performance under high-temperature conditions. This certification guarantees that the testing process adheres to international standards, thereby increasing the credibility of the acquired data. Furthermore, the chamber's control systems continuously monitor temperature and other environmental factors, ensuring that the motor operates under realistic conditions throughout the entire testing period. This configuration enables a comprehensive evaluation of the motor's functionality and resilience in extreme heat, allowing for precise analysis of its performance under the defined parameters.

E. Test Equipment

The materials used for this test include a closed-body squirrel cage AC induction motor, a thermocouple for acquiring temperature data from the motor casing, two NTC sensors located inside the motor, and control software that monitors the motor's temperature. The thermocouple continuously tracks the external surface temperature of the motor, providing critical data. The NTC sensors measure the internal temperature of the motor, supplying necessary information for performance analysis. The control software monitors the temperature throughout the test and reports an error, halting the test if a temperature above 135 °C is detected. These materials are vital for the safe and effective evaluation of the motor under high-temperature conditions.

F. Test Procedure

The test motor was assessed for functionality under high-temperature conditions following the guidelines of MIL-STD-810G Method 501.5 Procedure I for storage at a constant temperature of +63°C and MIL-STD-810G Method 501.5 Procedure II for operation at +50°C. Initially, the motor was connected to the test bench, and the procedural steps were carried out at room temperature, during which the relevant data was recorded. With no issues observed, the test chamber was adjusted to maintain a temperature of +63°C. Based on the thermocouple readings affixed to the motor casing, the temperature was stabilized at +63°C with a tolerance of 2 degrees, and a 4-hour acclimatization period was completed. Throughout this waiting phase, both the test setup and the

motor remained unpowered. After the 4-hour waiting period, the temperature of the test chamber was reduced to +50°C. It was expected that the temperature reading taken from the motor casing would stabilize within a tolerance of 2 degrees. Once the temperature value was stabilized, a 2-hour waiting period was implemented. After the 4-hour waiting period, the high-temperature operation test for the motor began. The test protocol initiated with 2 minutes of operation under no load, followed by the application of a counter load of 8 N·m, which is 80% of the nominal torque capacity, for a duration of 6 minutes. This 8-minute duration was classified as one complete cycle. In total, 6 cycles were performed during the testing phase, resulting in the motor running continuously for a total of 48 minutes. Throughout this period, measurements of the motor's operating temperature, current, voltage, and torque values were recorded, allowing for close observation of the motor's performance. The collected data was then analyzed to evaluate the motor's functionality and durability when subjected to high-temperature conditions.

III. RESULTS

The operational testing commenced after a 6-hour waiting phase. For the initial 2 minutes, the motor was run without any load applied. At the beginning of the test process, the internal temperature of the motor was determined to be 50 °C based on the data obtained from the NTC sensor. Similarly, the temperature of the motor body was also measured at 50 °C according to the thermocouple data. Since the motor has an insulation class of F, the test software was set with a maximum temperature threshold of 135 °C. This setting establishes a critical limit for the safe operation of the motor. During the initial phase of the test, the motor was operated in an unloaded condition for 2 minutes. This unloaded operation is an important step for evaluating the basic functionality of the motor and for identifying any potential issues at the outset. As no problems were observed during the unloaded operation, the test progressed to the next stage. Subsequently, in order to realistically simulate the working conditions of the motor, a counter load of 8 N·m was applied, and the motor was operated for 6 minutes. During this phase, the performance of the motor under load was carefully monitored. When the motor began operating under load, the NTC sensor indicated that the internal temperature of the motor was 73 °C. This temperature serves as a significant reference point for the operational conditions of the motor at the start. At the end of the first cycle, the internal temperature of the motor reached 103 °C. Upon reaching this temperature, the rapid increase in the motor's temperature was regarded as a critical engineering concern. Therefore, it was decided to add a 1-minute waiting period at the end of each cycle in the software. This waiting period aims to help stabilize the temperature values of the motor at a more consistent level. After the waiting period, the motor began the second cycle at 99 °C and completed it at 120 °C. The motor was then allowed to rest again for 1 minute. The motor started the third cycle at 115 °C and reached a temperature of 136 °C during this cycle. This temperature indicates that the motor requires further cooling. At the end of the third cycle, the data from the motor's temperature sensor exceeded 135 °C, prompting an update in the software to raise the maximum protection limit to 155 °C. After applying a 1-minute waiting period, the motor began the fourth cycle at 121 °C and completed it at 147 °C. Following another minute of waiting, the motor started the fifth cycle at 138 °C. However, this cycle

was halted by the software at the 302nd second due to the motor temperature exceeding 155 °C. Throughout the test process, the motor body temperature gradually increased to 85 °C. At this stage, the burning varnish odor emanating from the motor connector covers indicated that the motor was overheating and signaled a potential failure condition; therefore, the test was immediately halted. The test chamber was returned to room temperature, and temperature measurements from the motor body continued during this process. The test chamber reached room temperature in approximately 3 hours. By the end of this period, the surface temperature data collected from the chamber and reference samples measured 36 °C. However, the motor body's temperature was recorded at approximately 63 °C during this time. After returning to room temperature, the cooling process of the motor body was monitored. After a 1-hour waiting period, the temperature measurement indicated that the motor body temperature had decreased to 52.8 °C.



Figure 3 Motor body temperature measurement

Ultimately, following a total of 5 hours at room temperature, the motor body reached 28 °C, leading to the finalization of the test. The performance of the motor under high-temperature conditions was carefully monitored, particularly in relation to the temperature increase and the burning odor from the connectors. These observations raise questions about the effectiveness of the motor's cooling system and highlight the need for further improvements.

Table 1 High temperature test results

Phase & Waiting Time / Load Condition	Temperature (°C)	Software Warning
Initial State (No Load)	50	-
1st Cycle (Under Load: 8 N·m, 1 min wait)	73 → 103	-
2nd Cycle (Under Load: 8 N·m, 1 min wait)	99 → 120	-
3rd Cycle (Under Load: 8 N·m, 1 min wait)	115 → 136	Exceeded 135 °C, updated to 155 °C
4th Cycle (Under Load: 8 N·m, 1 min wait)	121 → 147	-
5th Cycle (Under Load: 8 N·m)	138 → >155	Test Stopped

IV. DISCUSSION

In this study, the performance of the motor under high-temperature conditions has been examined in detail. At the beginning of the testing process, it was observed that the internal temperature of the motor was 50 °C, which was confirmed by the data from the NTC sensors. During the first phase of the test, the motor was operated in an unloaded condition, and since no issues were observed, the performance of the motor was evaluated under realistic operating conditions. The tests conducted under load revealed the potential for the motor to overheat and provided critical data regarding the reliability of the motor. The rapid increase in the motor's temperature is a matter that must be considered from an engineering perspective. Notably, during the first cycle, the motor's temperature reached 103 °C, and it was observed that the one-minute waiting periods added at the end of each cycle were an effective method for controlling the temperature rise. However, at the end of the third cycle, the motor's temperature exceeded 135 °C, raising significant concerns about the effectiveness of the cooling system. Updating the maximum protection level in the software to 155 °C was one of the precautions taken to ensure the safe operation of the motor. Nevertheless, the motor's temperature exceeding 155 °C during the fifth cycle indicates that the motor design and cooling system require further improvements. Due to the high IP protection ratings frequently demanded in military systems, motor body designs have evolved into fully enclosed structures. While high IP protection requirements provide resistance to dust and sand and ensure leakage protection, they can negatively impact motor performance and lifespan. This study has highlighted the adverse effects of operating a fully enclosed AC induction motor solely relying on surface cooling (convective cooling). These findings assist in identifying the necessary requirements for improving the durability and performance of the motor under high-temperature conditions. Developing a more effective cooling system against overheating situations will enhance the overall efficiency of the motor.

V. CONCLUSION

In conclusion, this study has comprehensively evaluated the performance of the AC induction motor under high-temperature conditions. Throughout the testing process, the motor was operated with a starting internal temperature of 50 °C, and excessive heating tendencies were observed during load tests. The one-minute waiting periods applied at the end of each cycle helped control the temperature increase; however, the motor exceeding 135 °C during the third cycle raised concerns about the effectiveness of the cooling system. The adjustment of the software's maximum protection level to 155 °C stands out as a protective measure. It has been emphasized that fully enclosed motor designs are beneficial for meeting high IP protection requirements, yet they also introduce thermal management issues. These findings highlight the need for improved cooling solutions to enhance the durability of motors under high-temperature conditions. Future studies should focus on optimizing designs and cooling systems to ensure the reliable operation of motors in extreme conditions.

REFERENCES

- [1] M. H. Rashid, "Performance Analysis of Squirrel Cage Induction Motors under Different Load Conditions," *IEEE Transactions on Industry Applications*, vol. 55, no. 3, pp. 2385-2392, 2019.
- [2] J. Smith and R. Davis, "Induction Motors in Harsh Environments: Military Applications," *Defense Technology Review*, 2016.
- [3] M. S. V. R. Mohan, "Electrical Failures in Induction Motors: Causes and Prevention," in *Proceedings of the IEEE Industrial Applications Society Annual Meeting*, pp. 1-8, 2018.
- [4] S. K. Jain and K. R. Ranjan, "Cooling Techniques for Electric Motors," *International Journal of Electrical Engineering and Technology*, vol. 9, no. 1, pp. 15-24, 2018.
- [5] T. K. Gupta, "Advancements in Cooling Technologies for Induction Motors," *Journal of Electrical Engineering and Technology*, vol. 17, no. 3, pp. 215-222, 2020.
- [6] A. P. Singh and B. R. Sharma, "Energy Efficiency Challenges for Induction Motors in Cold Environments," *International Journal of Energy Research*, vol. 45, no. 9, pp. 1230-1240, 2021.
- [7] K. R. Ranjan and S. K. Jain, "Challenges in the Speed Control of Squirrel Cage Induction Motors," *International Journal of Electrical Engineering and Technology*, vol. 9, no. 1, pp. 15-24, 2018.
- [8] J. H. Wang and M. K. Li, "Thermal Analysis of Squirrel Cage Induction Motors Under Low Temperature Conditions," *Journal of Thermal Engineering*, vol. 6, no. 1, pp. 200-209, 2020.
- [9] S. K. Jain, "Cooling Techniques for Electric Motors," *International Journal of Electrical Engineering and Technology*, vol. 9, no. 1, pp. 15-24, 2018.
- [10] J. Lee and J. Hwang, "Performance Analysis of NTC Thermistors for Motor Temperature Control," *Journal of Electrical Engineering & Technology*, vol. 11, no. 2, pp. 576-582, 2016.

MOSFET H Köprüsü ile Asenkron Motor Sürücü PCB Tasarımı

Enes Şahiner^{1*}, Can Kaya¹ ve Tuncay Soylu¹

¹Elektrik-Elektronik Mühendisliği, Samsun Üniversitesi, Samsun, Türkiye
*enesahiner@gmail.com

Özet – Bu çalışma, Sinüzoidal Darbe Genişlik Modülasyonu (SPWM) tekniği kullanılarak çok alanlı simülasyon ve model tabanlı tasarım için bir blok diyagram ortamı olan MATLAB/SIMULINK platformunda MOSFET H köprüsü kullanılarak gerçekleştirdiğimiz asenkron motor sürücü tasarımımızın Baskı Devre (PCB) tasarımına odaklanmaktadır. Çalışmanın ana amacı maksimum verim elde etmek ve düşük maliyet sağlamaktır. Bu hedefe ulaşmak, asenkron motoru sürmek için gerekli olan motor sürücü tasarımına ek olarak, PCB tasarımında kullanılan malzemelerin seçim nedenleri ve bu malzemelerin diğer alternatiflere göre sağladığı teknik ve maliyet avantajları ayrıntılı şekilde ele alınmaktadır. Ayrıca, tasarlanan bu sistemin üretim sürecinde düşük maliyetle maksimum verimi elde etmek amacıyla detaylı bir malzeme kalem bazlı yaklaşık fiyat analizi gerçekleştirilmiştir. Kullanılan komponentlerin hem performans hem de dayanıklılık açısından en uygun olanlarının seçilmesi, tasarım sürecinin önemli bir aşaması olarak ele alınmıştır. Tasarım süreci boyunca yapılan analizler, maliyet-etkin, yüksek performanslı ve uzun ömürlü bir motor sürücü sistemi oluşturmayı amaçlamaktadır. Ayrıca bu sistemin çevresel etkileri ve sürdürülebilirliği de göz önünde bulundurulmuştur.

Anahtar Kelimeler – H köprüsü, Asenkron motor, PCB tasarımı, Motor sürücü, Düşük maliyet

Asynchronous Motor Driver PCB Design with MOSFET H Bridge

Abstract – This study focuses on the Printed Circuit (PCB) design of our asynchronous motor drive design using MOSFET H-bridge in MATLAB/SIMULINK platform, a block diagram environment for multi-domain simulation and model-based design using Sinusoidal Pulse Width Modulation (SPWM) technique. The main objective of the study is to achieve maximum efficiency and low cost. To achieve this goal, in addition to the motor driver design required to drive the induction motor, the reasons for the selection of the materials used in the PCB design and the technical and cost advantages of these materials over other alternatives are discussed in detail. In addition, a detailed material item-based approximate price analysis has been carried out in order to achieve maximum efficiency at low cost in the production process of this designed system. The selection of the most suitable components in terms of both performance and durability is considered as an important stage of the design process. The analyses performed throughout the design process aim to create a cost-effective, high-performance and long-lasting motor drive system. Environmental impacts and sustainability of this system have also been taken into consideration.

Keywords – H bridge, Induction motor, PCB design, Motor driver, Low cost

I. GİRİŞ

Asenkron motor sürücüleri, endüstriyel uygulamalarda yaygın olarak kullanılan ve yüksek verimlilik sağlayan elektrik motorlarıdır. Bu motorların kontrolü ve optimizasyonu üzerine yapılan araştırmalar, hem enerji tasarrufu hem de performans iyileştirmesi açısından büyük önem taşımaktadır. Literatürde, asenkron motorların verimliliğini artırmak için çeşitli yöntemler ve kontrol teknikleri önerilmektedir.

Birçok çalışmada, asenkron motorların enerji verimliliğini artırmak için matematiksel modelleme ve optimizasyon yöntemleri kullanılmaktadır. Örneğin, Pirmatov ve arkadaşları, asenkron motorların statik ve dinamik modlarının elektromanyetik enerji dönüşümündeki enerji tasarrufu yöntemlerini belirlemişlerdir [1]. Ayrıca, Zhang ve ekibi, modelden bağımsız adaptif doğrudan tork kontrolü (DTC) yöntemini tanıtarak, asenkron motorların hız düzenlemesinde sistemin dayanıklılığını artırmayı hedeflemişlerdir [2]. Bu tür

kontrol yöntemleri, motorun performansını artırmak için kritik öneme sahiptir.

Asenkron motorların verimliliğini optimize etmek için kullanılan bir diğer yöntem, parçacık sürüsü algoritmasıdır. Tong, bu yöntemi kullanarak asenkron motorların verimliliğini artırmanın yollarını araştırmıştır [3]. Ayrıca, Wang, üç fazlı asenkron motorlar için doğrudan tork kontrolü teknolojisini gelişimini incelemiş ve bu teknolojinin, vektör kontrolünden sonra gelen yüksek performanslı AC hız düzenleme teknolojisi olduğunu belirtmiştir [4]. Bu tür yenilikçi kontrol yöntemleri, motorların daha verimli çalışmasını sağlamaktadır.

Asenkron motorların kontrolü, genellikle karmaşık bir yapıya sahiptir. Yang ve arkadaşları, manyetik alan modülasyonu prensibi ve asenkron manyetik bağlantının iletim oranını hesaplama üzerine çalışmalar yapmışlardır [5]. Bu tür çalışmalar, motorların daha stabil ve güvenilir bir şekilde çalışmasını sağlamak için önemlidir. Ayrıca, Gong ve Li, asenkron motorların vektör kontrolü üzerine simülasyon

araştırmaları yapmış ve bu motorların kontrolündeki zorlukları ele almışlardır [6].

Asenkron motor kontrolünde yapay zeka ve bulanık mantık gibi modern yöntemlerin kullanımı da artmaktadır. Örneğin, Kirankumar ve arkadaşları, çok seviyeli inverter ile alan yönlendirmeli kontrolü incelemişlerdir [7]. Bu tür yenilikçi yaklaşımlar, motor kontrol sistemlerinin daha esnek ve dayanıklı olmasını sağlamaktadır.

Sonuç olarak, asenkron motor sürücüleri üzerine yapılan araştırmalar, enerji verimliliği, kontrol teknikleri ve optimizasyon yöntemleri açısından zengin bir literatüre sahiptir. Bu çalışmalar, asenkron motorların endüstriyel uygulamalardaki performansını artırmak için kritik öneme sahiptir.

Bu çalışmada Sinüzoidal Darbe Genişlik Modülasyonu (SPWM) tekniği kullanılarak MATLAB/SIMULINK ortamında tasarlanan H köprüsü ile asenkron motor sürücü tasarımının maksimum verim ve düşük maliyetle gerçekleştirilmesini konu almaktadır. Asenkron motor sürücü tasarımında kullanılan malzemelerin seçim nedenleri, maliyet analizleri ve tasarımın detayları ayrıntılı bir şekilde ele alınmıştır. Amacımız, üç faz asenkron motor sürücüsü olarak işlev gören entegre ve çok yönlü bir PCB devresi tasarlamak ve geliştirmektir. Bu bağlamda, motor sürücüsü ve kontrol yapıları, iletişim ve veri depolama çözümleri, görselleştirme ve kontrol arayüzleri, kullanıcı etkileşimi ve güç ölçüm modüllerine dair kapsamlı bilgiler sunulmuştur. Çalışmamız, hem akademik araştırmalar hem de endüstriyel uygulamalar için uygun, yüksek verimli ve güvenilir bir platform oluşturarak, gelecekteki projeler için önemli avantajlar sağlamayı hedeflemektedir.

II. MATERYALLER VE METHOD

Bu kısımda, kullanılan donanım ve malzemeler, PCB tasarım süreci ve prototip üretimi ve test aşamaları yer almaktadır.

A. Kullanılan Donanım ve Malzemeler

1) STM32F103C8T6 Mikrodenetleyici

Projede kullandığımız STM32F103C8T6 mikroişlemcisi STMicroelectronics tarafından üretilen bir mikroişlemci olup tercih edilmesinde ARM Cortex-M3 mimarisi ve sunduğu geliştirme ortamları büyük rol oynamaktadır. Yaptığımız projenin SPI, I2C, CAN Bus, Timerlar ve I/O gibi gereksinimleri yukarıda belirtilen özelliklerden yola çıkarak minimum maliyetle maksimum verim elde edilebilmesi amacı ile projemizde kullanılmak üzere STM32F103C8T6 mikroişlemcisi tercih edilmiştir.



Şekil 1. STM32F103C8T6

Aynı serinin STM32F103C4 mikroişlemcisinin maliyeti daha düşük olmasına rağmen CAN Bus iletişim protokolü bulunmadığından dolayı proje için uygun görülmemiştir.

2) OLED Ekran

Projemizde, 128x64 çözünürlüğe sahip 0.96 inç OLED grafik ekran kullanılmıştır. Bu ekranın tercih sebebi I²C bağlantısının bulunması, bu bağlantı ile yüksek hızlı veri iletimi sağlayarak ekranın hızlı ve verimli bir şekilde güncellenmesini mümkün kılmaktadır. Ayrıca LCD yerine OLED tercih edilme nedeni kendi ışığını üretmesi, arka ışık gerektirmemesi ve bu sayede düşük güç tüketimi sağlayarak adaptör ömrünün uzaması sağlamıştır.



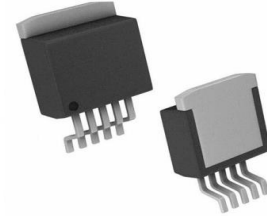
Şekil 2. OLED Ekran

3) Buck Converter

Çeşitli bileşenler için gerekli olan farklı voltaj seviyelerini sağlamak amacıyla projemizde farklı tip iki adet Buck converter kullanılmıştır.

3.1 LM2596S-5

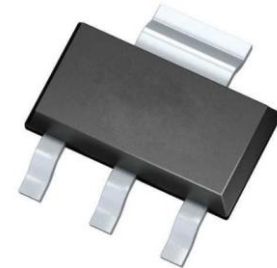
LM2596S-5.0, anahtarlama bir regülatör olup 12V'luk giriş gerilimini 5V'a düşürmek için kullanılmıştır. Bu regülatörün kullanılma amacı daha yüksek akım gereksinimi karşılamak, anahtarlama yapısı sayesinde enerji verimliliği sunarak ısınma problemlerini minimumda tutmaktır.



Şekil 3. LM2596S-5

3.2 AMS1117-3.3

AMS1117-3.3, lineer regülatör olup projemizde 12V'luk giriş gerilimini 3.3V'a düşürmek için kullanılmaktadır. Mikrodenetleyici ve sensör gibi düşük voltaj gereksinimi olan bileşenlere enerji sağlamaktadır.

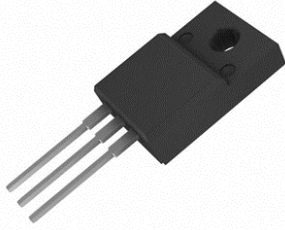


Şekil 4. AMS1117-3.3

4) MOSFET

Projemizde, anahtarlama uygulamaları için FCPF099N65S3 MOSFET kullanılmıştır. Projede bu MOSFET'in tercih edilme sebebi diğer MOSFET'lere kıyasla yüksek akım ve

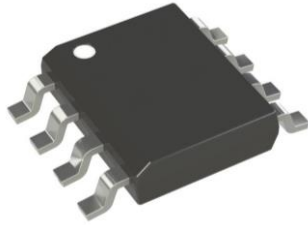
gerilim uygulamaları için uygun olması, Düşük Rds(on) ile ısınma problemlerinin minimize edilmesidir.



Şekil 5. FCPF099N65S3

5) Gate Driver

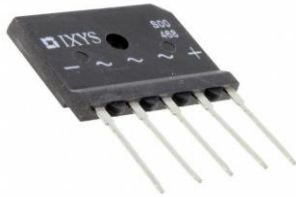
FCPF099N65S3 gibi yüksek akımlı MOSFET'leri 6A'lık çıkış akımı ile etkin bir şekilde sürebilme yeteneği sayesinde projemiz için TC4420COA gate driver'ı uygun görülmüştür. FCPF099N65S3 MOSFET için en az 13V gate sürücü gerilimi önerilmekte olup TC4420COA'nın 3V ila 18V arasındaki giriş gerilimide bu gereksinimi karşılamaktadır. Ayrıca aşırı akım koruması ve termal kapanma gibi güvenlik özellikleriyle öne çıkmaktadır.



Şekil 6. TC4420COA.

6) Doğrultucu

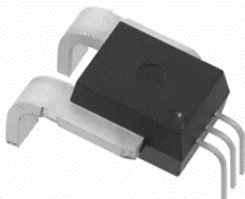
Yüksek verimli güç dönüştürme ve doğrultma işlemleri için DMA40U1800GU doğrultucusu kullanılmıştır. Motor sürücü sisteminizin temel bileşenlerinden biri olup üç fazlı AC gerilimi doğru gerilime (DC) dönüştürmekte ve motorumuz için gerekli gücü elde etmemize yardımcı olmaktadır.



Şekil 7. 238-DMA40U1800GU-ND.

7) Akım Sensörü

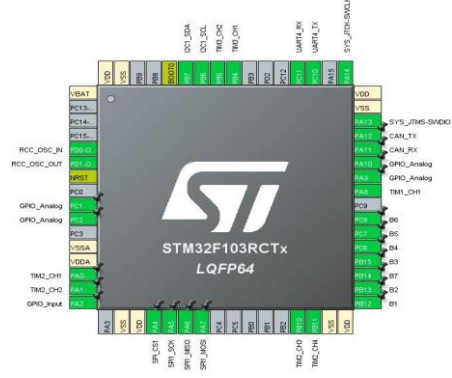
ACS758xCB-100B yüksek akım ölçümü için tasarlanmış olan bir akım sensörüdür. Projemizde motorun besleme akımını ölçmek için kullanılmaktadır. Akım ölçümü, motorun performansını değerlendirmek ve olası aşırı akım durumlarında koruma sağlamak için kritik öneme sahiptir. Ayrıca kullandığımız bu sensör AC ve DC akımlarını hassas bir şekilde ölçme yeteneğine sahip olup endüstriyel uygulamalar için kullanımı uygundur.



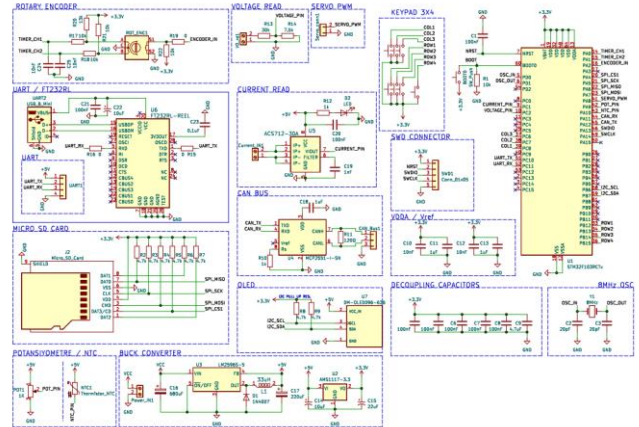
Şekil 8. ACS758xCB-100B

B. Şematik Tasarımı

Bu aşamada, STM32F103C8T6 mikrodenetleyicisinin çevre birim bağlantıları, motor sürücü devresindeki H-köprüsü yapılandırması ve MOSFET tetiklemeleri gibi kritik bileşenler optimize edilerek en verimli çalışma sağlanmış; tüm bileşenlerin özellikleri dikkate alınarak en uygun yerleşimle bağlantı yolları tasarlanmıştır.



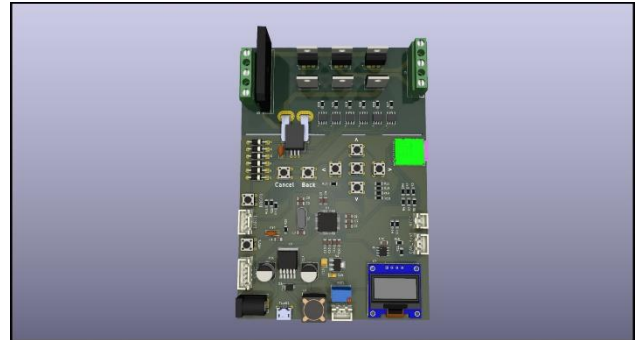
Şekil 9. Mikroişlemci I/O Konfigürasyonu



Şekil 10. Şematik Tasarımı

C. PCB Tasarımı

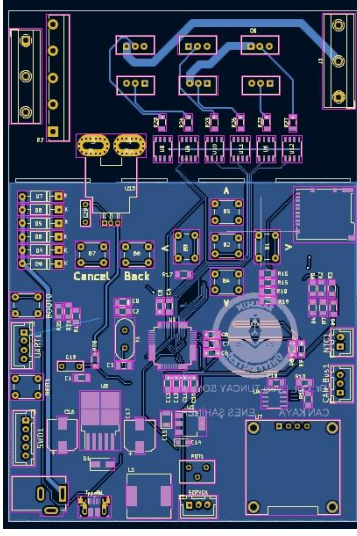
PCB tasarımında, motor sürücü devresinin yüksek verimle çalışabilmesi için çift katmanlı bir yapı tercih edilmiştir. Bu tasarım, sinyal yollarının güç yollarından ayrılmasına ve güç yollarının optimize edilmesine olanak sağlamaktadır. Yüksek akım taşıyan yollar geniş tutulmuş, ayrıca MOSFET'lerin sıcaklık yönetimi için ısı dağıtım stratejileri uygulanmıştır.



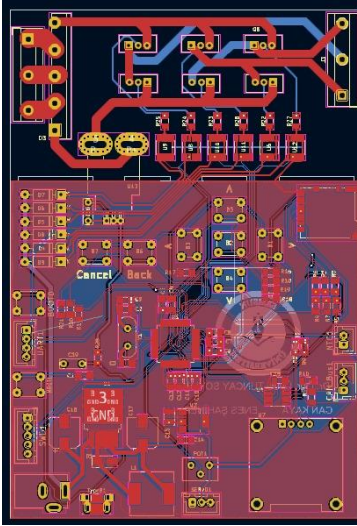
Şekil 11. PCB 3B görsel

Motor sürücü kısmındaki MOSFET'in güç besleme yolları, yüksek kalkış akımları gibi olası sorunların önüne geçilmesi

için PCB'de kaplamasız olarak yapılmış ve lehim veya tel ile desteklenmiştir. MOSFET bacak aralığından ve alan kısıtlamasından dolayı yollar kalınlaştırılmamış, bu çözüm tercih edilmiştir.



Şekil 12. PCB Çizimi



Şekil 13. PCB Çizimi

D. Malzeme Kalem Bazlı Fiyat Analizi

Tablo 1. Motor Sürücü Fiyat

Malzeme Kalemi	Malzeme Türü	Miktar	Birim Fiyat	Toplam Fiyat
10k	Direnç	8	0,19	1,52
4.7k	Direnç	8	0,19	1,52
1k	Direnç	2	0,12	0,24
1K	Direnç	2	0,2	0,4
30k	Direnç	2	12,5	25
7.5k	Direnç	2	0,48	0,96
120Ω	Direnç	1	0,48	0,48
FCPF099N65S3	MOSFET	6	167,648	1005,8904
8MHz	Kristal	1	4,85	4,85
M Power	Güç Kaynağı	1	90	90
Jack-DC	Dc Güç Giriş Konnektörü	1	7,08	7,08
USB_B_Mini	USB Konnektörü	1	12,996	12,996
Motor IN	Konnektör	1	5	5

Güç IN	Konnektör	1	5	5
Conn_01x02	Konnektör	1	2,5	2,5
Conn_01x03	Konnektör	2	1,37	2,74
Conn_01x04	Konnektör	1	1,8	1,8
Conn_01x05	Konnektör	1	139,76	139,76
SW_Push	Anahtar	9	1,68	15,12
1N4007	Diyot	6	0,61	3,66
100nF	Kondansatör	7	1,41	9,87
22uF	Kondansatör	1	3,8988	3,8988
1nF	Kondansatör	1	3,6	3,6
10nF	Kondansatör	2	0,62	1,24
4.7uF	Kondansatör	1	83	83
20pF	Kondansatör	2	0,31	0,62
680uF	Kondansatör	1	3,6	3,6
10uF	Kondansatör	1	160,826	160,8255
1uF	Kondansatör	3	0,78	2,34
220uF	Kondansatör	1	6,47	6,47
ACS758xCB-100B	Akım Sensörü	1	252,33	252,33
MCP2551-I-SN	CAN entegresi	1	63,35	63,35
Micro_SD	Micro SD Kart Giriş	1	95,7356	95,7356
TC4420COA	MOSFET Sürücü	6	63	378
LED	LED	1	5,66028	5,66028
33uH	Endüktör	1	117,939	117,9387
STM32F103RCTX	Mikrodenetleyici	1	80,82	80,82
DM-OLED096-636	OLED Ekran	1	162,45	162,45
DMA40U1800GU	Doğrultucu	1	479,69	479,69
AMS1117-3.3	Regülatör	1	2,42	2,42
LM2596S-5	Regülatör	1	74,727	74,727
Pcb	Baskı Devre Kartı	1	64,98	64,98
Toplam			₺3.380,08	

III. SONUÇLAR

Tasarımını gerçekleştirdiğimiz H-köprüsü ile motor sürücü PCB devresinin performansı, entegre bileşenler ve kontrol sistemleri aracılığıyla kapsamlı bir şekilde değerlendirilmiştir. Proje kapsamında, üç faz asenkron motor sürücüsü olarak işlev gören PCB, temel bileşenlerin ve modüllerin entegrasyonu sayesinde başarılı bir şekilde tasarlanmıştır.

Geliştirilen sistemde kullanılan FCPF099N65S3 MOSFET'ler, motor kontrol sinyalleri ile etkili bir şekilde tetiklenerek, motorun istenen performansı sergilemesine olanak tanımıştır. H-köprüsü konfigürasyonu, motor sürücüsünün yüksek verimlilikle çalışmasını sağlarken, TC4420COA gate sürücüsü ile kontrol edilen bu MOSFET'ler sayesinde enerji kayıpları minimize edilmiştir.

Projenin bir diğer önemli başarısı, motor besleme gerilimini düzenlemek, doğrultma görevini üstlenmek için kullanılan DMA40U1800GU doğrultucusu olmuştur. Bu bileşen, motorun stabil ve güvenilir bir şekilde çalışmasını sağlamakta kritik bir rol oynamıştır.

Devrede kullanılan UART, I2C, SPI ve CAN Bus protokolleri ile genişletilebilirlik ve veri iletişimi açısından önemli bir avantaj sağlamıştır. Micro SD kart modülü aracılığıyla, sistemin çalışma verileri etkili bir şekilde depolanmış ve geri çağırma işlemleri kolaylaştırılmıştır. Ayrıca görselleştirme ve kontrol aşamasında, I2C protokolü ile

bağlı OLED ekran, motor parametrelerinin ve sistem durumunun anlık izlenebilmesini sağlamıştır.

Sonuç olarak, projenin her aşamasında elde edilen sonuçlar, sistemin güvenilir ve verimli çalıştığını doğrulamakta ve hem akademik hem de endüstriyel uygulamalar için uygun bir platform sunduğunu göstermektedir.

IV. TARTIŞMA

Farklı iletişim protokolleri (UART, I2C, SPI, CAN Bus) sayesinde sistemin genişletilebilirliği ve veri yönetimi artırılmıştır. Motorun besleme akımının ACS758xCB-100B sensörü ile izlenmesi, aşırı akım koruma mekanizmalarıyla birlikte motor performansının sürekli olarak değerlendirilmesine olanak tanımaktadır. Sonuç olarak, bu tasarım hem akademik araştırmalar hem de endüstriyel uygulamalar için güçlü bir platform oluşturmakta ve gelecekteki projeler için önemli avantajlar sunmaktadır.

V. SONUÇ

Sistem, yüksek verimlilik, düşük güç kaybı ve hassas motor kontrolü özellikleri ile öne çıkmakta olup, gelecekteki projelerde ve uygulamalarda önemli avantajlar sağlamaktadır.

REFERENCES

- [1] N. Pirmatov, A. Panoev, G. Samatova, & O. Berdiyrov, "Determination of methods of achieving the energy savings through mathematical modeling of static and dynamic modes of electromagnetic energy conversion in asynchronous motors used in feed crushers", *E3s Web of Conferences*, vol. 383, p. 04046, 2023. <https://doi.org/10.1051/e3sconf/202338304046>
- [2] Z. Zhang, S. Jin, G. Liu, Z. Hou, & J. Zheng, "Model-free adaptive direct torque control for the speed regulation of asynchronous motors", *Processes*, vol. 8, no. 3, p. 333, 2020. <https://doi.org/10.3390/pr8030333>
- [3] D. Tong, "Efficiency optimization of asynchronous motor with particle swarm algorithm incorporating parameter identification", *Journal of Physics Conference Series*, vol. 2522, no. 1, p. 012003, 2023. <https://doi.org/10.1088/1742-6596/2522/1/012003>
- [4] L. Wang, "Study on direct torque control of three phase asynchronous motor", 2018. <https://doi.org/10.2991/mcei-18.2018.44>
- [5] C. Yang, D. Lu, Y. Hu, X. Chen, R. Yu, & L. Kong, "Magnetic-field modulation principle and transmission ratio calculation of field-modulated asynchronous magnetic coupling", *Applied Mechanics and Materials*, vol. 535, p. 48-52, 2014. <https://doi.org/10.4028/www.scientific.net/amm.535.48>
- [6] Y. Gong and X. Li, "The simulation research and modeling of asynchronous motor's vector control", *Applied Mechanics and Materials*, vol. 336-338, p. 484-488, 2013. <https://doi.org/10.4028/www.scientific.net/amm.336-338.484>
- [7] B. Kirankumar, Y. Reddy, & M. Vijayakumar, "Multilevel inverter with space vector modulation: intelligence direct torque control of induction motor", *Iet Power Electronics*, vol. 10, no. 10, p. 1129-1137, 2017. <https://doi.org/10.1049/iet-pe.2016.0287>

Açısal Hareket Sistemlerinin Hızını Ölçmek İçin BNO055 Sensör ve ESP32-WROOM-32 Mikrodenetleyici Kullanılarak Açısal Hareket Sistemlerinin Donanım Geliştirilmesi ve Ölçeklendirilmesi

Serhat Çindemir^{1*}, Süleyman Erdoğan²

¹Rollmech Automotive, Araştırma Geliştirme, Bursa, Türkiye

²Rollmech Automotive, Araştırma Geliştirme, Bursa, Türkiye

*serhat.cindemir@rollmech.com

Özet – Hareket sırasında dairesel alanları tarayan sistemlerde, hareket hızını ölçmek için yaygın olarak jiroskoplar, takometreler ve kodlayıcılar kullanılır. Bu çalışmada, manyetometre, jiroskop ve ivmeölçer içeren BNO055 sensörü açısal hareketi ölçmek için kullanılmıştır. Sensörden gelen jiroskop ve ivmeölçer verileri açısal hızı ölçmek için kullanılmış ve veri işleme için bir ESP32-WROOM-32 mikrodenetleyici seçilmiştir. Bileşenler özel olarak tasarlanmış bir PCB'ye monte edilmiştir. Elektronik ölçüm cihazı vantuzlarla dönen bir sisteme sabitlenmiş ve sistemin belirli noktadaki anlık doğrusal hızı hesaplanmıştır. Dairesel hareketin olduğu çeşitli sistemlerde kullanılabilmesi için sensör ile dönme merkezi arasındaki mesafe manuel olarak ölçülmüş ve Bluetooth aracılığıyla sisteme iletilmiştir. Sensörün vantuzlu montajı kullanım kolaylığını artırmıştır. Ayrıca PCB, anakarta veri aktarımını sağlayan RS485 haberleşmesi ile donatılmıştır. Anakart üzerindeki ESP32-WROOM-32E, WiFi bağlantısı sayesinde sensör verilerinin internet üzerinden bir sunucuya yüklenmesine olanak tanır. Böylece çeşitli uygulamalara uygun bir açısal hız ve açı ölçüm sistemi geliştirildi.

Anahtar Sözcükler – BNO055, ESP32WROOM32, açı ölçümü, açısal hız hesaplama

Hardware Development and Scale-up of Angular Motion Systems Using BNO055 Sensor and ESP32-WROOM-32 Microcontroller to Measure the Speed of Angular Motion Systems

Abstract – In systems that scan circular areas during movement, gyroscopes, tachometers, and encoders are commonly used to measure movement speed. In this study, the BNO055 sensor, which includes a magnetometer, gyroscope, and accelerometer, was used to measure angular motion. Gyroscope and accelerometer data from the sensor were utilized to measure angular velocity, and an ESP32-WROOM-32 microcontroller was selected for data processing. The components were mounted on a custom-designed PCB. The electronic measurement device was fixed to a rotating system using suction cups, and the system's instantaneous linear velocity at specific points was calculated. To allow use in various systems with circular motion, the distance between the sensor and the center of rotation was manually measured and transmitted to the system via Bluetooth. The suction cup mounting of the sensor facilitated ease of use. Additionally, the PCB was equipped with RS485 communication, enabling data transfer to the mainboard. The ESP32-WROOM-32E on the mainboard, with its WiFi connectivity, allows sensor data to be uploaded to a server via the internet. Thus, an angular velocity and angle measurement system suitable for various applications was developed.

Keywords – BNO055, ESP32WROOM32, angle measurement, angular velocity calculation

I. GİRİŞ

Jiroskoplar ve ivmeölçerler gibi atalet sensörleri, navigasyon, otomotiv endüstrisi, robotik ve askeri alanlar gibi çeşitli alanlarda yoğun bir şekilde talep görmektedir [1] – [4]. Son on yılda, BNO055 (Bosch Sensortec tarafından geliştirilen), BNO080/85/86 (Hillcrest Labs ve Bosch Sensortec'in ortak çalışması) ve MPU9250 (InvenSense tarafından üretilen) gibi çeşitli IMU'lar, araştırmacılar arasında büyük bir popülerlik kazandı. Bu IMU'ların popülerliğinin

arkasındaki en önemli nedenlerden biri, yüksek hızda gerçek zamanlı yönelim verilerini (kuaterniyonlar ve/veya Euler açıları şeklinde) çıkarabilmeleridir. Bu işlem, sensörün içerisine entegre edilmiş bir mikrodenetleyici tarafından, genellikle 100 Hz gibi yüksek örnekleme hızlarında, bir sensör füzyon algoritması kullanılarak gerçekleştirilir. Örneğin, BNO055 IMU'su, 100 Hz'de yönelim verilerini kuaterniyonlar veya Euler açıları şeklinde işleyebilmek için 32 bitlik bir mikrodenetleyiciye sahiptir. Bu mikrodenetleyici, Kalman

filtresi tabanlı bir sensör füzyon algoritması uygular. Bu sayede, ivmeölçer, jiroskop ve manyetometre gibi farklı sensörlerden gelen verileri birleştirerek, doğruluk ve kararlılığı yüksek yönelim verilerini sağlar. Sensör füzyon algoritmaları, özellikle gerçek zamanlı izleme, robotik ve otonom sistemlerde büyük avantajlar sunar.[9] – [10]

Birden fazla sensörün kombinasyonundan oluşan atalet ölçüm birimleri IMU'lar, dönme hızı ve yerçekimi kuvveti gibi dönme ve doğrusal atalet verilerini ölçmek için bir gerekliliktir. IMU'lar, açısal dönüşleri ölçmek için jiroskopları ve atalet ivmelerini ölçmek için ivmeölçerleri kullanır [5]. Her iki sensör de üç eksende ölçüm yapabilen üç serbestlik derecesine sahiptir. IMU teknolojisi, bu iki ölçüm türünü tek bir cihazda entegre ederek önemli bir ilerleme kaydetmiştir [6]. Dokuz serbestlik derecesine sahip (9-DOF) bir IMU, ivmeölçer ve jiroskopik sensörler içerir ve 3 eksende ivme ile jiroskopik değerlerle 6 serbestlik derecesi sunar. İvmeölçerler bir nesnenin doğrusal ivmesini ölçerken, bu veriler nesnenin duruşunu belirlemek için yerçekimi kuvvetini de içerir. IMU sensör verileri, konum ve hızı belirlemek için kullanılabilir. [7]-[8]

Açısal hareket eden sistemlerin hızını doğru ve hassas bir şekilde ölçmek, mühendislik uygulamalarında ve bilimsel araştırmalarda öneme sahiptir. Bu tür ölçümler, robotik sistemlerin stabilizasyonu, otomotiv endüstrisi, havacılık mühendisliği, uzay araştırmaları ve spor performans analizi gibi çeşitli alanlarda geniş bir uygulama alanına sahiptir. Açısal hız, bir cismin belirli bir eksen etrafındaki dönme hızını ifade eder ve genellikle derece/saniye ($^{\circ}/s$) biriminde ölçülür.

Bu çalışmada, BNO055 sensörü ve ESP32 mikrodenetleyicisi kullanılarak açısal hız ölçümü için bir sistem geliştirilmiştir. BNO055 sensörü, Bosch Sensortec tarafından üretilen ve jiroskop, ivmeölçer ve manyetometre özelliklerini bir arada sunan bir hareket takip sensörüdür. 100 Hz'de örnekleme hassasiyeti sağladığı için açısal hız ölçümlerinde tercih edilen bir çözüm olmuştur. ESP32-WROOM-32 mikrodenetleyicisi ise Espressif Systems tarafından geliştirilmiş olup geniş bellek kapasitesi ve güçlü veri işleme yetenekleri sunar. Özellikle entegre WiFi ve Bluetooth özelliği sayesinde, sensör verilerinin gerçek zamanlı olarak iletilmesi ve uzaktan erişim imkânı sağlanabilmektedir. Bu özellikler, sistemin saha içi ve saha dışı uygulamalarda kullanılabilirliğini artırmaktadır.

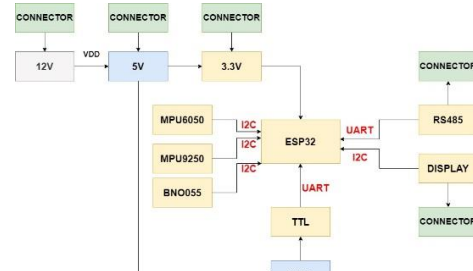
Bu çalışmanın amacı, BNO055 sensörü ve ESP32-WROOM-32 mikrodenetleyicisi tabanlı yeni bir donanım ve yazılım sistemi geliştirerek açısal hareket eden sistemlerde hız ve açı ölçümü için doğru, hassas ve güvenilir ölçümler yapabilen bir teknoloji sunmaktır. Donanım tasarımı, sensör verilerinin güvenilir bir şekilde toplanmasını ve işlenmesini sağlamak için özel olarak yapılandırılmıştır. Yazılım bileşenleri ise veri analizi ve farklı platformlarda kullanılabilirlik konularında esneklik sunmaktadır.

Bu makalenin ilerleyen bölümlerinde, geliştirilen sistem detaylı bir şekilde açıklanacak, yapılan deneysel çalışmaların sonuçları tartışılacak ve sistemin performansı değerlendirilecektir. Gerçekleştirilen bu çalışma, endüstriyel ve bilimsel uygulamalarda kullanılabilirliğini artırmayı hedeflemektedir.

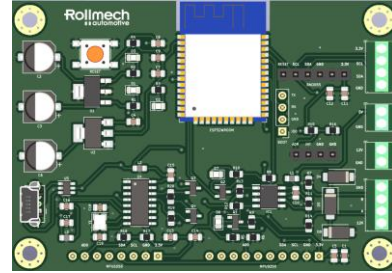
II. YÖNTEM

A. Devre Kartı

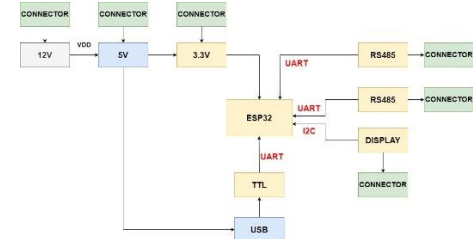
Şekil 1 ve Şekil 3'te blok diyagramda görüldüğü üzere, sarı renkli kutular 3.3V çalışma voltajını, mavi renkli kutular 5V çalışma voltajını temsil etmektedir. Şekil 2'de sensörün bulunduğu ve ölçümü gerçekleştiren devre kartı ve Şekil 4'te sensörlerden anlık ölçüm sonuçlarını RS485 ile alan ve sunucu ile Wifi kullanarak bağlantı kuran haberleşme devre kartı tasarımının 3D görüntüsü görülmektedir.



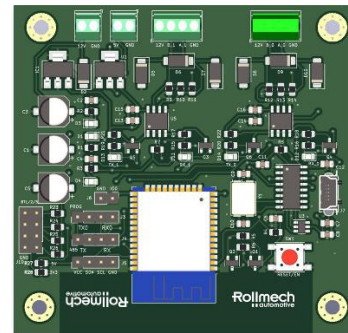
Şekil 1: Sensör devre kartının blok diyagramı.



Şekil 2: Sensör devre kartının tasarımı üç boyutlu görüntüsü.



Şekil 3: Haberleşme devre kartının blok diyagramı.



Şekil 4: Haberleşme devre kartının tasarımı üç boyutlu görüntüsü.

B. Mikrodenetleyici

Gelen sinyalleri alıp işlemek için, Şekil 1'deki blok diyagramda görüldüğü üzere, ESP32-WROOM-32 mikrodenetleyicisi kullanılmıştır. Mikrodenetleyici, çift çekirdekli 240 MHz çalışma frekansına sahip olup, WiFi ve Bluetooth özellikleri içermektedir. Toplamda 34 adet giriş-çıkışı pini, 3 tane UART, 2 tane I2C, SPI, ADC ve Timer

modüllerine sahiptir. Pinlerin sayısı bu işlem için fazlasıyla yeterlidir. Programlama pinleri, devre kartı üzerinde CH340G USB seri çevirici ile bağlantı kurulacak şekilde tasarlanmıştır. Devre kartı üzerinde bir harici reset butonu bulunmakta ve giriş sinyalleri için bir alçak geçiren filtre yapısı kullanılmıştır. Güç beslemesi, adaptör veya USB bağlantısı üzerinden sağlanmaktadır. Güç besleme kısmında, voltaj kararlılığını artırmak için bypass kondansatörleri ve devreye gelen gürültüleri bastırmak için ferrit boncuk kullanılmıştır.

C. Jiroskop Sensör

Şekil 1'deki blok diyagramda görüldüğü üzere, BNO055 9 serbestlik dereceli (9-DOF) mutlak konum sensörü tercih edilmiştir. Bu sensör, 3 eksenli ivmeölçer, jiroskop ve manyometre bileşenlerini içeren entegre bir yapıya sahiptir ve bu sayede doğrudan açısal hız, eğim ve konum hesaplamalarını gerçekleştirebilmektedir.

Açısal hız (ω), birim zamandaki açı değişimini ifade eder ve Denklem 1'deki şekilde formüle edilir.

$$\omega = \frac{\Delta\theta}{\Delta t} \quad (1)$$

Bu denklemde:

$$\omega = \text{Açısal hız}(\text{rad/s})$$

$$\Delta\theta = \text{Açı değişimi}(\text{rad})$$

$$\Delta t = \text{Zaman değişimi}(\text{s})$$

Denklem 1'de görüldüğü üzere birim zamandaki açı değişiminin, açısal hızın temel belirleyicisi olduğunu ortaya koymaktadır. Bu ifade, jiroskop gibi sensörler aracılığıyla ölçülen veri üzerinden açısal hızın hesaplanmasında kullanılır. Doğrusal hız (ϑ) ise, açısal hızın yarıçap ile çarpılmasıyla elde edilir ve Denklem 2'deki şekilde formüle edilir.

$$\vartheta = \omega * r \quad (2)$$

Bu denklemde:

$$\vartheta = \text{Doğrusal hız}(\text{m/s})$$

$$\omega = \text{Açısal hız}(\text{rad/s})$$

$$r = \text{Yarıçap}(\text{m})$$

Denklem 2'de açısal hızın yarıçapla orantılı olarak doğrusal hıza dönüştürebileceğini ifade eder. Bu, bir nesnenin dögüsel hareketinin doğrusal hıza nasıl yansıdığını matematiksel olarak ifade etmektedir.

Açı ölçümü, manyometre verileri kullanılarak hesaplanabilen başka bir önemli parametredir. Heading açısı (θ_h), özellikle yön belirleme uygulamalarında kullanılır ve manyometrenin x ve y eksenlerindeki bileşenlerden türetilir. Heading açısının hesaplanması Denklem 3'te formüle edilmektedir.

$$\theta_h = \arctan2(M_y, M_x) \quad (3)$$

$$\theta_h = \text{Heading açısı}(\text{rad})$$

$$M_x, M_y = \text{Manyometre x ve y eksen bileşenleri}$$

Denklem 3, heading açısının, manyetik alan vektörlerinin x ve y bileşenlerinin ters tanjant fonksiyonuna uygulanmasıyla

hesaplandığını gösterir. Bu yöntem, z eksenli etrafındaki dönüş açısını tespit etmek için yaygın olarak kullanılmaktadır.

Sonuç olarak, açısal hız ve açı ölçümü gibi temel parametreler, sensör verilerinin matematiksel modeller ile işlenmesi yoluyla elde edilir. BNO055 gibi entegre sensör sistemleri, bu tür hesaplamaları doğrudan ve yüksek doğrulukla gerçekleştirme kapasitesine sahip olup, yönelim ve konum tespiti uygulamalarında önemli bir yere sahiptir.

D. Programlama ve Seri Port Bağlantı Devresi

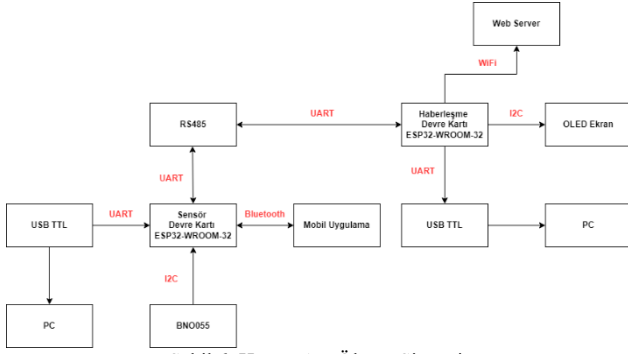
Bilgisayar üzerinde hazırlanan seri port ekranı uygulamaları ile BNO055 sensöründen alınan verilerin okunması için devre kartı üzerinde, Şekil 1'deki blok diyagramda görülen TTL (Transistor to Transistor Logic) ile USB seri port üzerinden verilerin aktarılması için devre tasarımı yapılmıştır. Bu devre tasarımında, ESP32-WROOM-32 ile bilgisayar arasındaki veri iletişimi ve mikrodenetleyicinin programlama işlemleri USB üzerinden sağlanmıştır. Yapılan tasarımda devre kartı ve bilgisayar arasında USB kablo bağlantısı sağlanarak, seri port üzerinden gönderilen veriler bilgisayar ortamında hazırlanan yazılım uygulamasında, grafik ile anlaşılmış ve sayısal değerleri görüntülenmiştir. Ölçümü görüntülenen veriler, .xlsx, .txt ve .png formatında gün, saat, dakika olarak sayısal ölçüm sonucu ve grafik değeri kaydedilip raporlanabilmektedir.

E. RS485 Haberleşme Sistemi

Sensör verilerinin aktarılması için RS485 haberleşme protokolü kullanılmıştır. RS485, uzun mesafelerde elektromanyetik parazitlere dayanıklı, dengeli (balanced) bir haberleşme standardıdır. Yarı çift yönlü (half-duplex) modda çalışan sistemde, sensörden gelen açısal hız ve açı verileri tek bir hat üzerinden ESP32-WROOM-32 mikrodenetleyicisine iletilmiştir. RS485 sürücüsü, düşük enerji tüketimi ve yüksek elektromanyetik uyumluluk sağlayan bir transceiver modülü ile tasarlanmıştır. Bu sayede, veriler toplanarak mikrodenetleyici üzerinden WiFi aracılığıyla sunucuya aktarılmıştır.

F. Hız ve Açı Ölçüm Sistemi

Aşağıda Şekil 6'da gösterilen hız ve açı ölçme sisteminin bileşenleri, blok diyagramda belirtilen şekilde gerçekleştirilmiştir. Sistem, mobil uygulama ile sensör devre kartı arasında Bluetooth bağlantısı kurar. Sensör devre kartının dönme merkezine olan uzaklığı manuel olarak bluetooth ile sensör devre kartına tanıtılır, Sensör devre kartında, BNO055 sensöründen alınan sinyaller ESP32-WROOM-32 mikrodenetleyicisinde işlenir. Mikrodenetleyici, gelen sinyali gerekli parametrelerle filtreler ve kalibrasyon işlemini tamamlar. Ardından, hız ve açı bilgisi RS485 haberleşme protokolü üzerinden haberleşme devre kartına aktarılır. Haberleşme devre kartı, bu veriyi hem OLED ekrana hem de bilgisayara seri port üzerinden iletir. Ayrıca, haberleşme devre kartının WiFi özelliği sayesinde hız ve açı bilgileri bir servera anlık olarak aktarılır.



Şekil 6: Hız ve Açılı Ölçme Sistemi.

G. Ölçüm Sonuçları

Mekanik açı ölçüm cihazı kullanılarak ayarlanan referans açı değerleri tasarlanan sistem kullanılarak Tablo 1'de belirtilen açı değerleri için ölçümlenmiştir ve sonuçları Tablo 1'de belirtilmiştir.

Tablo 1: Referans açı değerleri ve sensör açı ölçüm sonuçları.

Açı Değeri	Mekanik Açı Ölçer	Açı Ölçüm Sonucu1	Açı Ölçüm Sonucu2	Açı Ölçüm Sonucu3
0	0	0	0	0
10	10	10.06	10.00	10.06
20	20	20.06	20.00	20.06
30	30	30.00	30.06	30.00
40	40	39.94	39.94	39.06
50	50	50.06	50.06	50.06
60	60	59.94	59.94	60.00
70	70	69.94	70.06	70.00
80	80	80.00	79.94	80.06
90	90	90.00	90.06	90.19

H. Yazılım

Sistem iki ana kod parçasından oluşmaktadır.

H.A.1 Sensör Birimi Kodu

Bu kısımda, BNO055 sensöründen gelen verileri toplayarak RS485 üzerinden haberleşme cihazına ileten bir ESP32 WROOM-32 mikrodeneleyicisinde çalışmaktadır.

H.A.2 Kütüphaneler ve Tanımlamalar

Gerekli kütüphaneler dahil edilmiştir: Wire.h, Adafruit_Sensor.h, Adafruit_BNO055.h, Bluetooth Serial.h, vb. SensorData yapısı tanımlanmıştır; sensörden elde edilecek verileri tutar.

H.A.3 Kurulum Fonksiyonu

- Seri haberleşme ve Bluetooth başlatılır.
- BNO055 sensörü başlatılır ve doğru şekilde çalıştığı kontrol edilir.
- RS485 için gerekli pinler ve seri portlar ayarlanır.

H.A.4 Ana Döngü

- Bluetooth üzerinden yarıçap bilgisi alınır.
- BNO055 sensöründen Euler açıları okunur ve başlık (heading) değeri hesaplanır.
- Açısal hız ve doğrusal hız hesaplamaları yapılır
- Hesaplanan veriler SensorData yapısına kaydedilir.
- Veriler RS485 üzerinden ana cihaza gönderilir.

H.B.1 Haberleşme Birimi Kodu

Bu kod, sensör biriminden gelen verileri alır, ekranda gösterir ve sunucuya gönderir.

H.B.2 Kütüphaneler ve Tanımlamalar

- OLED ekran için Adafruit_GFX.h ve Adafruit_SSD1306.h kütüphaneleri kullanılır.
- Wi-Fi ve HTTP işlemleri için gerekli kütüphaneler dahil edilir.
- SensorData yapıları tanımlanır, sensörden gelen verileri tutar.
- Wi-Fi bağlantı bilgileri ve sunucu adresi tanımlanır.

H.B.3 Kurulum Fonksiyonu

- Seri haberleşme başlatılır ve Wi-Fi ağına bağlanılır.
- RS485 portları ve ilgili pinler ayarlanır.
- OLED ekran başlatılır ve başlangıç görseli gösterilir.

H.B.4 Ana Döngü

- RS485 üzerinden her iki sensörden gelen veriler okunur ve ilgili yapılara kaydedilir.
- Veri alma işlemi sırasında iletişim hatları etkinleştirilir ve sonrasında devre dışı bırakılır.
- OLED ekranda sensörlerden gelen başlık, yarıçap ve doğrusal hız değerleri görüntülenir.
- Her 10 saniyede bir, Wi-Fi üzerinden sunucuya HTTP POST isteği gönderilir.
- Gönderilen JSON verisi, cihaz kimliği ve sensör verilerini içerir.
- HTTP isteğinin yanıtı ve durumu seri monitöre yazdırılır.
- Eğer Wi-Fi bağlantısı koparsa, yeniden bağlanma işlemi gerçekleştirilir.

III. SONUÇLAR

Bu çalışma kapsamında BNO055 kullanılarak açısal ölçümler yapılmış olup, ölçüm sonuçlarının doğruluğu mekanik açı ölçer kullanılarak 0°, 10°, 20°, 30°, 40°, 50°, 60°, 70°, 80° ve 90° açılarında karşılaştırılmıştır. Elde edilen ölçüm sonuçları mekanik açı ölçer referansında yüzde doğruluk ve Kare kök ortalama hatası (RMSE) olarak hesaplanmış ve bildirinin tartışmalar kısmında detaylı olarak belirtilmiştir. Elde edilen hız ölçümleri çalışma kapsamında paylaşılmamıştır ve teorik olarak bu ölçümün yapılabileceğinden bahsedilmiştir.

IV. TARTIŞMA

Kurulan sistem için herhangi kalibrasyonu yapılmış manuel açı ölçer kullanılarak ölçüm sonuçlarının doğruluğu kontrol edilmiştir.

Denklem 4'te görüldüğü gibi, her bir açı için yapılan üç ölçüm sonucunun ortalaması hesaplanmıştır. Denklem 5'te ise, ortalama ölçüm değeri ile gerçek açı arasındaki fark kullanılarak yüzde doğruluk hesaplanmıştır.

$$\text{Ortalama Ölçüm} = \frac{Açı\ Ölçümü1 + Açı\ Ölçümü2 + Açı\ Ölçümü3}{3} \quad (4)$$

$$\text{Yüzde Doğruluk} = \left(1 - \frac{\text{Gerçek Açı} - \text{Ortalama Ölçüm}}{\text{Gerçek Açı}}\right) \times 100 \quad (5)$$

Ölçümlerin ortalama doğruluğu = %99.82

$$\text{RMSE} = \sqrt{\frac{1}{n} \sum_{i=1}^n (y_i - \hat{y}_i)^2} \quad (6)$$

Kare kök ortalama hatası (RMSE) $\cong 0.119$

V. SONUÇ

Elde edilen ölçüm sonuçlarına göre yüzde doğruluk oranı Denklem 5'te belirtildiği gibi hesaplanarak %99.82 olarak bulunmuştur.

RMSE değeri ise Denklem 6 kullanılarak hesaplanmış olup $\cong 0.119$ olarak bulunmuştur.

Tüm bu doğruluk ve hata oranları kululan sistemin güvenilir ölçüm sonuçları için kullanılabileceğini kanıtlar niteliktedir.

TEŞEKKÜR

Tüm Rollmech çalışanlarına ve Rollmech Ar-Ge Ekibi'ne destekleri için teşekkür ederiz.

KAYNAKLAR

- [1] V. Saahar and R. Durai, "Designing MEMS Based Tuning Fork Gyroscope For Navigation Purpose", International conference on Communication and Signal Processing, pp. 1102-1107, April 2013.
- [2] B. Mashadi and M. Gowdini, "Vehicle Dynamics Control by Using an Active Gyroscopic Device", Journal of Dynamic Systems Measurement and Control, vol. 137, pp. 1-12, 2015.
- [3] C. Acar, A. Schofield, A.R. Trusov, L.E Costlow and A.M. Shkel, "Environmentally robust MEMS vibratory gyroscopes for automotive applications", IEEE Sensors Journal, vol. 9, pp. 1895-1906, 2009.
- [4] D. Dobriborsci, A. Kapitonov and N. Nikolaev, "The basics of the identification localization and navigation for mobile robots", International Conference on Information and Digital Technologies (IDT), pp. 100-105, 2017.
- [5] A.S. Kundu, O. Mazumder, P.K. Lenka and S. Bhaumik, "Hand Gesture Recognition Based Omnidirectional Wheelchair Control Using IMU and EMG Sensors", Journal of Intelligent and Robotic Systems., vol. 91, pp. 529-541, 2018.
- [6] K. Okada, T. Kakutani, H. Itano, Y. Matsu and S. Sugiyama, "Development of 6-axis Motion Sensors Using Piezoelectric Elements", Proceedings of the 21st Sensor Symposium, 2004.
- [7] Bakhshi, S., Mahoor, M. H., & Davidson, B. S. (2011). Development of a body joint angle measurement system using IMU sensors. Paper presented at the 2011 Annual International Conference of the IEEE Engineering in Medicine and Biology Society
- [8] Yuan, Q., & Chen, I.-M. (2014). Localization and velocity tracking of human via 3 IMU sensors. Sensors and Actuators A: Physical, 212, 25-33.
- [9] H. Liu, X. Xie, M. Millar, M. Edmonds, F. Gao, Y. Zhu ve diğerleri, "Eklem pozisyonu ve kuvvet algılama yoluyla el-nesne manipülasyonunu incelemek için eldiven tabanlı bir sistem", IEEE/RSJ Uluslararası Intell. Robot Sistemleri Konferansı (IROS) Bildirileri, s. 6617-6624, Eylül 2017.
- [10] F. Fei, S. Xian, X. Xie, C. Wu, D. Yang, K. Yin ve diğerleri, "El kinematiki değerlendirilmesi için çoklu sensörlere sahip giyilebilir bir eldiven sisteminin geliştirilmesi", Micromachines, cilt 12, sayı 4, s. 362, Mart 2021.

Enhancing Urban Parking Management with SSD-Based Satellite Detection Systems

Ipek Neslihan Alpugan¹, Behiye Sahin^{2*}, Köksal Semercigil¹

Department of Computer Engineering, Faculty of Engineering, Ankara University, Ankara, Türkiye
Aerospace Engineering Department, Faculty of Aeronautics and Astronautics, Tarsus University, Mersin, Türkiye
** (behiye_sahin@tarsus.edu.tr)*

Abstract – The rapid urbanization and exponential growth in vehicle numbers have significantly increased the demand for parking spaces in metropolitan areas, creating challenges for drivers and urban planners alike. Effective detection of available parking spaces is crucial, as it impacts traffic flow, environmental sustainability, public safety, and the efficient use of urban land. Studies show that a significant portion of urban traffic consists of vehicles searching for parking, leading to increased energy consumption, higher emissions, and more congestion. This paper explores the use of advanced parking detection systems, specifically leveraging satellite technology and single-stage object detection algorithm Single Shot Multibox Detector (SSD). By analyzing the performance of the SSD model in detecting empty parking spaces from satellite images, this study offers a comprehensive evaluation of its strengths and weaknesses in various scenarios. The findings contribute to the ongoing development of smart parking solutions, which are essential for reducing environmental impacts, enhancing safety, and improving the quality of life in urban environments. This study is among the first to assess the SSD model's effectiveness in this critical area of urban infrastructure.

Keywords – parking management, smart city, deep learning, object detection, SSD

I. INTRODUCTION

Modern urbanization has caused an exponential increase in the number of cars on the road. As a result, the demand for parking spaces in metropolitan areas has increased, posing a significant dilemma for both drivers and municipal planners. Detecting available parking spaces is more than just a convenience for drivers; it is an important part of urban infrastructure that affects traffic flow, environmental sustainability [1] and the overall quality of life in cities. One of the main reasons for detecting empty parking spaces is that it directly affects traffic congestion. According to studies, in many cities, 20 to 30% of urban traffic consists of vehicles searching for parking spaces [2]. This increases per capita energy consumption of residents in metropolitan areas [3], leading to higher carbon emissions [4] and gasoline consumption [5], as well as more air pollution [6] and traffic congestion on a regional scale. By accurately detecting available parking spots in cities, it can also significantly reduce the hours drivers spend looking for a place to park. This leads to better traffic, less pollution and less stress in city center traffic jams. Open parking spaces are also critically important for achieving better space utilization efficiency, and this has been a challenge in large cities for many years. Cities facing parking shortages need to make the best use of available land [7]. Parking lots and garages are often underused or unevenly used; some spaces are full, others are empty [8]. Real-time information on parking availability can be provided and better utilized through advanced parking detection systems [9].

Parking management is an important revenue stream for cities, and an inefficient matching system can easily mean that parking revenues are missed [10]. For example, urban areas where smart detector systems are available can make the most

of parking spaces to ensure that the space is used and that revenues collected from customers are collected effectively [11]. This recognition can result in a potential increase in revenue that municipal governments can spend on other important urban infrastructure projects. Finally, it is not possible to ignore the safety component of detecting empty parking lots [12]. Finding an empty space in a large parking lot can sometimes lead to erratic driving behaviors, such as unexpected stops or lane changes, which increases the probability of traffic accidents [13]. These technologies reduce the probability of such incidents by directing cars directly to accessible spaces, which helps to create a safer parking environment. To summarize, the importance of detecting empty parking spaces goes far beyond practicality. It is an important part of contemporary urban infrastructure that affects public safety, economic efficiency, land use, environmental sustainability and traffic management [14]. As cities expand and the number of vehicles on the roads increases, finding effective and smart parking solutions will become increasingly important. By investing in advanced parking detection systems, cities can reduce their environmental impact, improve the quality of life of residents and create more sustainable, efficient and safe urban environments.

The detection of objects, structural analysis, and identification of existing parking areas using satellite systems [15] are crucial steps in urban planning and the development of smart cities. Satellite technology can greatly minimize the time vehicles spend searching for parking spaces, resulting in reduced traffic congestion and pollution. Drivers can be guided directly to available spaces by providing real-time data to navigation systems or mobile applications, thus optimizing

routes and avoiding unnecessary journeys. Satellite-based parking detection systems also help with more effective urban planning and management. Urban planners can use the data obtained by these systems to study parking trends, identify high-demand locations, and make informed decisions about infrastructure development, such as building more parking spaces or implementing dynamic pricing models. This system can also be applied to driverless vehicles that rely on precise data for navigation and parking. As autonomous vehicles become increasingly common, the ability to autonomously detect and navigate to available parking spaces will be critical to their mainstream acceptance.

Single Shot Multibox Detector (SSD) [16] and You Only Look Once (YOLO) [17] are prominent single-stage object detection algorithms known for their efficiency and speed in real-time applications. Unlike two-stage detectors, which first generate region proposals and then classify them, single-stage detectors like SSD and YOLO directly predict bounding boxes and class probabilities in a single forward pass of the network. SSD excels in detecting objects at different scales by employing a series of convolutional filters, each responsible for detecting objects at varying sizes. YOLO, on the other hand, divides the image into a grid and predicts bounding boxes and class probabilities for each grid cell, enabling rapid and accurate object detection. Both models are widely used in applications that require real-time processing, such as autonomous driving, where quick identification of pedestrians, vehicles, and other road hazards is crucial, and in surveillance systems, where timely detection of objects can enhance security and monitoring effectiveness. Their ability to balance speed and accuracy makes them ideal for tasks where computational resources and time are limited, but reliable detection is essential.

In this study, a detailed analysis of the detection performance of the SSD model is performed for the detection of empty parking spaces from images of parking areas captured from satellite systems. The detection capabilities of the SSD model in various scenarios are evaluated comprehensively. In addition, the performance parameters of the algorithm in question are measured and the performance of the SSD model is analyzed quantitatively. As a result of the measurement, the strengths and weaknesses of the detection capability of the SSD model are evaluated comprehensively. In this context, the study is one of the first applications that evaluates the SSD model in the detection of empty parking spaces.

II. MATERIALS AND METHOD

A. SSD Network Structure

The SSD model can be examined in three main parts: the backbone network part, the original bounding box generation part, and the convolution estimation part. In applications, it can be seen that the backbone network part is divided into the basic network and the additional feature extraction layer. The first operation in the working principle of the algorithm is to feed the images to the deep neural networks in order to extract the features of the images. Then, default frames are designed by extracting feature maps at different scales. Then, the features in the frames are extracted to estimate what the object to be detected is and its location. Finally, Non-Maximum Suppression (NMS) is used to select the prediction that is most

compatible with the real target frame. NMS is a technique widely used in object detection and computer vision applications. If there is more than one prediction box for a detected object, it eliminates the extra boxes and selects the box with the highest accuracy rate. This application of NMS prevents overlapping in predictions and multiple predictions for a single object.

The network architecture of the SSD model is shown in Fig. 1. The network architecture generally consists of a main network and additional layers. The main network of SSD is created using a pre-trained convolutional neural network that extracts features from images [18]. The most commonly used basic network is VGG-16. VGG-16 is a convolutional neural network with a weight layer and consists of several convolutional layers and max-pooling layers. Each of these layers has a specific filter and extracts feature maps from the input image. The last layers of VGG16 consist of fully connected layers, but in SSD, additional convolutional layers are added instead of these layers. Each of these layers added after the main network produces feature maps at different resolutions and thus plays a role in recognizing objects of different sizes. SSD adds prediction layers for each feature map. These layers determine the possible classification for each position and the prediction boxes corresponding to the classification.

B. Loss Function

The SSD loss function combines the classification and location loss to optimize both the classification accuracy and location accuracy of the object detection model. These two loss components constitute the total loss function. The classification loss estimates whether each default box belongs to any class. This loss is usually calculated as follows:

$$L_{cls}(x, c) = -\sum_{i \in Pos} x_{ij} \log(c_i) - \sum_{i \in Neg} \log(c_0) \quad (1)$$

Positive examples predict local object classes, while negative examples predict background classes.

Location loss estimates how much each default box overlaps with the real object box. This loss is usually calculated as L1 or L2 loss and is expressed as follows.

$$L_{loc}(x, l, g) = \sum_{i \in Pos} x_{ij} smooth_{L1}(l_i - g_i) \quad (2)$$

where, the term $smooth_{L1}(z)$ in (2) is defined as:

$$smooth_{L1}(z) = \begin{cases} 0.5z^2, & \text{if } |z| < 1 \\ |z| - 0.5, & \text{otherwise} \end{cases} \quad (3)$$

The total loss is calculated as the sum of the classification and location loss and is as follows:

$$L(x, c, l, g) = \frac{1}{N} (L_{cls}(x, c) + \alpha L_{loc}(x, l, g)) \quad (4)$$

Here, N is the number of positive default boxes, and α is the weight coefficient used to determine the importance of location loss.

In SSD, the abundance of negative examples makes training inefficient. When faced with such a problem, the hard negative mining technique is used to solve the problem. This technique calculates a classification loss by selecting the subset of negative examples with high loss. Thanks to this technique, the network is trained with more efficient negative examples and its imbalance is reduced.

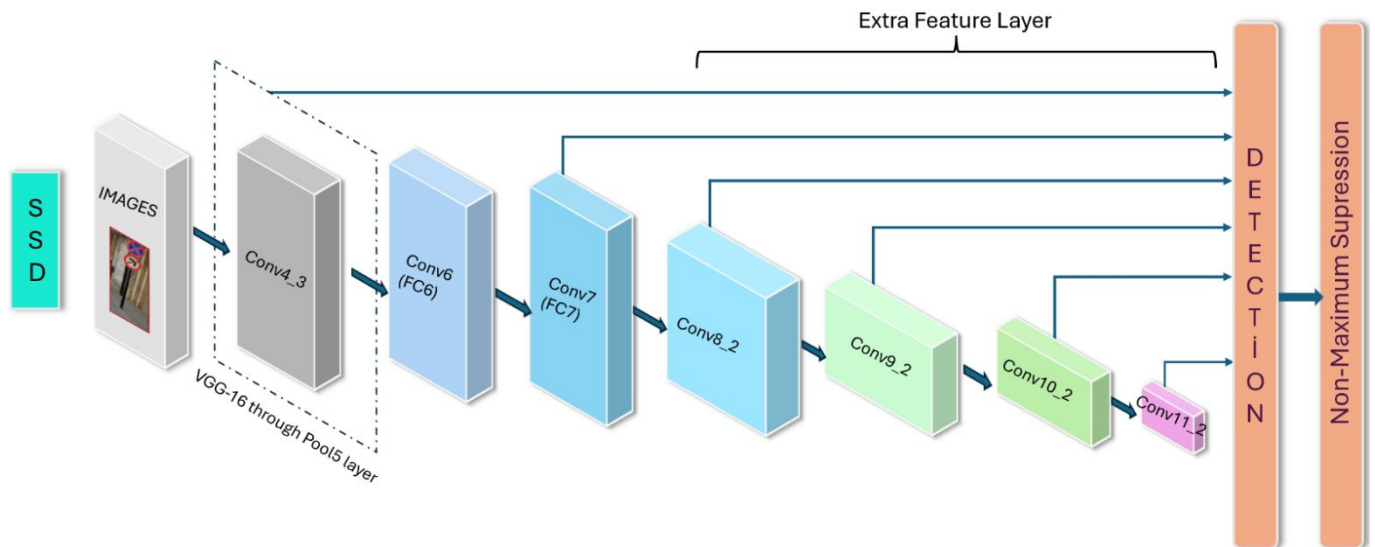


Fig. 1. Network architecture of the SSD model.

III. RESULTS

A comprehensive dataset obtained from satellite images was created to evaluate the performance of the SSD model. The comprehensive creation of the dataset directly affects the performance of the model. The created dataset includes images from many challenging conditions. In order to investigate the effect of the shadow factor on the detection ability, images taken at different times of the day were added to the dataset. With the inclusion of images from different conditions, the dataset contains a total of 3750 images. The dataset was divided into three parts for the training, validation and testing stages of the model. In order to provide comprehensive training to the model, the majority of the dataset was used for training. Therefore, 2150:950:650 images were selected for the training, validation and testing dataset, respectively.

Fig. 2 presents various examples of the SSD model's detection of empty parking spaces across different scenarios, illustrating both its strengths and limitations. In example 1, an open parking lot with roughly half occupancy is shown. The parking spaces are demarcated by two parallel white lines, and the SSD model successfully detects the empty spaces when these lines are not obstructed by vehicles. However, in the lower-left section of the image, the model fails to detect an empty parking space due to the white lines being obscured by parked cars. This suggests that the visibility of parking lines is critical for accurate detection. Example 2 features an angled and somewhat distant view of the parking area, where the white parking lines are less distinct due to low image resolution. Unlike the previous case, the reduced visibility of the lines, rather than vehicle obstruction, affects the detection. Consequently, the model correctly identifies only the more clearly visible spaces.

Example 3 is similar to the first, with a top section of the parking area clearly visible, allowing the model to accurately detect the empty spaces. In other sections, irregularly parked vehicles obscure the parking lines, causing detection errors. This reinforces the importance of clear, visible lines for effective performance. In example 4, the model performs better overall, largely due to the image being taken from a lower altitude, resulting in sharper parking lines. Despite this, the SSD model still struggles to detect spaces between vehicles where the lines are less visible. Example 5 shows that while

the model successfully detects most parking spaces, it occasionally draws bounding boxes smaller than the actual spaces, even including parts of a white vehicle in one of the parking spaces. This issue may arise because the vehicle's color closely matches the parking lines.

Example 6 involves a close-up view of the parking area with clearly visible lines. Similar to the previous example, the model mistakenly includes part of a white car in the bounding box and also detects an occupied space (with a black car) as empty. This error likely occurs because the parking lines on either side of the vehicle remain clearly visible, misleading the algorithm. Example 7 showcases an image captured from a low altitude with excellent resolution, allowing the SSD model to accurately detect most of the empty spaces. However, it again mistakenly includes part of a white car within a bounding box and identifies some areas incorrectly as parking spaces, possibly due to the similar color of the car and the parking lines. As expected, the model struggles in areas where vehicles obscure the parking lines. Finally, in example 8, the image is taken at a close angle, and the model successfully detects almost all the empty spaces. However, in some cases, it combines two adjacent empty spaces into one, likely due to the parking line between them being unclear.

The performance evaluation of the SSD algorithm for detecting empty parking spaces was carried out using four key performance metrics: precision, recall, mean Average Precision (mAP), and F1 score. In terms of precision, which measures the proportion of correctly predicted empty parking spaces out of all spaces identified by the model, the SSD algorithm demonstrated strong results with a precision score of 0.771. This indicates that approximately 77.1% of the detections made by the model were accurate and truly represented empty parking spaces, highlighting the model's reliability in minimizing false positives. The recall metric, which quantifies the proportion of actual empty parking spaces that were successfully detected by the algorithm, further supports the precision score. The SSD model achieved a recall value of 0.702, meaning it was able to correctly identify 70.2% of the true empty parking spaces present in the dataset. The close relationship between the precision and recall values indicates that the model is not only accurate but also effective at capturing a significant portion of the relevant empty parking spaces.



Fig. 2. Examples of vacant parking space detection using the SSD algorithm in various scenarios.

Another important metric, mAP, which is the average of precision values across all detection thresholds, was calculated as 0.744. This value represents the model's ability to maintain a high degree of accuracy over a range of detection scenarios, confirming that the SSD algorithm's detection capabilities are consistently strong across different levels of difficulty and various environmental conditions. Moreover, the F1 score, which is the harmonic mean of precision and recall, was measured at 0.735. The F1 score provides a balanced assessment of the model's performance by considering both the precision and recall values. This score highlights the overall effectiveness of the SSD model in maintaining a good balance between detecting as many empty parking spaces as possible while minimizing incorrect detections.

IV. CONCLUSION

In this study, the performance of the SSD algorithm was thoroughly evaluated for its ability to detect empty parking spaces in various scenarios using key performance metrics, including precision, recall, mean Average Precision (mAP), and F1 score. The results demonstrate that the SSD algorithm exhibits strong detection capabilities, with a precision score of 0.771, indicating a high accuracy rate in identifying true empty parking spaces. The recall score of 0.702 supports the algorithm's ability to capture a significant portion of actual empty spaces. The mAP value of 0.744 further emphasizes the model's consistent performance across diverse detection thresholds, while the F1 score of 0.735 reflects a balanced integration of precision and recall. These findings confirm the SSD model's suitability for automated parking space detection systems, where real-time identification of available spaces is crucial. The algorithm's robustness across varying

environmental conditions and image qualities makes it an effective tool for parking management solutions. However, while the SSD algorithm shows considerable promise, there is still room for improvement, particularly in addressing the limitations related to occlusions and low visibility of parking lines, which may affect detection accuracy. Future work could focus on refining the model to enhance its performance under more challenging conditions, further solidifying its role in intelligent transportation systems and smart city applications.

REFERENCES

- [1] A. Binmahfooz et al., "IoT-Based Sustainable Parking Lot," *2023 7th International Conference on Smart Grid and Smart Cities (ICSGSC)*, Lanzhou, China, pp. 210-215, 2023. <https://doi.org/10.1109/ICSGSC59580.2023.10319164>
- [2] Y. Ma, Y. Liu, L. Zhang, Y. Cao, et al., "Research review on parking space detection method," *Symmetry*, vol. 13, no.1, 2021. <https://doi.org/10.3390/sym13010128>
- [3] L. Baroffio, L. Bondi, M. Cesana, A. E. Redondi and M. Tagliasacchi, "A visual sensor network for parking lot occupancy detection in Smart Cities," *2015 IEEE 2nd World Forum on Internet of Things (WF-IoT)*, Milan, Italy, pp. 745-750, 2015. <https://doi.org/10.1109/WF-IoT-2015.7389147>
- [4] V. Paidi, J. Håkansson, H. Fleyeh, R. G. Nyberg, "CO₂ emissions induced by vehicles cruising for empty parking space in an open parking lot," *Sustainability*, vol.14, no.7, 2022. <https://doi.org/10.3390/su14073742>
- [5] B. Xu, O. Wolfson, J. Yang, L. Stenneth, P. S. Yu and P. C. Nelson, "Real-Time Street Parking Availability Estimation," *2013 IEEE 14th International Conference on Mobile Data Management*, Milan, Italy, pp. 16-25, 2013. <https://doi.org/10.1109/MDM.2013.12>
- [6] S. J. Faraji, M. J. Nozar, "Smart parking: An efficient approach to city's smart management and air pollution reduction," *Archives*, vol.4, no.1, 2019. <https://doi.org/10.18502/japh.v4i1.603>
- [7] M. Bakirci and I. Bayraktar, "Refining Transportation Automation with Convolutional Neural Network-Based Vehicle Detection via UAVs," *2024 International Russian Automation Conference (RusAutoCon)*,

- Sochi, Russian Federation, 2024, pp. 150-155. <https://doi.org/10.1109/RusAutoCon61949.2024.10694108>
- [8] A. Varghese and G. Sreelekha, "An Efficient Algorithm for Detection of Vacant Spaces in Delimited and Non-Delimited Parking Lots," in *IEEE Transactions on Intelligent Transportation Systems*, vol. 21, no. 10, pp. 4052-4062, Oct. 2020. <https://doi.org/10.1109/TITS.2019.2934574>
- [9] N. Bibi, M. N. Majid, H. Dawood and P. Guo, "Automatic Parking Space Detection System," *2017 2nd International Conference on Multimedia and Image Processing (ICMIP)*, Wuhan, China, pp. 11-15, 2017. <https://doi.org/10.1109/ICMIP.2017.4>
- [10] V. Paidi, H. Fleyeh, J. Håkansson, R. G. Nyberg, "Smart parking sensors, technologies and applications for open parking lots: A review," *IET Intelligent Transport Systems*, vol.12, no.8, pp. 735-741, 2018. <https://doi.org/10.1049/iet-its.2017.0406>
- [11] L. Baroffio, L. Bondi, M. Cesana, A. E. Redondi and M. Tagliasacchi, "A visual sensor network for parking lot occupancy detection in Smart Cities," *2015 IEEE 2nd World Forum on Internet of Things (WF-IoT)*, Milan, Italy, pp. 745-750, 2015. <https://doi.org/10.1109/WF-IoT.2015.7389147>
- [12] S. K. Thangallapally, R. Maripeddi, V. K. Banoth, C. Naveen and V. R. Satpute, "E-Security System for Vehicle Number Tracking at Parking Lot (Application for VNIT Gate Security)," *2018 IEEE International Students' Conference on Electrical, Electronics and Computer Science (SCEECS)*, Bhopal, India, pp. 1-4, 2018. <https://doi.org/10.1109/SCEECS.2018.8546903>
- [13] G. Ciaburro, "Sound event detection in underground parking garage using convolutional neural network," *Big Data Analytics for Social Services*, vol.4, no.3, 2020. <https://doi.org/10.3390/bdca4030020>
- [14] M. Bakirci and I. Bayraktar, "YOLOv9-Enabled Vehicle Detection for Urban Security and Forensics Applications," *2024 12th International Symposium on Digital Forensics and Security (ISDFS)*, San Antonio, TX, USA, 2024, pp. 1-6. <https://doi.org/10.1109/ISDFS60797.2024.10527304>
- [15] M. Bakirci and I. Bayraktar, "Improving Coastal and Port Management in Smart Cities with UAVs and Deep Learning," *2024 Mediterranean Smart Cities Conference (MSCC)*, Martil - Tetuan, Morocco, 2024, pp. 1-6. <https://doi.org/10.1109/MSCC62288.2024.10697069>
- [16] M. Bakirci and I. Bayraktar, "Integrating UAV-Based Aerial Monitoring and SSD for Enhanced Traffic Management in Smart Cities," *2024 Mediterranean Smart Cities Conference (MSCC)*, Martil - Tetuan, Morocco, 2024, pp. 1-6. <https://doi.org/10.1109/MSCC62288.2024.10696996>
- [17] M. Bakirci and I. Bayraktar, "Boosting Aircraft Monitoring and Security through Ground Surveillance Optimization with YOLOv9," *2024 12th International Symposium on Digital Forensics and Security (ISDFS)*, San Antonio, TX, USA, 2024, pp. 1-6. <https://doi.org/10.1109/ISDFS60797.2024.10527349>
- [18] Liu, W., Anguelov, D., Erhan, D., Szegedy, C., Reed, S., Fu, C. Y., & Berg, A. C. (2016). Ssd: Single shot multibox detector. In *Computer Vision—ECCV 2016: 14th European Conference, Amsterdam, The Netherlands, October 11–14, 2016, Proceedings, Part I 14* (pp. 21-37). Springer International Publishing. https://doi.org/10.1007/978-3-319-46448-0_2

Transformatörlerde Buşing Bağlantılarının Önemi

Tuğçe Kayalak¹, Furkan Ekşi², Şeyma Nur Gökmen³, Ahmet Doğuhan Mermer⁴, Melis Öder^{5*}

¹SEM Transformatör A.Ş., Ankara, Türkiye

²SEM Transformatör A.Ş., Ankara, Türkiye

³SEM Transformatör A.Ş., Ankara, Türkiye

⁴SEM Transformatör A.Ş., Ankara, Türkiye

^{5*}SEM Transformatör A.Ş., Ankara, Türkiye

*(melis.oder@semtransformator.com.tr) Email of the corresponding author

Özet – Bu çalışma, transformatörlerde alçak gerilim (AG) tijlerinin kararmasına yol açan aşırı ısınma sorunlarını ve bu sorunların çözümünü ele almaktadır. Transformatörler, elektrik enerjisini alçak gerilimden yüksek gerilime veya tam tersine çevirerek, enerjinin uzun mesafelere verimli bir şekilde iletilmesini sağlar. Transformatörlerin sahada kurulması ve bağlanması çeşitli elektriksel ve mekanik bağlantıları gerektiren bir süreçtir. Bağlantılarda ve montajda oluşan hatalar; elektrik kaçaklarına, kısa devre oluşmasına ve hatta sistemin bozulmasına sebep olabilir.

Çalışma kapsamında saha ortamında alıcının yanlış bağlantısından dolayı trafonun alçak gerilim tijlerindeki aşırı ısınmaya bağlı olarak kararmaların ana nedenini belirlemek hedeflenmiştir. Aşırı ısınma yaşayan AG buşinglerin direnç değerlerinin yüksek olduğu tespit edilmiştir, fazlar arası direnç değerlerinde anormal artışlar gözlemlenmiştir. Isınmaya bağlı kararmaların yüksek direnç noktalarındaki transformatör terminalleri ve buşing bileşenleri arasındaki bağlantılarda problem olabileceği konusu öne çıkmıştır. Ayrıca buşinglerdeki aşırı ısınmaya bağlı olarak yapılan kısa devre testleri ve termal görüntüleme çalışmaları, sorunların altında yatan ana nedenin daha iyi anlaşılmasını sağlamıştır. Analizler sonucunda, fazlar arası sargı dirençleri dengelenmiştir ve sorunun alçak gerilim buşinglerinin montajında olduğu tespit edilmiştir. Sonuç olarak, hasarlı terminaller ve contalar değiştirilmiş, gevşek bağlantılar sıkılaştırılmış ve uygun tork değerleri sağlanmıştır. 8D analiz metoduyla sistemli bir şekilde sorunun kök nedenleri belirlenmiştir ve kalıcı çözümler geliştirilmiştir. Bu çözümler sahada başarıyla uygulanarak test edilmiştir. Böylece transformatörlerin daha güvenli ve verimli çalışması sağlanmıştır.

Anahtar Kelimeler – Güç Sistemleri, Transformatör, Aşırı Isınma, Buşing, 8D Analizi, Montaj Hataları

The Importance of Bushing Connections in Transformers

Abstract – This study addresses the overheating issues that cause the low-voltage (LV) busbars of transformers to become discolored due to excessive heating, as well as the solutions to these issues. Transformers are essential for efficiently transmitting electrical energy over long distances by converting it from low voltage to high voltage or vice versa. The installation and connection of transformers in the field require various electrical and mechanical connections. Errors in these connections and installation processes can lead to electrical leaks, short circuits, and even system failures.

The aim of this study is to identify the root cause of the discoloration of the low-voltage busbars in the transformer, which is due to excessive heating caused by incorrect connections made by the customer in the field. It was found that the resistance values of the overheated LV bushings were high, and abnormal increases were observed in the resistance values between phases. It was concluded that the discoloration due to overheating could be related to issues in the connections between the high-resistance points of the transformer terminals and the bushing components. Additionally, short-circuit tests and thermal imaging studies related to the overheating of the bushings helped better understand the underlying causes of the problem. As a result of the analysis, phase-to-phase winding resistances were balanced, and it was determined that the problem originated from the installation of the low-voltage bushings. Damaged terminals and gaskets were replaced, loose connections were tightened, and appropriate torque values were applied. Using the 8D analysis method, the root causes of the issue were systematically identified, and permanent solutions were developed. These solutions were successfully implemented and tested in the field, ensuring the transformers operated more safely and efficiently.

Key words – Power Systems, Transformer, Overheating, Bushing, 8D Analysis, Assembly Defects

I. GİRİŞ

Güç Sistemlerinde elektrik enerjisinin iletimi ve dağıtımı için transformatörler oldukça önemlidir. Elektrik enerjisinin iletimi, dağıtımı ve kullanımı için gerilim seviyesini değiştiren elektrik makineleridir. Hareketli parçalara sahip olmayan bu makineler, manyetik indüksiyon ile çalışarak gerilim

seviyesini yükseltir veya düşürür. Ancak bu dönüşüm esnasında frekansında herhangi bir değişiklik olmamaktadır. Bu sayede elektrik enerjisi, daha az kayıplar ile uzun mesafelere ulaştırılır. Aynı zamanda enerjinin güvenli bir şekilde iletimi ve kullanımı sağlanır [1].

Elektrik üretim santrallerinde, üretilen elektrik enerjisi genellikle daha düşük gerilim seviyelerinde olur. Santrallerde üretilen elektriğin üretildiği yerde tamamen tüketilmesi

mümkün olmadığından; kullanım bölgelerine taşınması gerekir. Ancak, bu enerjinin uzak mesafedeki tüketim alanlarına güvenli bir şekilde iletilmesi için gerilim seviyesinin yükseltilmelidir. Yüksek gerilimli enerji iletimi, uzun mesafelerde enerji kaybını önemli ölçüde azaltır. Böylelikle verimli bir iletim sağlanır. Elektrik enerjisi kullanıcıya ulaştığında ise gerilim seviyesinin düşürülmesi gerekmektedir. Çünkü dağıtım hatlarında yüksek gerilim, güvenlik riskleri oluşturabilir. Bu sebeple, enerjinin güvenli bir seviyeye ve kullanılabilir hale getirilmesi için gerilim dağıtım merkezlerinde transformatörlerle yeniden dönüştürülür [2].

Transformatörlerin görevlerinin yerine getirirken saha kurulumunun ve bağlantılarının doğru bir şekilde yapılması oldukça önemlidir. Yanlış yapılan bağlantılar ve sahadaki hatalar, transformatör arızalarının en büyük nedenlerinden biridir. Arızaların belirlenmesi verimli ve kaliteli çalışma koşullarının devamlılığını sağlar [3]. Sahadaki bağlantılar, transformatörün primer ve sekonder sargılarının doğru ve güvenli bir şekilde enerjilendirilme görevini yerine getirir. Primer sargıya gerilim uygulandığında oluşan manyetik alan, sekonder sargıda uygun gerilim seviyesini oluşturur. Enerjinin yüksek gerilim hattından alçak gerilim hattına güvenli bir şekilde aktarılması için bağlantıların sağlam yapılması ve yalıtım önlemlerinin alınması büyük önem arz etmektedir. Çünkü yanlış bağlantılar, aşırı ısınma ve yağ kaçaklarına neden olabilir, bu da ciddi hasarlara ve sistemin durmasına yol açar [4][5].

Transformatörün metal gövdesi ile toprak arasındaki bağlantının da doğru yapılması gerekmektedir. Çünkü topraklama, kaçak akımları güvenli bir şekilde toprağa ileterek, transformatörü ve çevresini korumaya alır. Ayrıca transformatörlerde önemli bir diğer konu ise buşing bağlantılarıdır. Buşingler, transformatörün içindeki yüksek gerilimli enerjinin dışarıya güvenli bir şekilde aktarılmasını sağlamaktadır. Bu işlevi yerine getirirken elektriksel yalıtıma ve mekaniksel sağlamlığa uygun olması gerekir. Yanlış yapılan bağlantılar hem mekanik hem de elektriksel sorunlara yol açarak ciddi güvenlik riskleri oluşturur. Bu nedenle, bağlantıların doğru yapılması, sadece sistemin verimli çalışmasını sağlamakla kalmaz; aynı zamanda enerjinin güvenli ve sorunsuz bir şekilde iletilmesine, çevreye herhangi bir zarar vermemesine de katkıda bulunur. Düzgün bir kurulum, olası riskleri en aza indirir, güvenliği artırır ve transformatörün daha uzun ömürlü olmasını sağlar [6].

II. MATERYAL VE METOD

Buşinglerin en önemli görevlerinden biri, yüksek gerilimli elektrik akımını izolasyonunu sağlayarak elektrik kaçaklarının engellemektir. Transformatörde dönüştürülen enerji genellikle yüksek gerilimde olur. Bu gerilimin trafonun dışına, yani transformatörün gövdesine ya da çevresindeki bileşenlere geçmesini önlemek buşinglerin temel işlevidir. Sağlanan elektriksel yalıtım ile oluşabilecek ciddi elektrik kazaları engellenmektedir. Montajı yanlış yapılmış veya zamanla aşınmış buşingler, kaçak akımlara, kısa devrelere ve hatta yangın risklerine yol açabilir [7] [8].

Buşingler yalnızca elektriksel bir yalıtım sağlamaz; aynı zamanda transformatör ile sistem arasındaki mekanik bağlantıyı da kurar. Buşinglerin düzgün monte edilmesi, özellikle yüksek akım geçişlerinde kritik önem taşımaktadır. Ayrıca, mekanik sağlamlık, transformatörün iç yapısının titreşim, mekanik darbeler, sıcaklık değişimleri gibi çevresel

faktörlere dayanmasını sağlar. Eğer buşing bağlantıları yeterince sağlam değilse, elektrik iletimi sırasında temas sorunları yaşanabilir, bu da performans düşüklüğüne, ısınmalara ve enerji kayıplarına yol açar.

III. BULGULAR VE TARTIŞMALAR

Müşteri şikâyeti olan aşırı ısınma nedeniyle Alçak Gerilim (AG) buşinglerinin kararması Şekil 1.'de gösterildiği gibidir.



Şekil 1. Tijleri kararmış AG buşingler

Aşırı ısınmadan dolayı meydana gelen alçak gerilim buşinglerinin termal kameradaki görüntüsü Şekil 2.'de verilmiştir.



Şekil 2. Aşırı ısınmanın gözlemlendiği alçak gerilim buşinglerinin termal kamera görüntüleri

Alçak gerilim terminallerinde sahada tespit edilen sıcak noktaların kaynağını belirlemek için transformatörde tanı testleri gerçekleştirildi.

Yağı boşaltmadan ve transformatör tanktan çıkarmadan önce, transformatörde düşük voltaj testleri gerçekleştirilmiştir. Test sonuçları Tablo 1.'de verilmiştir.

Tablo 1. Test sonuçları

Ölçüm Sonuçları								
A (a2-b2)			B (b2-c2)			C (c2-a2)		
R _m	R _d	R _c	R _m	R _d	R _c	R _m	R _d	R _c
7,68	0,00	7,68	6,95	0,00	6,95	6,18	0,00	6,18
1 µΩ	8 %	1 µΩ	9 µΩ	8 %	9 µΩ	9 µΩ	8 %	9 µΩ

Bu testlerin sonucunda, aşırı ısınmaya maruz kalan AG sargı direnci beklenen değerlerden yüksek gelmiştir. Fazlar arası fark %16,7 katı direnç değerlerinin arttığı görülmüştür.

Sonuçlar göz önüne alındığında, yağın boşaltılmasına, aktif kısmın tankın dışına çıkarılmasına, aynı sargıların dirençlerinin ölçülmesine, buşinglerinin etkisinin ortadan

kaldırılmasına ve kapağın altından ölçülmesine karar verilmiştir.

Buşinglerin etkisini ortadan kaldırmak için kullanılan ölçüm noktaları Şekil 3.'te verilmiştir.



Şekil 3. Buşinglerin etkisini ortadan kaldırmak için kullanılan ölçüm noktaları

Bu işlemlerin sonucunda fazlar arasındaki sargı dirençleri doğru ve dengeli hale geldiği değerler Tablo 2.'de paylaşılmıştır.

Tablo 2. Test sonuçları

Ölçüm Sonuçları								
A (a2-b2)			B (b2-c2)			C (c2-a2)		
R_m	R_d	R_c	R_m	R_d	R_c	R_m	R_d	R_c
658,	0,00	658,	664,	0,00	664,	673,	0,00	673,
80	5%	80	65	6%	65	80	7%	80
$\mu\Omega$		$\mu\Omega$	$\mu\Omega$		$\mu\Omega$	$\mu\Omega$		$\mu\Omega$

Bu, problemin yüksek direnç noktalarının alçak gerilim buşinglerinde bulunduğu anlamına gelir; ancak bunu tekrar kontrol etmek için transformatörde kısa devre testi gerçekleştirildi. Önce buşinglerin kendisinde kısa devre yapıldı ve ardından buşinglerin etkisini ortadan kaldırmak için bakır bağlantı baraları kısa devre yapıldı.



Şekil 4. Buşing kısa devre ölçümü

Buşing kısa devre ölçümünün termal kamera görüntüleri Şekil 5'te verilmiştir.



Şekil 5. Buşing kısa devre ölçümünün termal görüntüleme sonucu

Termal görüntüleme kamerasıyla yapılan incelemenin sonucuna göre buşingler kısa devre yapıldığında, tijlerin 30 saniyeden kısa bir sürede çok hızlı bir şekilde ısındığını ve yüksek voltaj sargısında 50 amperlik, yani nominal akımının %30'undan daha az bir akımla kısa devre yapılmasına rağmen yüksek sıcaklıklara ulaştığını göstermektedir.

Ancak, aynı kısa devre testi bakır bağlantı baralarında yapıldığında, buşingler de veya bağlantıyı oluşturan diğer bakır tijlerde aşırı ısınma gözlemlenmemektedir.

Tij ile bara bağlantısı arasındaki ölçüm Şekil 6.'da verilmiştir.



Şekil 6. Tij ile bara bağlantısı arasındaki ölçüm

Tij ile bara bağlantısı arasında yapılan ölçümlerin termal kamera görüntüleri Şekil 7.'de verilmiştir.



Şekil 7. Tij ile bara bağlantısı arasındaki ölçümün termal görüntüleme sonucu

Bu ölçüm sonuçları transformatörde meydana gelen yüksek direnç noktalarının buşinglerde olduğu teorisini güçlendirdi. Bu teoriyi kesin olarak doğrulamak için, bayrak bara ile tij arasında ve tij ile bara bağlantı noktası arasında bir temas direnci testi gerçekleştirilmiştir.

Sonuçlar yüksek direnç noktasının bayrak bara ile tij arasında olduğunu göstermektedir. Elde edilen değerler Tablo 3.'te yer almaktadır.

Tablo 3. Test sonuçları

Ölçüm Sonuçları					
Bayrak bara ve tij			Tij ve tabanı		
R _m	R _d	R _c	R _m	R _d	R _c
4,77 mΩ	0,002%	4,77 mΩ	2,30 μΩ	0,003%	2,30 μΩ

Tüm bu test ve kontroller tamamlandıktan sonra hasarlı terminallerden biri çıkarılıp incelenmiştir. Hasarlı terminallerin görüntüsü Şekil 8.'de verilmiştir.



Şekil 8. Hasarlı terminallerin görüntüsü

Şekil 8'de görüldüğü gibi, tijin kendisinde erimiş malzeme izleri bulunmaktadır. Bu durum ulaşılan yüksek sıcaklıkların göstergesidir.

Trafo muayenesi sonucunda, bakır bayrak baranın montajının gevşek bağlanmasından kaynaklı aşırı ısınmadan dolayı tijin karardığı ve kontak direnci geçişinin normalden çok daha yüksek olduğu tespit edilmiştir. Transformatorün aktif kısmında herhangi bir sorunla karşılaşılması. Mevcut tijler çıkarılmış ve 3 tij yenileriyle değiştirilmiştir. AG buşing contaları ve üst kapak altındaki mantar conta yenileriyle değiştirilerek müşteriye teslim edilmiştir.

Sahadaki transformatorlerde yaşanan sıcak nokta ve yağ kaçağı sorunlarının çözümünde 8D analizi etkin bir şekilde uygulanmıştır. Bu sürecin sonunda, saha bağlantılarındaki montaj hataları ve çevresel etkilerin, yağ kaçağı ve sızdırmazlık problemlerini artırdığı görülmüştür.

Aşağıda 8D analizinin aşamaları yer almaktadır.

1D - Ekip Oluşturma

- **Amaç:** Aşırı ısınma sorununun ve yağ kaçağının çözümü için her birimden gerekli uzmanlıklara sahip ekip oluşturuldu.
- **Ekip Üyeleri:** Elektrik mühendisi, makine mühendisi, üretim mühendisi, kalite kontrol uzmanı.
- **Sahada Çalışan Ekip Üyeleri:** Bakım mühendisi, elektrik teknisyeni, test mühendisi ve saha mühendisi.

2D - Problemin Tanımlanması

- **Sorun Tanımı:** AG bağlantılarında aşırı ısınma ve yağ kaçağı gözlemlenmiştir. Transformatorde yağ kaçağı ve bağlantı civatalarında renk değişikliği raporlanmıştır.
- **Etkilenen Alanlar:** AG buşing bileşenleri

3D - Geçici Önlemler Alınması

- **Önlemler:** Sıcak noktaların olduğu alanlarda yağ seviyeleri düzenli olarak kontrol edildi. Hasarlı conta bölgelerinde geçici olarak sızdırmazlık malzemesi eklendi.
- **Amaç:** Transformatorlerin anlık güvenliğini sağlamak ve daha ciddi arızaların önüne geçmek oldu.

4D - Kök Neden Analizi

- **Kök Neden Analizi:** Buşinglerdeki yüksek direnç ve hatalı saha montajı sonucu aşırı ısınma sonucu sıcak noktalar oluşmuş ve bu da contaların yıpranmasına yol açmıştır. Ayrıca, bağlantı noktalarındaki aşırı yük, termal stres ile birleşerek yağ kaçağına neden olmuştur.

5D - Kalıcı Çözümler Geliştirilmesi

- **Çözümler:**
- **Bağlantı Torklarının Düzeltilmesi:** Montaj sırasında uygun tork değerlerinin sağlanması için bir kontrol süreci oluşturuldu.
- **Yüksek Kaliteli Conta ve Bağlantı Elemanları Kullanımı:** AG terminalleri için kullanılan contalar yeterli olsa da aşırı ısınma sonucu yüksek kaliteli contalar kullanıldı.

6D - Çözümlerin Uygulanması

- **Uygulama:** Hasarlı buşingler, contalar ve bağlantı elemanları değiştirildi. Yüksek sıcaklık oluşumunu engellemek için buşing bağlantı noktalarındaki direnç azaltacak ekipman yerleştirildi.
- **Amaç:** Sorunun temel nedenlerine yönelik kalıcı çözümler uygulayarak transformatorlerin güvenli çalışmasını sağlamaktır.

7D - Çözümlerin Doğrulanması

- **Doğrulama ve Test:** Transformatorler çalıştırılarak bağlantı noktalarında termal kamera ile izleme yapılır. Yağ sızıntısı ve sıcak nokta problemlerinin giderildiği doğrulanmıştır.
- **Sonuçlar:** Uygulanan çözümler, sorunları etkili bir şekilde ortadan kaldırmıştır.

8D - Standartlaştırma

- **Standartlaştırma:** Tork kontrolü, yüksek kaliteli conta kullanımı ve çevresel koruma prosedürleri müşterinin saha montajı için bakım standartlarına dahil edilir.

IV. SONUÇ

Transformatorde yapılan tüm test ve kontrollerin sonucunda, gevşek bayrak tijinin neden olduğu terminal bayrağı ile hasarlı buşinglerin tijler arasında yüksek direnç noktası oluşumunda aşırı ısınma görülmüştür. Bunun sonucunda tijin karardığı ve

temas direnci geçişinin normalden çok yüksek olduğu tespit edilmiştir. Ayrıca contaların işlevlerini yitirecek şekilde hasar görmesine neden olmuştur. Hasar gören conta da transformatörde yağ sızıntılarının görülmesine sebep olmuştur.

Yaşanan bu tür sorunlar, saha bağlantılarının doğru ve güvenli bir şekilde yapılmasının ne kadar kritik olduğunu göstermektedir. Saha bağlantıları, sadece transformatörün güvenli ve verimli çalışmasını değil, aynı zamanda uzun ömürlü olmasını da doğrudan etkiler.

Doğru yapılan saha bağlantıları, transformatörde elektriksel akımların düzgün bir şekilde iletilmesini sağlayarak enerji kayıplarını minimumda tutar. Yanlış veya hatalı bağlantılar ise fazlar arasında dengesiz akımlara, aşırı ısınmaya ve hem termal hem de mekanik strese neden olabilir. Bu tür hatalar, zamanla transformatörün yalıtımının bozulmasına bozulan yalıtım sonucunda ömrünün azalmasına, yağ sızıntılarına ve en önemlisi transformatörün tamamen arızalanmasına yol açabilir.

Ayrıca, bağlantıların doğru yapılması, aşırı yüklenme, kısa devre gibi durumlarda koruma sistemlerinin doğru çalışmasını sağlar. Koruma sistemlerinin devreye girmesi, transformatörün hasar almasını önler ve olası maliyetli onarımların ya da sistemin devre dışı kalmasının önüne geçer.

Sonuç olarak, saha bağlantılarında gerçekleşen ihmal veya oluşacak olan hata, transformatörün performansını olumsuz etkileyip ömrünü kısaltabilir. Bu nedenle, saha bağlantıları transformatörün hem güvenli hem de uzun yıllar verimli çalışmasını sağlamak adına önemli bir rol oynar.

TEŞEKKÜR

Bu çalışmaya vermiş olduğu katkı ve desteklerinden dolayı SEM Transformatör A.Ş.'ye teşekkür ederiz.

KAYNAKLAR

- [1] Tören,M. (2022).Yağlı tip transformatörlerde hibrit bir soğutma sistem tasarımının FEM ve CFD analizleri ,Niğde Ömer Halisdemir Üniversitesi Mühendislik Bilimleri Dergisi. 11(3), 611-619.
 - [2] Karabacak,K.(2011).Elektronik Burun Kullanarak Trafolarında Arıza Analizi. Dumlupınar Üniversitesi, Yüksek Lisans Tezi.
 - [3] Atalar,F. & Kuntman,A. (2022). Bulanık Mantık Yöntemi Kullanılarak Güç Transformatörleri Arızalarının Belirlenmesi. Elektrik Mühendisleri Odası Yayınları.
 - [4] Kemik,E.(2016)Güç Transformatörü hatalarının Bulanık Mantık ve Öz Düzenlemeli Haritalama Yöntemi ile Belirlenmesi. Pamukkale Üniversitesi Fen Bilimleri Enstitüsü
- Elektrik-Elektronik Mühendisliği Anabilim Dalı.
- [5] Yıldız, C., Çelik, İ., & Şekkeli, M. (2022). Güç Trafosu Arızasının Farklı Yöntemler ile Tahmini: 403 MVA'lık Bir Trafoda Uygulama ve Ekonomik Analizi. Bingol University Journal of Technical Science.
 - [6] Saraswati D, Marie I A, Witonohadi A. Power Transformer Failures Evaluation Using Failure Mode Effect and Criticality Analysis (FMECA) Method. Asian Journal of Engineering and Technology. 2014; 2(06).
 - [7] Kruger, M., Kraetge, A., Koch, M., Rethmeier, K., Pütter, M., Hulka, L., Muhr, M., Summereder, C., "New Diagnostic Tools For High Voltage Bushing", Cigre VI Workspot-International Workshop On Power Transformers, 25-28 April 2010.

- [8] Pekin,H. (2020) Transformatör Arızaları ve Sebepleri. Elektrik Mühendisliği Araştırmaları Dergisi.